University of Stuttgart
Germany

Faculty 6: Aerospace Engineering and Geodesy

Annual Report **2022**

Geodesy & Geoinformatics

GIS

INS

ifp

editing and layout:
volker walter, markus antoni, martin metzner, aloysius wehr

Dear friends and colleagues,

It is our great pleasure to present to you this annual report on the 2022 activities and academic highlights of the four institutes

- Institute of Geodesy (GIS),
- Institute for Photogrammetry (ifp),
- Institute of Navigation (INS),
- Institute of Engineering Geodesy (IIGS),

which contribute to the curricula of Geodesy and Geoinformatics at the University of Stuttgart and which are part of the Faculty of Aerospace Engineering and Geodesy.

Preface

With the overcome of the Corona crisis we have moved back to normal operations in the way how we teach our students but also how we do research. Regaining the possibility to interact face-to-face with our students and work in research teams who are physically gathered, makes us realize how important such human interactions are in our research disciplines. Thus, it is no surprise that the back-to-normal mode has boosted our productivity and increased the coherency in our institutes even further. We saw new research projects being launched and many research proposals, which are covering new and creative ideas, being submitted to different funding organizations.

In general, it can be stated that all institutes had a very prosperous year in their research work, when establishing new collaborations or attracting new undergraduate and graduate students. Thus, we can surely say that we were able to increase the visibility of Geodesy and Geoinformatics on national and international levels.

Research

This annual report documents our research contributions in many diverse fields of Geodesy and Geoinformatics: from satellite and physical geodesy through navigation, remote sensing, engineering surveying and telematics to photogrammetry, geographical information systems and location based services. Detailed information on projects and research output can be found in the following individual institutes' sections.

Teaching

We were able to welcome 14 new BSc students in winter term 2021/2022. For the first semester of the MSc program for Geodesy and Geoinformatics we welcomed 14. Please visit our website

www.geodaesie.uni-stuttgart.de

or check our Instagram account

https://www.instagram.com/geodaesie_stuttgart/

for additional information on the programs.

Our successful international MSc program Geomatics Engineering (GeoEngine) exists already 17 years. Probably due establishment of tuition fees for non-EU students in 2018, we saw a decline of new students since then. We welcomed only 4 students in 2022. We believe one reason for the decline in the number of students actually showing up could be a general reluctance to study abroad as well as the manifold of international master programs that are available.

Awards and Scholarships

We want to express our gratitude to our friends and sponsors, most notably:

- Verein Freunde des Studienganges Geodäsie und Geoinformatik an der Universität Stuttgart e.V. (F2GeoS),
- Ingenieur-Gesellschaft für Interfaces mbH (IGI),
- DVW Landesverein Baden-Württemberg,

who support our programs and our students with scholarships, awards and travel support. Below is the list of the recipients of the 2022 awards and scholarships. The criterion for all prizes is academic performance; for some prizes GPA-based, for other prizes based on thesis work. Congratulations to all recipients!

Award	**Recipient**	**Sponsor**	**Programme**
Karl-Ramsayer Preis	Ms. Sigi Ke	Department of Geodesy & Geoinformatics	Geodesy & Geoinformatics
BSc Thesis Award	Ms. Paula Peitschat	F2GeoS	Geodesy & Geoinformatics
MSc Thesis Award	Mr. Joachim Schulz	F2GeoS	Geodesy & Geoinformatics

Thomas Hobinger, Associate Dean (Academic)

thomas.hobiger@ins.uni-stuttgart.de

Institute of Engineering Geodesy

Geschwister-Scholl-Str. 24 D
70174 Stuttgart
Germany
Tel.: +49 711 685 84041
Fax: +49 711 685 84044
sekretariat@iigs.uni-stuttgart.de or
firstname.secondname@iigs.uni-stuttgart.de
http://https://www.iigs.uni-stuttgart.de/

Head of Institute

Prof. Dr.-Ing. habil. Dr. h.c. Volker Schwieger

Secretary

Elke Rawe
Désirée Schreib

Scientific Staff

M.Sc. Sahar Abolhasani (since 01.01.2022)	Sensor Fusion
M.Sc. Laura Balangé	Quality Modeling
M.Sc. Urs Basalla (until 30.06.2022)	Terrestrial Laser Scanning
M.Sc. Rudolf Frolow (since 15.07.2022)	Sensor Fusion
Dipl.-Ing. Lyudmila Gorokhova	Kinematic Positioning
Dipl.-Ing. Susanne Haußmann (until 30.06.2022)	Kinematic Positioning
M.Sc. Gabriel Kerekes	Terrestrial Laser Scanning
Dr.-Ing. Otto Lerke (until 30.06.2022)	Machine Guidance
M.Sc. Philipp Luz	Digital Map
Dr.-Ing. Martin Metzner	Engineering Geodesy
M.Sc. Christoph Sebald	GIS for Climate Data
Dr.-Ing. Li Zhang	Engineering Geodesy

Technical Staff

Dipl.-Ing. (FH) Andreas Kanzler
Martin Knihs, Mechanikermeister
Dipl.-Geogr. Lars Plate

External Teaching Staff

Dipl.-Ing. Jürgen Eisenmann	Geschäftsbereichsleiter Landratsamt Ostalbkreis, Geoinformation und Landentwicklung
Dr.-Ing. Frank Friesecke	Prokurist der STEG Stadtentwicklung GmbH
M. Eng. Jonas Stadler	Landratsamt Alb-Donau-Kreis Flurneuordnung der Landkreise Alb-Donau-Kreis und Biberach
Dipl.-Math. Ulrich Völter	Geschäftsführer der Fa. Intermetric - Gesellschaft für Ingenieurmessung und raumbezogene Informationssysteme mbH
Dr.-Ing. Thomas Wiltschko	Daimler AG, Mercedes-Benz Cars; Research and Development

PhD Students

M.Sc. Julia Aichinger	Terrestrial Laser Scanning
Dipl.-Ing. Patric Hindenberger	Location Referencing
M.Sc. Yu Li	Digital Map
M.Sc. Annette Schmitt	Multi-Sensor-Systems
M.Sc. Tobias Schröder	Automation of Production Process
M.Sc. Yihui Yang	Multi-Sensor-Systems
M.Sc. Christian Bader	Kinematic Laser Scanning

General View

The Institute of Engineering Geodesy (IIGS) is directed by Prof. Dr.-Ing. habil. Dr. h.c. Volker Schwieger. It is part of Faculty 6 “Aerospace Engineering and Geodesy” within the University of Stuttgart. Prof. Schwieger holds the chair in “Engineering Geodesy and Geodetic Measurements”.

In addition to being a member of Faculty 6, Prof. Schwieger is co-opted to Faculty 2 “Civil and Environmental Engineering”. Furthermore, the IIGS is involved in the Center for Transportation Research of the University of Stuttgart (FOVUS). Thus, the IIGS actively continues the close collaboration with all institutes in the field of transportation, especially with those belonging to Faculty 2.

Since 2011, Prof. Schwieger is a full member of the German Geodetic Commission (Deutsche Geodätische Kommission - DGK). Furthermore, since 2020 he is head of the section “Engineering Geodesy” within the DGK.

The institute’s main tasks in education focus on geodetic and industrial measurement techniques, kinematic positioning and multi-sensor systems, statistics and error theory, engineering geodesy and monitoring, GIS-based data acquisition, and transport telematics. Here, IIGS is responsible for the above-mentioned fields within the curricula of "Geodesy and Geoinformatics" (Master and Bachelor in German) and for "GEOENGINE" (Master for Geomatics Engineering in English). In addition, the IIGS provides several courses in German for the curricula of "Aerospace Engineering" (Bachelor and Master), "Civil Engineering" (Bachelor and Master), "Transport Engineering" (Bachelor and Master) and "Technique and Economy of Real Estate" (Bachelor and Master). Furthermore, lectures are given in English to students within the Master course "Infrastructure Planning".

The cluster "Integrative Computational Design and Construction for Architecture" (IntCDC), which is part of the excellence strategy to strengthen cutting-edge research in Germany, was awarded funding in 2018 for the next seven years. The cluster IntCDC aims to harness the full potential of digital technologies in order to rethink design and construction, and enable ground breaking innovations for the building sector through a systematic, holistic, and integrative computational approach. As a member of the cluster (IntCDC), the institute's research in the field of new construction methods is intensified in cooperation with architects, civil engineers, computer scientists, production engineers, and other scientists from various research institutions within and outside the University of Stuttgart.

The current research and project work of the institute is expressed in the course contents, thus always presenting the actual state-of-the-art to the students. As a benefit of this, student research projects and theses are often implemented in close cooperation with the industry and external research partners. The main research focuses on kinematic and static positioning, analysis of engineering geodetic processes and construction processes, machine guidance, monitoring, transport and aviation telematics, process and quality modeling. The daily work is characterized by intensive co-operation with other engineering disciplines, especially with traffic engineering, civil engineering, architecture, and aerospace engineering.

Research and Development

AI-supported Collaborative Control and Trajectory Generation of Mobile Manipulators for Indoor Construction Tasks

Gefördert durch DFG Deutsche Forschungsgemeinschaft
IntCDC CLUSTER OF EXCELLENCE

For the automation of indoor construction tasks specifically in existing buildings, mobile robots offer great flexibility and provide digital support for time-consuming tasks such as the positioning of building elements. Within the framework of the Cluster of Excellence IntCDC, the research project RP 26 focuses on collaborative path and trajectory generation for a heterogeneous group of collaborating mobile robots. These robots, which are depicted in Figure 1, are equipped with sensors including cameras, LIDAR, IMU and different manipulator arms and operate under Robot Operating System (ROS). In this project three institutes from Stuttgart University cooperate: Institute of System Dynamics (ISYS), Institute of Photogrammetry (IFP) and Institute of Engineering Geodesy (IIGS).

Simultaneous Localization and Mapping (SLAM) is a special form of Structure-from-Motion (SfM), focused on real-time accurate tracking of robot trajectories while simultaneously building a map of the respective environment. The main goal of IIGS is to use the capability of robot total stations (RTS) in seamless absolute positioning to improve SLAM methods to reach the high accuracy levels necessary for automatic assembly or manipulation.

Figure 1: Robots Overview (© IIGS/Abolhasani)

To initiate the tracking and positioning of robots with RTS a test case was arranged by placing a prism on the sensor robot in IntCDC Laboratory for Large-Scale Construction Robotics (LCRL). Using a GPS receiver, a NTP time server was developed to synchronize the total station with other sensors. Having compared the results with those of SLAM, developed by IFP, in the next step the absolute coordinates resulting from sensor fusion are to integrate in SLAM.

Supported by the Deutsche Forschungsgemeinschaft (DFG, German Research Foundation) under Germany's Excellence Strategy - EXC 2120/1 - 390831618.

CYBER-PHYSICAL ON-SITE CONSTRUCTION PROCESSES USING A SPIDER CRANE ROBOTIC PLATFORM

In a frame of the Cluster of Excellence IntCDC, the research project cyber-physical construction had been improved and further developed. The project itself deals with development of a cyber-physical construction (CPC) instrumentation platform, including two types of robotic cranes (see Figure 2), for the automated or partly automated assembly of building components, where the accurate position of the platform has to be provided by a network of total stations. The position of the being developed platform can be achieved using different opportunities, for example: by tracking the prism, installed on the platform, or by tracking the object itself, using it's images. Based on it, the whole research project can be divided on two parts, which are being connected to each other.

Gefördert durch
DFG Deutsche Forschungsgemeinschaft
IntCDC
CLUSTER OF EXCELLENCE

In the first phase of the project, from July 2019 until June 2022, a real time robotic image assisted total station (IATS) network was realized, which was capable of calculating and transmitting the pose seamlessly to the mini crane. Additionally, in order to evaluate the performance of the network two criteria of reliability and accuracy were taken into consideration in simulation and real-world tests leading to satisfactory results. Furthermore, in a period since July until December 2022, the first version of the completed system had been additionally tested out in respect to the internal uncertainties and errors. The local geodetic network, being used for positioning of the cranes, had been measured again and the coordinates of the network points had been examined in respect to its stability.

After the successful implementation of the first part of the project, the second had started from July 2022. The aim of it is to use the whole potential of the robotic total stations, by usage of the integrated camera for the absolute tracking and positioning purposes via image-processing techniques. It requires at first to calibrate the robotic total stations in order to provide the accurate tracking algorithm. The development of the proper calibration procedure is in process in order to realize the correct conversion from a pixel-based image coordinate system into metric IATS coordinate system. The robotic total stations, being already involved in developed on the first step of the project network, had been checked in respect to the quality of the integrated cameras and its possible further usage in the project. It is planned to integrate the calibration procedure on all robotic total stations, which are used in the network.

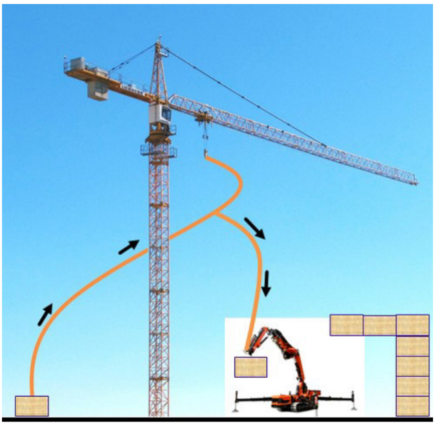

Figure 2: Example of the cooperation between two cranes for the automated/partly automated construction

Supported by the Deutsche Forschungsgsmeinschaft (DFG, German Research Foundation) under Germany's Excellence Strategy - EXC 2120/1 - 390831618.

Holistic Quality Model for Existing Buildings - Social, Environmental, Technical and Economic Integration

As part of the cluster of excellence Integrative Computational Design and Construction for Architecture (IntCDC), the research project "Holistic Quality Model for IntCDC building systems" is concerned with the development of a holistic quality model. This is done in close cooperation with the Institute of Acoustics and Building Physics (IABP) for the environmental quality and the Institute of Social Sciences (SOWI) for the social quality. The objective of the IIGS here is to consider the technical quality.

Gefördert durch DFG Deutsche Forschungsgemeinschaft

IntCDC CLUSTER OF EXCELLENCE

In the final phase of the first research period the focus of the interdisciplinary work was to detect and map the dependencies of quality characteristics between the different disciplines. Special attention was paid to the interpretation of the agent-object dependencies between the quality characteristics of different disciplines.

For the disciplinary work the focus of the IIGS was the development of a quality assessment concept for the application of coreless filament winding. Therefore, algorithms for the autonomous detection of fiber segments from laser scanner point cloud are developed and implemented. Also the mapping of the data to the available fiber syntax was one of the main challenges. In addition, investigations of the calculation of the fiber cross-sections were carried out by using different methods (see Figure 3).

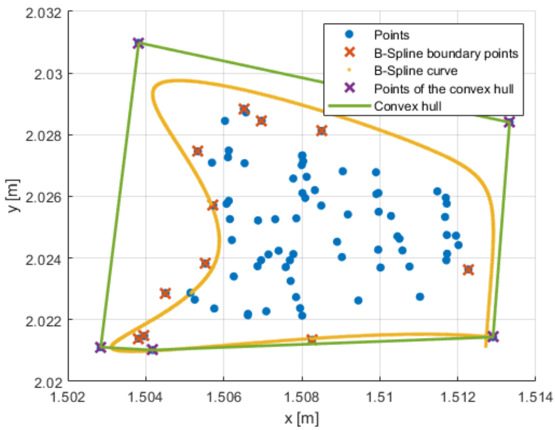

Figure 3: Computed boundary of fiber segments using convex hull and B-spline approach.

With the start of the second project phase in the middle of the year, another dimension was added to the quality model. Since July, the Institute for Construction Management (IBL) has been part of the project, which integrates besides the social, environmental and technical components now also the economic component into the model to assess the economic life cycle, cost efficiency as well as flexibility and adaptability of IntCDC building systems. Another focus of the second project phase is to not only assess the quality of new buildings, but also the quality of existing buildings. Therefore, in a first step different measures for the building stock extension are defined and investigations are carried out about the social, environmental, economic and technical drivers for the building stock extension.

Supported by the Deutsche Forschungsgemeinschaft (DFG, German Research Foundation) under Germany's Excellence Strategy - EXC 2120/1 - 390831618.

Automated Assembly of a Wooden Pavilion

Monitoring the geometry is of major importance in the construction industry. Since automation is becoming more and more important and many processes are carried out robotically, determining the position of the construction robots is also of crucial importance in addition to monitoring the geometry of the building itself. In the framework of the FIT construction project (FIT - Freiburg Center for Interactive Materials and Bioinspired Technologies), which is a timber pavilion built with 127 individual wooden cassettes. The project is a cooperation between the two clusters of excellence livMatS at the University of Freiburg and IntCDC at the University of Stuttgart. For IntCDC the project serves a building demonstrator.

The geodetic contribution to the FIT Pavilion consists of two main parts: Geodetic control of the construction robots and geometric quality assurance. Regarding the first part, initially a three-dimensional coordinate system was defined as a frame of reference for subsequent observations and geometry calculations, followed by bringing the cranes according to the desired alignment at precisely predefined points inside and outside the pavilion. Subsequently with the aim of integration of geodetic techniques for localization and control of the construction robots a highly accurate real-time total station network consisting of four total stations was developed. Two total stations determined the position of one construction robot and the two remaining total stations that of the second one. From this fully automatic real-time measuring system, which is depicted in Figure 4, the positions of the reflectors were transmitted to control the construction robots. The goal was an accuracy in the range of a few millimeters.

In order to be able to guarantee a fluent assembly of complex buildings with double-curved shells, quality assurance is of major importance. In the following, special emphasis is placed on the geometric quality of the components and the construction. The aim was to accompany a previously defined number of components through the manufacturing process in order to be able to detect possible changes in the geometry. For this purpose, 3D point clouds of the selected cassettes were generated using a terrestrial laser scanner, which could then be compared with the nominal geometry from the planning. These measurements were carried out after production in Blaustein, on the construction site in Freiburg before assembly, as

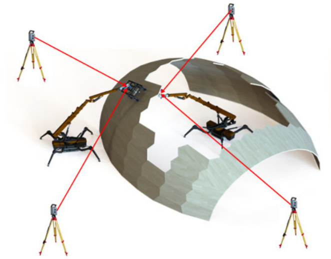

Figure 4: Configuration of total station Network

well as in the installed state (see Figure 5). In order to be able to carry out a final geometric quality assurance, a scan of the finished shell was also taken in order to finally evaluate the geometry.

Figure 5: TLS measurements of timber shell

Supported by the Deutsche Forschungsgemeinschaft (DFG, German Research Foundation) under Germany's Excellence Strategy - EXC 2120/1 - 390831618.

Patch-based M3C2: Towards Lower-uncertainty and Higher-resolution Deformation Analysis of 3D Point Clouds

Multitemporal acquisitions of 3D point clouds for geomonitoring tasks allow the quantification and analysis of geometric changes of monitored objects by advanced processing algorithms, further revealing the underlying deformation mechanism. Among numerous approaches proposed in the geoscientific domain for point cloud-based deformation analysis, the Multiscale Model-to-Model Cloud Comparison (M3C2) is the most widely applied for distance quantification between two point clouds with high surface roughness. Small-magnitude deformations under complex topographies, however, are still challenging to be accurately quantified and analyzed by a statistical significance test when using standard M3C2, for (1) average positions may deviate from the actual surface in cylindrical neighborhoods and (2) empirical uncertainties represented by local roughness are overestimated in highly variable areas. Besides, the resolution of derived deformation is limited by original point densities and algorithm limitations. In this contribution, an extended alternative called patch-based M3C2 is proposed, which inherits the basic framework of standard M3C2 for its simplicity. This novel approach does not need surface meshing and identification of semantic or instance correspondences for point clouds. Lower uncertainty is achieved by generating locally planar patches and projecting measurements on associated patch planes, allowing better detection of small deformations in complex 3D topographies. Besides, the patch-based M3C2 could assign a deformation value to any position located within the overlapping areas, enabling a higher resolution of deformation analysis. The proposed method is demonstrated and evaluated on three datasets. The experimental results indicate that patch-based M3C2 exhibits higher accuracy and lower uncertainties on distance computations between two surfaces. Figure 6 shows the general workflow of patch-based M3C2.

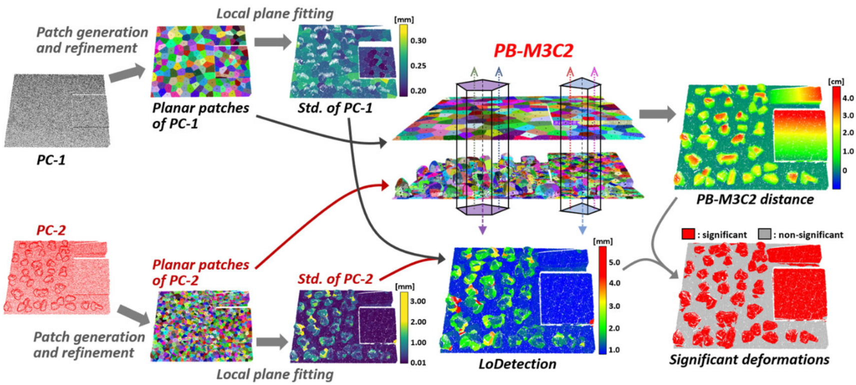

Figure 6: The workflow of patch-based M3C2 (PB-M3C2)

Integrated space-time modeling based on correlated measurements for the determination of survey configurations and the description of deformation processes (IMKAD)

The report for the DFG (Deutsche Forschungsgemeinschaft) IMKAD II was completed in 2022. To sum up the main objectives, the project addressed the analysis of deformation processes with high spatial-temporal resolution. The intended applications are related to monitoring of civil engineering buildings and constructions with complex shapes.

Gefördert durch
DFG Deutsche Forschungsgemeinschaft

The project was carried out together with a partner, the Department of Geodesy and Geoinformation of the Vienna University of Technology. Several study cases show this, out of which the Urbach Tower (Figure 7 left) is shortly presented.

The scanned object is a unique double-curved wooden 14 m tall tower, called the Urbach Tower, designed and constructed in 2018 with new self-shaping processes. Since it has complex façade geometry, it is an interesting and challenging object for B-spline modeling and Terrestrial Laser Scanning (TLS) deformation analysis.

A novel method, which allows the statistically based deformation analysis using the epochal and space-continuous estimated B-spline surfaces, was developed. The surface parameters define the point correspondences on different B-spline surfaces. Using these correspondences, a RANSAC-approach is implied to estimate the parameters of the rigid body movement. The resulting consensus set initially defines the non-distorted areas of the object, which are extended and statistically verified in a second step. Distorted regions can be reliably detected and the parameters of the rigid body movement can be simultaneously determined if the appropriate stochastic model is considered. In this project, the synthetic variance-covariance matrix (SVCM) defines the stochastic model. The results show that by stochastical and B-spline surface modeling, the measurement noise is reduced and distorted regions are detectable in a statistically correct way even in mm level (Figure 7 middle & right).

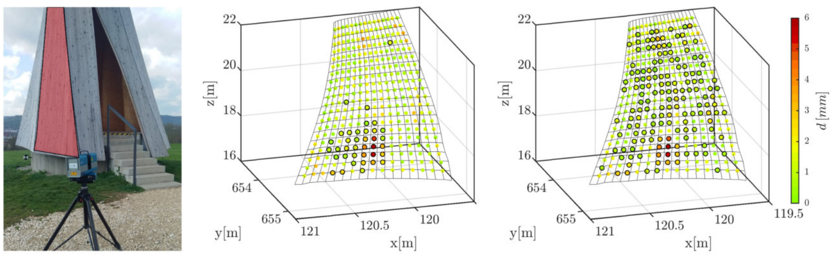

Figure 7: left: Urbach Tower façade element (red); middle: statistically identified deformation area (circled points) with fully-populated SVCM; right: falsely identified deformation areas with diagonal SVCM.

This research was funded by DFG (German Research Foundation), SCHW 838/7-3 and the Austrian Science Fund (FWF), I3869.

Studies on deformation analysis of TLS point clouds using B-splines

High-resolution point clouds of terrestrial laser scan measurements present advantages for epoch-wise comparisons of deformation analyses. However, since there are no identical points between the epoch-wise laser scans, modeling by means of B-splines offer an opportunity to superimpose the B-spline surfaces using feature-based methods and to identify deformations. Compared to current methods, the generation of the B-spline surfaces is based on a direct use of control points for the first time. In many current methods, the B-splines are generated via a control point estimation. The novel approach, in which control points are used directly, currently consists of a mapping method that ensures a superposition location of two B-spline curves based on the ranks of curvature values in combination with the determination of rank correlation functions in order to calculate coordinate differences. A stochastic model based on a variance-covariance propagation is used in parallel to this procedure and allows the performance of a significance test for each curve point to determine possible deformations.

On the basis of the developed fundamentals, this novel method is to be applied to B-spline surfaces. Here, a preparation of the control point grid structure by a knot insertion algorithm to create a uniform grid using Boehm's algorithm is necessary. A mapping algorithm to determine the superposition location of B-spline surfaces from different epochs is to be developed.

Achieving Road Boundary Detection in a Neural Network based Semantic Segmentation Pipeline

To achieve vehicle autonomy, road boundary detection is one essential component in the environment perception stack. The precise detection of the road geometry not only improves the vehicle localization, but also facilitates the motion planning task, thus the vehicle control efficiency. LiDAR sensors have been widely used for this task. Existing rule-based detection approaches still require handcrafted filters to achieve rational result. Usually, it is hard to adapt these handcrafted filters on different sensor models, and the diverse road conditions pose additional challenges to this problem. To overcome these issues, the semantic segmentation technique that is based on convolutional neural network provides another possible solution.

In the first step, the unordered 3D point cloud is converted into an efficient data representation, so that the power of convolutional neural network can be leveraged. In our experiment, both the Bird's Eye View (BEV) and Cylindrical Projection (CP) are used as the LiDAR representations. Then, a semantic segmentation neural network with the standard encoder-decoder architecture is utilized to accomplish the inference task. There exists a variety of mature network designs for semantic segmentation task, such as U-Net and ENet. With the runtime and storage efficiency in mind, the comparison of existing networks in terms of their inference performance and the computational efficiency is realized. In addition, the influence of the network size on the inference result is investigated. Finally, as the output of a semantic segmentation network, an inferred binary mask image, where pixel value 1 stands for road boundary point and 0 for background, is received. The overall pipeline can be seen in Figure 8.

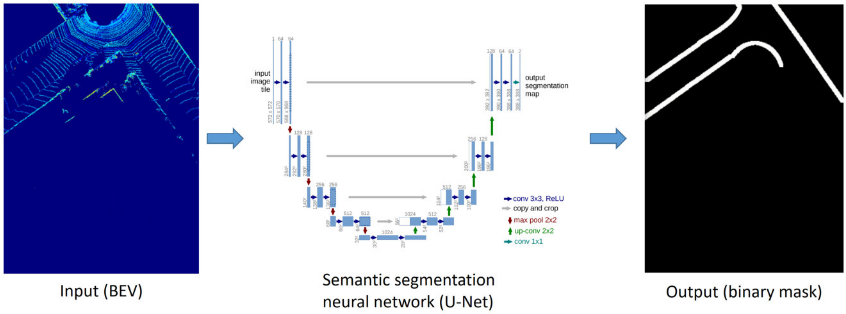

Figure 8: Overview of road boundary detection in a semantic segmentation pipeline

Dynamic Location Referencing: Probability and Fuzzy Logic Based Decision Systems

To share geoobjects between digital maps, location referencing is a well-known methodology typically used for exchanging traffic information such as traffic jams, road works etc. In some cases, there are no common databases between the systems (maps) being exchanged. For this, dynamic (on-the-fly) methods are developed to share Location References (LR, digital-map based geoobjects) between different maps in such particular cases where no common databases and/or common structures are available.

Generally, Location Referencing Methods follow a one-dimensional three-step process of encoding the LR in the sender system, transfer and decoding the LR in the receiver system without any iterations and typically limited bandwidth. Given the fact, that there are no dedicated links/common data structures between the maps, the key issue for Dynamic Location Referencing is to find the correct LR in the target map which corresponds to the LR in the source map (see Figure 9).

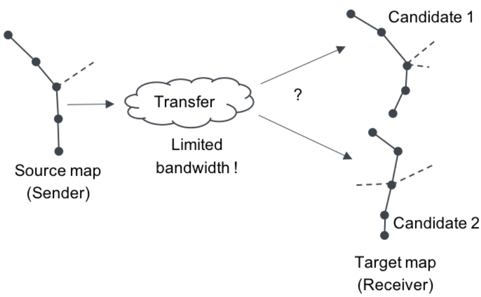

Figure 9: Identification of Location Reference

So far, deterministic algorithms have been defined and implemented. Based on the fact, that there is uncertainty in matching procedures for geodata, uncertainty-based decision systems are in process of research. That means in specific, a probability-based and a fuzzy-based approach as two different uncertainty-based concepts were specified and investigated in detail. For both, a set of decision criteria (geometrical, topological, syntactical and semantical) were defined and the decision algorithms formulated. Both approaches were implemented in an evaluation system and analyzed.

As a result, the probability-based and fuzzy-based approaches show similar results with an average hit rate up to 90% and improve the results of a comparable deterministic approach (OpenLR) in average by 12 percentage points.

As pointed out in the last report, new principles have been developed to validate the previous results and provide a broader basis. Most of these topics are done, specified and implemented in the existing evaluation system. Some first pre-tests show successful results, so the previous results are confirmed. In the course of the year this will be continued and brought to a final stage.

Ghosthunter III

The aim of the Ghosthunter III project (s. Figure 10) is to develop an app for Android smartphones that will help to reliably detect wrong-way drivers on freeways and their slip roads and warn the wrong-way drivers themselves as well as the other road users in the surroundings. This app, including the server infrastructure will be certified with regard to its functionality. The search for a future operator of the system will finalize the project. This project is carried out in cooperation with the Institute of Space Technology and Space Applications at the University of the Federal Armed Forces Munich and the company NavCert GmbH.

Supported by:

Federal Ministry for Economic Affairs and Climate Action

on the basis of a decision by the German Bundestag

Figure 10: Ghosthunter III project logo

A key component of the app is the digital map on the basis of which the map matching is performed. Since the app is to be provided free of charge, this map must be based on freely available open source data. For this purpose, a program was developed that filters the OSM (Open Street Maps) data according to its necessity for our use case and then creates an SQLite database from it. This way of storing the map information allows efficient access in the app with only a small memory footprint. Based on this database, the map matching algorithms used were adapted to ensure interoperability with them.

The Ghosthunter III research project is funded by the German Federal Ministry of Economic Affairs and Climate Action (BMWi) and the German Aerospace Center (DLR) under grant number 50 NA 2109.

The CoKLIMAx Project

The CoKLIMAx project started in November 2021. It deals with the use of COPERNICUS data for climate-relevant urban planning by the example of water, heat, and vegetation. The project consortium consists of four project partners. The project lead is with the City of Constance, supported by the Institute of Engineering Geodesy (IIGS) at the University of Stuttgart, the Constance University of Applied Sciences for Technology, Economics and Design (HTWG) Constance, and the Climate Service Center Germany (GERICS) at the Helmholtz Center Hereon.

Supported by:

Federal Ministry for Economic Affairs and Climate Action

on the basis of a decision by the German Bundestag

The use of climate date in municipal administrations is not common these days. Municipalities and their respective administrations, their specific divisions involved in city planning are increasingly interested to learn more and integrate the added value gained from climate data in their daily routines for better decision making. This is especially true because the data is now publicly available, via the Copernicus Climate Data Store. However, it remains a challenge for these administrative entities to simply use the data. This is mostly due to the lack of hardware and software, but also of expertise. Hence, it remains a challenge and it is difficult for municipal users in these administrative bodies, to identify and put the relevant data to effective use, since the sheer amount of data and its complexity must be known, understood and tackled. Having said that, it also depends very much on the available technology (e.g. hardware, software) and specific know-how available. Without the right tools or specialist expertise in place, the resource that most municipalities lack, it is about impossible to succeed and put the data to good use for better decision making. In this context it becomes clear that urban planning in cities requires rather practical tools that are easy to handle by staff. These are needed and shall help to assimilate Copernicus data with local (in situ) data, and to further process and use the results in municipal planning activities.

CoKLIMAx continues to develop new procedures and products for municipal users. A more practice-oriented approach for technical tools and applications is needed to derive and process data from some Copernicus services, and combining these with various local data. Thus, the project persists to develop an Advanced Municipal Climate Data Store toolbox (AMCDS Toolbox). The project members are currently working on the exemplary implementation, which is based on actual local needs of the city of Constance. New data products ought to be developed, implemented, applied and validated for better decision-making applications, for the respective study area and municipality.

2022, especially the first half year, was mainly dominated by continuous configuring and fine-tuning the numerous GIS Server software components of the distributed GIS Enterprise system on the CODE-DE server infrastructure. The initial setup of the installed system took place back in December 2021. After all, the GIS Enterprise system, installed on the Code-de IT infrastructure, required more attention, care and devotion as initially anticipated and planned. While the project partner from GERICS started to make use of many preinstalled applications available, the backend setup and configuration was ongoing. By the end of 2022, a myriad number of extra hours had to be invested into additional troubleshooting and system checks to make the system run smoothly. Meanwhile, ETL (extract, transform and load) processes were developed and tested to derive data from the CDS, and other sources.

In May 2022, the first consortium meeting took place in Constance. The first results were shared with colleagues from the Federal Ministry of Digital Affairs and Transport. The meeting was also a great opportunity for a dialogue with stakeholders from Constance and other participating partners form different cities, and the swords project UrbanGreenEye. In June 2022, IIGS staff and the project were invited and presented at the “National Forum for Remote Sensing and Copernicus 2022” in Berlin with the guiding slogan “Copernicus.Digital.Sustainable”. In the technical session E.1 “Designing the city of the future with Copernicus” the project titled “CoKLIMAx: Using COPERNICUS data and services for climate-resilient urban planning with municipal application potentials using the example of the city of Constance” were presented. In November 2022, the project CoKLIMAx was once again invited to Berlin, in order to present at the “10th German GeoForum”. The event is an annual networking event hosted by the German Association for Geoinformation. The slogan of the event was “Geoinformation for a sustainable future”. The forum draws together stakeholders from science, industry, government and municipal administrations. The presentation on the CoKLIMAx project was well received by the audience and the subsequent discussion made it clear that one of the biggest challenges is the consolidation of climate services within municipal administrative structures.

The CoKLIMAx research project is funded by the German Federal Ministry for Digital and Transport (BMDV) and the German Aerospace Center (DLR) as part of the “Climate Adaptation Strategies for Municipal Applications in Germany” under grant number 50EW2103C.

Advanced Automated Gap and Flush Measurement Assisted by a High Flexible and Accurate Robot System

A modular measurement system that is characterized by its hardware and software components is presented (s. Figure 11). Due to requirements, such as higher cars with more measurement points and complex surfaces (glass, chrome and painted plastic), a new sensor unit is necessary. The new sensor unit uses the ultraviolet wavelength to profit from the block layers in automobile materials. In addition, the performance of the system has been formally demonstrated through a measurement system analysis according to VDA (2021) and it is already being used in series. Furthermore, it is aimed to further flexibilize the composition of components into an overall system in order to eliminate the limitations in the implementation and adaptation of components. The modular referencing system showcased in this report is an important development in the field of measurement and positioning. It allows the use of components with significantly higher tolerances regarding their positioning accuracy (in the order of several centimeters), while still ensuring the required positional accuracy of ±4 mm of the overall system. This provides an advantage in terms of efficiency and cost savings, as components with higher tolerances can be used for the same results. Further information can be found in DVW Band 101/2022.

Figure 11: SME-SL for automated gap- and flush measurement

Multi Sensor Multi Object Tracking using the GM-PHD Filter and Sensor Models

Modern vehicles with advanced driver assistance systems (ADAS) fuse the detections of different sensors to obtain a comprehensive environment detection. This is often done by a Kalman filter, which requires data association as well as a track management to add or remove tracks. In order to eliminate error sources by the data association and the track management, filters of the random finite set (RFS) family can be used. These estimate both the states themselves and the number of states by using a random set variable. Thus, no explicit data association procedure and no direct track management is necessary. Both setups are shown schematically in the Figure 12 below.

The Gaussian Mixture Probability Hypothesis Density filter (GM-PHD) is a filter from the RFS family, which can achieve real time capability. To enable a fusion of several sensors with the GM-PHD filter, which have different field of views and different measurement properties, sensor models are developed. These model the parameters of the GM-PHD filter, such as the clutter density and the detection probability depending on the state space. The figure exemplary shows the detection probabilities' dependency of the distance in x- and y-direction.

Using the Karlsruhe Institute of Technology and Toyota Technological Institute (KITTI) data set, the performance of the Kalman filter setup is compared with that of the GM-PHD setup. Detections from camera and Lidar are fused and evaluated using the Higher Order Tracking Accuracy (HOTA) metric on the KITTI multi object tracking benchmark. The Kalman filter achieves a HOTA of 73.56%, while the GM-PHD filter achieves 77.11%, with runtime doubling in comparison.

When using modern electronic control units (ECUs) with increasing computation power, the use of RFS filters, such as the GM-PHD filter shown here, can therefore achieve improved environment perception.

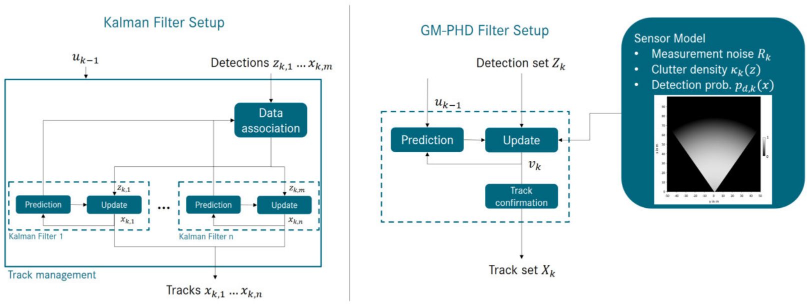

Figure 12: Comparison of Kalman filter and GM-PHD filter setup

Regional Ionosphere Model (RIM) for Single Frequency GNSS PPP Solution using Bernese GNSS Software - Case Study: Egyptian Nile Delta

Egypt is quickly constructing many infrastructures such as roadways and railways. Due to the spare coverage of the international GNSS service (IGS) network in North Africa, in January 2012, the Egyptian surveying authority (ESA) established the first permanent Egyptian continuously operating reference stations (CORS) network. This network is covering the Nile valley and its delta. In this study, a developed regional ionosphere model (RIM) is

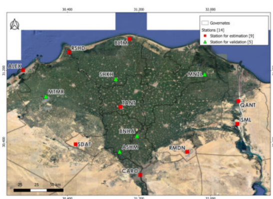

modeled for obtaining a single-frequency precise point positioning (SF-PPP) solution for the Nile delta. This solution is compared with the solution obtained using the Global Ionosphere model (GIM). A data set of six consecutive days 202-207/2019 of the ESA-CORS permanent stations was involved in the study. Nine stations were considered for RIM estimation and five stations are used for model validation. Bernese GNSS V. 5.2 software is used to model the regional ionosphere by using a geometry-free linear combination for code observation data (P4) Bernese GNSS v. 5.2 software developed at the Astronomical Institute of the University of Bern (AIUB), Switzerland is used to model the regional ionosphere and estimate the SFPPP solution.

The estimated accuracy of the SF-PPP solution using the modeled RIM model shows an average error for all stations of 0.06 m - 0.07 m (SD = 0.06 m - 0.07 m) in the east direction. For the north, the solution displays an approximate average error of 0.1 m (SD = 0.03 m - 0.04 m). Based on the results presented in this table, the height average error shows approximately 0.3 m (SD = 0.05 m - 0.10 m). Generally, the SF-PPP solution using the RIM model shows an average 2D accuracy of 0.13 m and a height of 0.30 m. In addition, the solution provides an average 3D accuracy of 0.33 m. Overall, these results indicate that the solution obtained by using the RIM model is better than the one from the CODE-GIM model. The solution is improved by 60%, 70%, and 67% in east, north, and height, respectively. This shows the benefit of using a regional rather than a global ionosphere model.

PhD Seminar

The 12th Doctoral Seminar of the Engineering Geodesy Section of DGK was organized by the Institute of Geo-Engineering at the Technical University Clausthal. The DGK PhD Seminar of the Engineering Geodesy Section was organized as a live event. It took place from October 6 to 7, 2022 at the Aula Academia in Clausthal. A total of 11 presentations mirrored the work of PhD candidates from Austria, Poland, and Germany. From the IIGS Laura Balangé and Yihui Yang presented their results. Fruitful discussions among the approximately 60 participants were possible during the coffee breaks and at the evening at the well-organized get-together including locally brewed beverages.

Publications

Refereed Publications

Abdallah, A., Agag, T., & Schwieger, V. (2022): Validation of CODE-GIM and Regional Ionosphere Model (RIM) for Single Frequency GNSS PPP Solution using Bernese GNSS software- Case Study, Egyptian Nile Delta. XXVII FIG Congress 2022, Warsaw, Poland. https://www.fig.net/resources/proceedings/fig_proceedings/fig2022/papers/ts08c/TS08C_abdallah_tarek_et_al_11375_abs.pdf

Aichinger, J., & Schwieger, V. (2022): Studies on deformation analysis of TLS point clouds using B-splines - A control point based approach (Part I). Journal of Applied Geodesy, 16(3), 279–298. https://doi.org/doi:10.1515/jag-2021-0065

Balangé, L., Harmening, C., Duque Estrada, R., Menges, A., Neuner, H., & Schwieger, V. (2022): Monitoring the production process of lightweight fibrous structures using terrestrial laser scanning. 5th Joint International Symposium on Deformation Monitoring, Valencia, Spain. https://doi.org/10.4995/JISDM2022.2022.13830

Frost, D., Gericke, O., Di Bari, R., Balangé, L., Zhang, L., Blagojevic, B., Nigl, D., Haag, P., Blandini, L., Jünger, H. C., Kropp, C., Leistner, P., Sawodny, O., Schwieger, V., & Sobek, W. (2022): Holistic Quality Model and Assessment - Supporting Decision-Making towards Sustainable Construction Using the Design and Production of Graded Concrete Components as an Example. Sustainability, 14(18), Article 18. https://doi.org/10.3390/su141811269

Gil-Pérez, M., Zechmeister, C., Kannenberg, F., Mindermann, P., Balangé, L., Guo, Y., Hügle, S., Gienger, A., Forster, D., Bischoff, M., Tarín, C., Middendorf, P., Schwieger, V., Gresser, G. T., Menges, A., & Knippers, J. (2022): Computational co-design framework for coreless wound fibre-polymer composite structures. Journal of Computational Design and Engineering, 9(2), 310–329. https://doi.org/10.1093/jcde/qwab081

Hassan, A., Zhang, L., Kerekes, G., & Schwieger, V. (2022): Geodetic Data Fusion for Rock Cliff Monitoring: A Case Study of the Lianzi Cliff in Three Gorges National Geological Park in China. XXVII FIG Congress 2022, Warsaw, Poland. https://fig.net/resources/proceedings/fig_proceedings/fig2022/papers/ts04d/TS04D_hassan_zhang_et_al_11340.pdf

Kerekes, G., Petrš, J., Schwieger, V., & Dahy, H. (2022): Geometric quality control for bio-based building elements: Study case segmented experimental shell. Journal of Applied Geodesy. https://doi.org/doi:10.1515/jag-2020-0035

Kerekes, G., Jakob, R., Harmening, C., Neuner, H., & Schwieger, V. (2022): Two-epoch TLS deformation analysis of a double curved wooden structure using approximating B-spline surfaces and fully-populated synthetic covariance matrices. 5th Joint International Symposium on Deformation Monitoring (JISDM), 20-22 April 2022, Valencia, Spain. http://ocs.editorial.upv.es/index.php/JISDM/JISDM2022/paper/viewFile/13816/7605

Yang, Y. & Schwieger, V. (2022): Supervoxel-based targetless registration and identification of stable areas for deformed point clouds. Journal of Applied Geodesy. https://doi.org/10.1515/jag-2022-0031

Non-Refereed Publications

Balangé, L., Zhang, L. & Schwieger, V. (2022): Qualitätssicherung im Rahmen des Exzellenzclusters IntCDC. 208. DVW-Seminar: Qualitätssicherung geodätischer Mess- und Auswerteverfahren, Berlin 2022, 2.-3.Juni.

Luz, P., Metzner, M., Mendes, P., Stapelfeld, M., Lichtenberger, C., Pany, T., Grzebellus, M. & Schwieger, V. (2022): Ghosthunter III - Detection of wrong-way drivers. XXVII FIG Congress 2022, Warsaw, Poland. https://www.fig.net/resources/proceedings/fig_proceedings/fig2022/papers/ts07c/TS07C_luz_pany_et_al_11527.pdf

Schröder, T. & Schwieger, V. (2022): Qualitätssicherungssystem zur automatisierten Spalt- und Übergangsmessung am Ende einer Produktionslinie. 208. DVW-Seminar „Qualitätssicherung geodätischer Mess- und Auswerteverfahren 2022“ 2.-3. Juni, Berlin.

Schwieger, V., Zhang, L., Lerke, O. & Balangé, L. (2022): The Research Cluster Integrative Computational Design and Construction (IntCDC) - Current Engineering Geodetic Contribution. XXVII FIG Congress 2022, Warsaw, Poland.

Wieser, A., Balangé, L., Bauer, P., Gehrmann, T., Hartmann, J., Holst, C., Jost, B., Kuhlmann, H., Lienhart, W., Maboudi, M., Mawas, K., Medic, T., Paffenholz, J.-A., Florian, P., Rafeld, E., Schill, F. & Schwieger, V. (2022): Erfahrungen aus einem koordinierten Vergleich aktueller Scanner. Beiträge zum 214. DVW-Seminar: Terrestrisches Laserscanning 2022, Fulda, 8.- 9. Dez., TLS 2022. https://geodaesie.info/sr/terrestrisches-laserscanning-2022-tls-2022/8860/4870

Presentations

Balangé, L., Di Bari, R., & Hos, P. D.: RP18: Holistic Quality Model for IntCDC Building Systems, IntCDC Research Network Colloquium 2021, 24.02.2022

Balangé, L: Technical Quality Modeling within IntCDC, RP18 Workshop Hirsau, 06.09.2022

Balangé, L.: Quality modeling and assurance concept for coreless filament winding, DGK PhD-Seminar Clausthal-Zellerfeld, 06.10.2022

Balangé, L., Di Bari, R. & Hos, P. D.: RP18: Holistic Quality Model, Status Seminar 2022 Bad Boll, 17.11.2022

Bühler, M., Sebald, C., Rechid, D., Baier, E., Michalski, A., Rothstein, B., Metzner, M., Schwieger, V., Harrs, J.A., Jacob, D., Panhuis, G., Rodríguez, R.C., Reinhart, V. & Scheffczyk, K.: Climate-resilient urban planning through the development of climate data integration strategies and tools based on information from the Copernicus Climate Data Store in the city of Constance, Germany, Poster Session at the European Space Agency (ESA) - Living Planet Symposium 2022, World Conference Center, Bonn, Germany, 23-27 May 2022.

Göbel, M., Schlopschnat, C., Treml, S., Yang, X., Gienger, A. Lauer, A., Abolhasani, S., Zhang, L., Balangé, L., Skoury, L. & Wood, D.: livMatS Biomimetic Shell Co-Design and Construction of an innovative segmented timber shell building, Status Seminar 2022 Bad Boll, 17.11.2022

Lauer, A., Lerke, O. & Gong, Y.: Robotic Platform for Cyber-Physical Assembly of Long-Span Fibre-Composite Structures, IntCDC Research Network Colloquium 2022, 24.02.2022

Lauer, A., Gorokhova, L. & Gong, Y.: Cyber-Physical On-Site Construction Processes Using a Spider Crane Robotic Platform, IntCDC Status Seminar 2023, 03.03.2023

Reinhart, V., Sebald, C., Vögt, V.: Das CoKLIMAx Projekt: Nutzung von Copernicus-Daten und Diensten für die klimaresiliente Stadtplanung mit kommunalen Anwendungspotentialen am Beispiel der Stadt Constance, Vortragsreihe "Fernerkundung / Copernicus für kommunale Anwendungen", 10. Deutsches GeoForum, Berlin, 23.-24.11.2022

Schwieger; V.: Quality in Engineering Geodesy - an introduction to the topic and to the workshop. Scientific Workshop on Uncertainty and Quality of Multi-Sensor Systems, FIG Congress 2022, Warsaw, 10.09.2022.

Schwieger, V.: Vorstellung der Abteilung Ingenieurgeodäsie, Jahressitzung des Ausschusses Geodäsie (DGK), Innsbruck, 21.09.2022.

Schwieger, V.: Vorarbeiten zur Entwicklung eines Gleisfehlerdetektionssystems mit Regelzügen und Low-Cost Sensorik, Hamburg, 213. DVW Seminar "MST 2022 - Multisensortechnologie: Von (A)nwendungen bis (Z)ukunftstechnologien Mulitsensorsysteme", 26.09.2022.

Schwieger, V.: Quality Control for Graded Concrete. IntCDC Conference 2022, Integrative Computational Design and Construction for Future Proof Architecture, Stuttgart, 12.10.2022.

Schwieger, V.: Map Matching Applications. Seminar SE 3.05 "GPS/INS-Integration und Multisensor-Navigation", Carl-Cranz-Gesellschaft e.V., Oberpfaffenhofen, 10.11.2022.

Sebald, C., Tewes, T.: CoKLIMAx - Nutzung von Copernicus-Daten und -Diensten für die klimaresiliente Stadtplanung mit kommunalen Anwendungspotentialen am Beispiel der Stadt Constance, Nationales Forum für Fernerkundung und Copernicus 2022, Berlin, 21.-23.06.2022.

Yang, Y.: Towards better targetless registration and deformation analysis of TLS point clouds using patch-based segmentation, DGK PhD-Seminar Clausthal-Zellerfeld, 07.10.2022.

Yang, Y. & Schwieger, V.: Supervoxel-based targetless registration and identification of stable areas for deformed point clouds. 5th Joint International Symposium on Deformation Monitoring (JISDM 2022), Valencia, Spain, 22.06.2022.

Activities at the University and in National and International Organizations

Volker Schwieger

Full member of the German Geodetic Commission (Deutsche Geodätische Kommission - DGK)
Head of the section "Engineering Geodesy" within the German Geodetic Commission (DGK)
Chief Editor of Peer Review Processes for FIG Working Weeks and Congresses
Member of the Editorial Board "Journal of Applied Geodesy"
Member of the Editorial Board "Journal of Applied Engineering Science"
Member of the Editorial Board "Journal of Geodesy and Geoinformation"

Martin Metzner

Member of the NA 005-03-01 AA "Geodäsie" at the DIN German Institute for Standardization
Course Director of the MSc Program GeoEngine at the University of Stuttgart

Li Zhang

Co-Chair of the Working Group 5.6 "Cost Effective Positioning" within the FIG Commission 5 (Positioning and Measurement)
Chair of the Working Group "Quality Assurance" within the Commission 3 "Measurement Methods and Systems" of "Deutscher Verein für Vermessungswesen (DVW)"

Master Theses

Dalloul, Ahmed: 3D model generation through autonomous scanning for infrastructure facilities. (Kerekes/Basalla, Schwieger)

Frolow, Rudolf: Entwicklung eines grid-basierten Map-Matching Algorithmus zur Anwendung auf spurgenauen Karten

Li, Zhan: Investigation of different approaches to tiling and memory management of map data for processing in map-matching. (Luz/Metzner)

Miehling, Ronja: Entwicklung und Evaluierung eines Algorithmus zur Liniensegmentierung aus Punktwolken für Faserverbundsysteme. (Balangé/Schwieger)

Yu, Huang: Investigation of the accuracy in the creation of 3D models using UAV. (Luz/Metzner)

Bachelor Theses

Airouta, Salam: Untersuchungen von Materialeigenschaften verschiedener Betonmischungen und Fertigungsmaterialien auf die Messgenauigkeit. (Balangé/Zhang)

Kassulat, Tim: Entwicklung und Evaluierung verschiedener Methoden zur Querschnittsflächenberechnung einzelner Fasern aus Faserverbundsystembauteilen. (Balangé/Schwieger)

Kunzi, Christian: Untersuchung der Registrierungsgenauigkeit bei Punktwolken am Beispiel des Turms an der Birke. (Gorokhova/Schwieger)

Speidel, Pauline: Evaluierung von unterschiedlichen Verfahren zur Bestimmung der Pose eines Bauroboters mittels eines RTS Netzwerks (Lerke/Schwieger)

Education

SS22 and WS22/23 with Lecture/Exercise/Practical Work/Seminar

Bachelor Geodesy and Geoinformatics (German)

Basic Geodetic Field Work (Kanzler)	0/0/5 days/0
Engineering Geodesy I (Schwieger, Abolhasani, Kerekes)	4/2/0/0
Engineering Geodesy II (Schwieger, Gorokhova)	1/1/0/0
Geodetic Measurement Techniques I (Metzner, Frolow)	3/1/0/0
Geodetic Measurement Techniques II (Haußmann/Kanzler/Frolow)	0/1/0/0
Integrated Field Work (Kerekes, Metzner)	0/0/10 days/0
Reorganisation of Rural Regions (Stadler)	1/0/0/0
Statistics and Error Theory (Schwieger, Balangé)	2/2/0/0

Master Geodesy and Geoinformatics (German)

Industrial Metrology (Schwieger, Gorokhova)	1/1/0/0
Land Development (Eisenmann)	1/0/0/0
Monitoring Measurements (Schwieger, Kerekes)	1/1/0/0
Terrestrial Multisensor Systems (Zhang, Frolow)	2/1/0/0
Geomobility (Zhang, Luz)	2/2/0/0
Projekt Geodäsie und Geoinformatik (Schwieger, Zhang, Abolhasani, Gorokhova)	0/0/0/6

Master GeoEngine (English)

Kinematic Measurement Systems (Schwieger, Basalla)	2/2/0/0
Monitoring (Schwieger, Balangé)	1/1/0/0
Thematic Cartography (Zhang, Frolow)	1/1/0/0
Transport Telematics (Metzner, Sebald)	2/1/0/0
Terrestrial Multisensor Systems (Zhang, Luz)	2/1/0/0

Bachelor and Master Aerospace Engineering (German)

Statistics for Aerospace Engineers (Zhang, Abolhasani)	1/1/0/0

Master Aerospace Engineering (German)

Industrial Metrology (Schwieger, Gorokhova)	1/1/0/0
Transport Telematics (Zhang, Luz)	2/2/0/0

Bachelor Civil Engineering (German)

Geodesy in Civil Engineering (Metzner, Luz, Kanzler)	2/2/0/0

Master Civil Engineering (German)

Geoinformation Systems (Metzner, Sebald)	2/1/0/0
Transport Telematics (Zhang, Luz)	2/1/0/0

Bachelor Technique and Economy of Real Estate (German)

Acquisition and Management of Planning Data and Statistics (Metzner, Sebald, Kanzler)	2/2/0/0

Bachelor Transport Engineering (German)

Statistics (Metzner, Zhang, Kanzler)	0.5/0.5/0/0
Seminar Introduction in Transport Engineering (Gorokhova)	0/0/0/1

Master Infrastructure Planning (English)

GIS-based Data Acquisition (Zhang, Sebald, Kanzler)	1/1/0/0

Institute of Geodesy

Geschwister-Scholl-Str. 24D
70174 Stuttgart
+49 711 685 83390
gis@gis.uni-stuttgart.de
www.gis.uni-stuttgart.de

Institute Management

Prof. Dr.-Ing. Nico Sneeuw	Head, Chair of Geodesy
Prof. Dr. James Foster	Chair of Space Geodetic Methods
Dr.-Ing. Mohammad Tourian	Senior Scientist, Satellite Geodesy

Retired

Prof. Dr. sc. techn. Wolfgang Keller

Academic Staff

Dr.-Ing. Markus Antoni	Physical Geodesy, Satellite Geodesy
M.Sc. Clara Bützler	Physical Geodesy, Seismology
Dr.-Ing. Jianqing Cai	Satellite Geodesy, Adjustment Theory
Dr. Karim Douch	Physical Geodesy, Seismology
Dr.-Ing. Omid Elmi	Remote Sensing
PD Dr.-Ing. habil. Johannes Engels	Physical Geodesy, Satellite Geodesy
M.Sc. Bruce Thomas	Physical Geodesy, Satellite Geodesy
Ph.D. Rudolf Widmer-Schnidrig	Physical Geodesy, Seismology

Research Associates

M.Sc. Sajedeh Behnia	Satellite Altimetry
M.Sc. Siqi Ke	Hydrology
M.Sc. Peyman Saemian	Satellite Geodesy, Hydrology
M.Sc. Bo Wang	Satellite Altimetry

Administrative/Technical Staff

B.A. Tamara De Francesco	Secretary
Dipl.-Ing. (FH) Thomas Götz	IT, Controlling
Dipl.-Ing. (FH) Ron Schlesinger	IT, Technical Support, Gravimetry

External Lecturers

Dipl.-Ing. Gerhard Grams	Ministerium für Ländlichen Raum und Verbraucherschutz Baden-Württemberg, Stuttgart
Dipl.-Ing. Dieter Heß	Ministerium für Ländlichen Raum und Verbraucherschutz Baden-Württemberg, Stuttgart

Guests

M.Sc. Lang Li	Tongji University, China, DAAD Fellow (01.11.2021–31.10.2022)
Assoc. Prof. Yi Lin	Tongji University, China (15.11.2021–15.07.2022)
Prof. Péter Varga	Institute of Earth Physics and Space Science, Hungary, Humboldt Fellow (07.04.2022–30.06.2022)
Dr. Yixiati Dilixiati	since June 2022
Tasnîme Louartani	ENSG Geomatics, France (23.05.2022–12.08.2022)

Research

Systematic errors of superconducting gravimeters

Clara Bützler

The value of gravity of about $9.81\,\mathrm{m/s^2}$ is not constant, neither in space nor in time. While the biggest spatial differences occur between the equator ($9.78\,\mathrm{m/s^2}$) and the poles ($9.83\,\mathrm{m/s^2}$) changes in time are much smaller. The biggest contribution are daily, half-daily and monthly tidal signals originating from the changing gravitational attraction from sun and moon. They reach up to $2\,\mathrm{\mu m/s^2}$. The second-biggest contribution are air pressure changes in the atmosphere above the gravimeter. They can produce gravity changes of about $150\,\mathrm{nm/s^2}$. If we correct these two contributions from gravity time series measured with superconducting gravimeters, long term gravity changes at the level of some tens of $\mathrm{nm/s^2}$ become visible. Two examples are gravity variations due to polar motion and gravity changes due to local hydrology. As these signals are on the edge of the accuracy of today's best gravimeters, knowing the error budget of the instruments is very important when studying these signals.

Figure 1: **Superconducting gravimeter SG056 at BFO**

The axis of rotation is not fixed inside the Earth, but slightly moving. The two main periods of this movement are one year and 430 days. This so-called polar motion influences gravity by two mechanisms. If the pole moves away from us first the centrifugal acceleration increases, which leads to a decrease of gravity. Secondly, the Earth deforms due to the change in centrifugal acceleration, which moves the gravimeter slightly away from the center of mass of the Earth. That again leads to a decrease of gravity. The second effect is about ten times smaller than the first one. However, if we accurately measure this second effect, we know how the Earth deformed due to the change in centrifugal acceleration. By this we could learn more about the viscosity of the mantle. In Figure 2 one can see a time series of gravity measured with the superconducting gravimeter SG056 at the Black Forest observatory (BFO). Additionally, the varying distance of the gravimeter to the rotation axis of the Earth is shown.

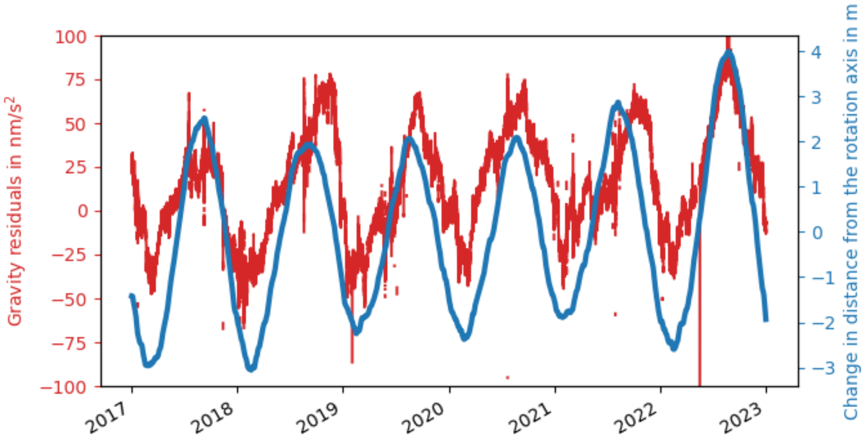

Figure 2: **Gravity and polar motion.** Gravity residuals at BFO are shown together with the variation in distance of the gravimeter to rotation axis of the Earth. The gravity signal was corrected for tides and air pressure variations, and major instrumental disturbances like linear drift and steps.

Local hydrology also influences gravity. In Figure 3 one can see gravity at BFO together with the monthly amount of rain. It can be seen, that gravity gets smaller in rainy periods. By combining gravity measurements with other measurements, like rainfall and soil moisture, we may learn more about the local hydrology.

Due to their low drift and good long term stability, superconducting gravimeters are used to study long term changes of gravity. They can measure gravity changes in time. In Figure 1 one can see a picture of the superconducting gravimeter at BFO. However, also superconducting gravimeters show systematical measurement errors. Dual sphere superconducting gravimeters offer one possibility to study them. These are instruments which have two sensing units. That means they are measuring gravity twice inside the instrument. In Figure 4 one can see the difference between the signals of the two sensors of SG056. For a perfect instrument they should be constant. However, even after removing a linear drift and major steps related to operator interventions, this difference still shows variations at the level of half the amplitude of the gravity residuals themselves. This means we have to be aware of these errors whenever studying long term gravity changes at the ten $\mathrm{nm/s^2}$ level.

At GIS and BFO we work on quantifying and characterizing these systematic errors and studying their influence on studies of long term gravity variations related to polar motion or hydrology.

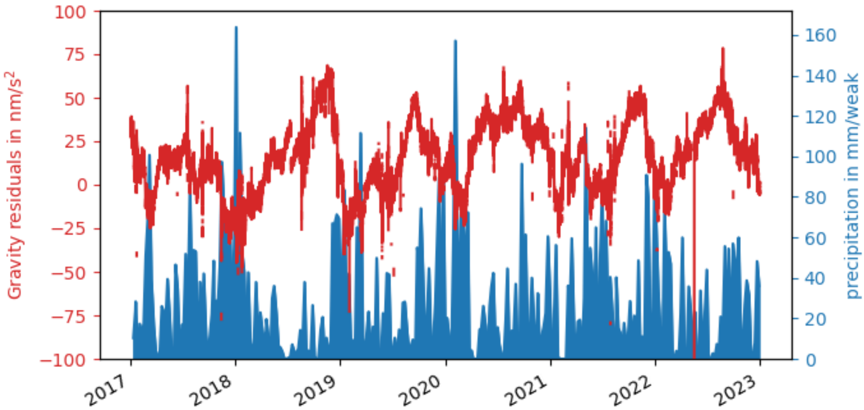

Figure 3: **Gravity and hydrology.** The figure shows gravity residuals and weakly amounts of rain at BFO. The gravity signal is the same as in Figure 2 but additionally corrected for polar motion

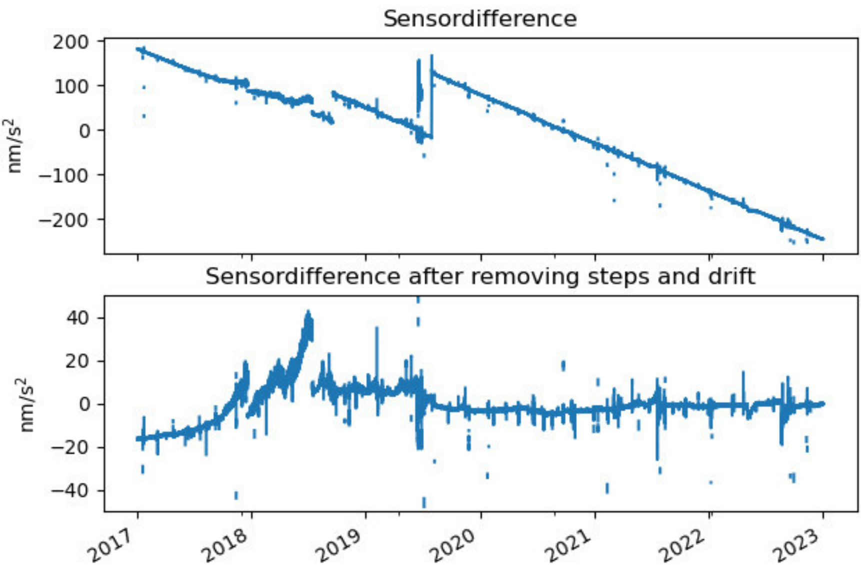

Figure 4: **Sensor difference of the gravimeter SG056 at BFO.** In the top panel the difference between the results of the two measurement units of the gravimeter SG056 at BFO are shown. In the lower panel major steps and drift were removed from the difference.

How seismometers tilt in response to atmospheric pressure—earthly lessons learned from Hunga Tonga and what they might mean for Mars

Rudolf Widmer-Schnidrig

This activity report summarizes a talk presented at the 25th InSight science team meeting in London in November 2022 and was co-authored by my colleagues at the Black Forest Observatory (BFO): Thomas Forbriger and Walter Zürn. The Hunga-Tonga volcano erupted in January 2022 and radiated energy in the atmosphere, the oceans and the solid Earth. A number of signals could be observed with unprecedented signal-to-noise ratio: seismic free oscillations of the solid Earth, meteo tsunamis in the oceans, globe circling Lamb waves in the atmosphere, to mention just a few. In this contribution we focus on the Lamb waves recorded by barometers and broad-band seismometers of the Global Seismic Network (GSN). With a phase velocity of approx. 315 m/s the Lamb wave was the fastest pressure signal propagating in the atmosphere with a dominant signal period of around 45 minutes. Except near the source, peak-to-peak amplitudes for the direct wave was typically 2–3 hPa.

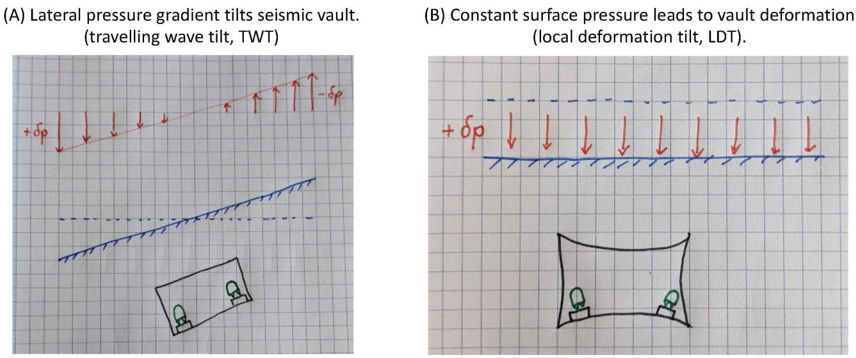

Figure 5: Cartoons of the two considered mechanisms which can tilt a seismometer: (A) a regional pressure gradient possibly from a travelling atmospheric pressure wave (hence travelling wave tilt or TWT) and (B) an illustration of the cavity effect: a warping of the vault floor due to an applied surface pressure.

Based on previous work (Zürn et al., GJI, 2021) we expect that the response of horizontal component seismometers at these long periods is dominated by tilts due to two distinct physical mechanisms: (A) tilt due to the local deformation of the vault in which the accelerometer is installed: e.g. warping of the vault floor in response to an atmospheric pressure change. We refer to this as local deformation tilt, LDT. (B) a regional tilt due to a lateral pressure gradient along the surface above the seismic vault. We call this travelling wave tilt, TWT. This nomenclature derives from the fact that for an elastic medium the tilt of the vault follows the free surface, and together they tilt in the direction of the surface pressure gradient (Figure 5). While LDT is in phase with the locally recorded atmospheric pressure change, the TWT is 90 degrees out of phase. Thus LDT is proportional to the pressure, p(t), while TWT is proportional to its Hilbert transform, H(p(t)). These two signals are linearly independent and in a regression where scaled versions of the two signals are sought to match the horizontal accelerograms one can separate the contributions of the two tilt mechanisms. The estimated TWT scale factors for the two horizontal components can be vectorially added and the resulting vector should align with the back-azimuth to Hunga Tonga. (Figure 6).

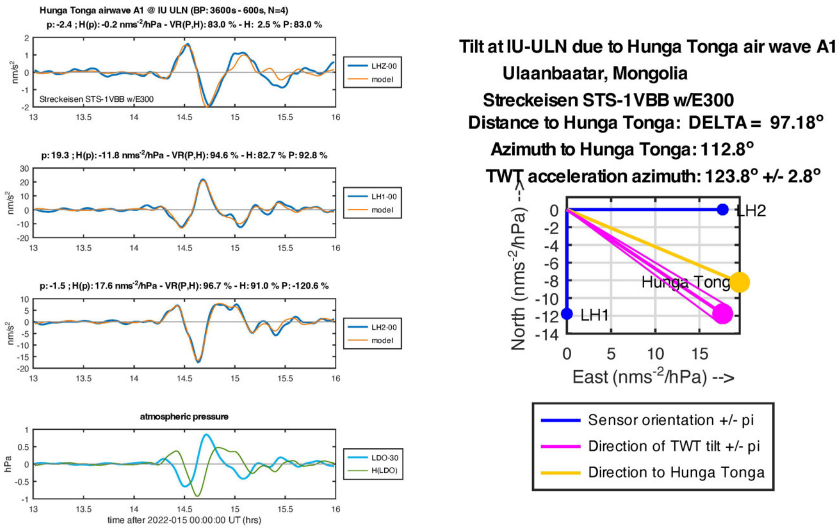

Figure 6: Example of the signal analysis for the station ULN (Ulanbatar, Mongolia). On the left the recordings of the direct Lamb wave A_1 are shown, recorded by the three seismometer components and the barometer (bottom panel). All three seismometer recordings can be well modelled by a linear combination of the barometric pressure and its Hilbert transform. The respective regression coefficients are given in the header of each panel. On the right is a map view of the station with the direction to Hunga Tonga (orange) and the direction of the estimated TWT seismometer tilt together with its 1 σ uncertainty (magenta). Here the seismometer tilts in the assumed direction of propagation of the Lamb wave, consistent with the TWT model.

We have inspected all the recordings by the Global Seismic Networks GSN and GEOSCOPE of the Hunga Tonga Lamb wave and only retained 21 stations with clean signals on all baro- and seismograms. 18 of these stations are also equipped with a secondary broad-band sensor for redundancy. Thanks to the secondary sensors, instrumental anomalies could be identified at 5 stations: ALE, TAU, FFC, KMBO, WCI. For any 3-component sensor the tilt due to vault deformation (LDT) points in a fixed, sensor specific direction independent of the Lamb wave propagation direction. This is in agreement with the vault deformation model. We find that LDT is larger than TWT at 80 % of retained GSN stations. While accelerations can be well modeled in most cases, pressure gradient induced ground tilts point towards Hunga Tonga for only seven stations: BFO, ESK, KAPI, WRAB, WVT, ULN, INCN.

Currently we lack any model which would allow us to explain the majority of the observed TWT tilt directions of the Hunga-Tonga Lamb wave as we do not think that Lamb wave front deformations due to wind or temperature variations in the atmosphere can account for the observed tilt misalignments.

For the analysis of observed atmospheric pressure drops and simultaneous seismometer tilts caused by the passage of dust devils near the lander of the NASA InSight mission to Mars the above findings will lead to a critical reevaluation of our models to interpret the observed seismometer tilt directions: so far in all studies the possibility of local deformation tilt due to, for example, heterogeneities in the regolith underneath the seismometer feet has been completely ignored.

Ability of a cargo-ship GNSS network to detect tsunamis

Bruce Thomas, Tasnîme Louartani, James Foster

Many of the most devastating natural hazards that impact our communities are generated over, or under, the oceans. The recent Tonga volcano eruption caused an unexpected tsunami that was poorly monitored, demonstrating the urgent need for more densely spaced observations and direct measurements from the areas between the source region and the communities that may be impacted – that is, across the oceans. Most of the existing observing capacity is located on land, close to the shore, or only sparse (seismic network, land-based GNSS, tide-gauges and DART array), limiting our ability to predict, detect and respond to these hazards. To fill the *geodetic desert* in the oceans and improve hazard mitigations, we propose the development of a network of ships with geodetic GNSS systems tracking changes in sea-surface height, that are able to detect even small amplitude tsunamis (~ 10 cm).

Using one year of navigation data from the commercial shipping fleet, we generated several statistical coverage maps of large ships for different epoch in the Pacific region. By overlapping these maps with tsunami source regions, we demonstrate that commercial shipping lines provide excellent temporal and spatial coverage of the ocean globally and, critically for local and regional early warning, are at their most dense near coastlines. More results, based on running tsunami models and analyzing predicted amplitudes, describe some first insights into how this proposed cargo-ship network might experience tsunamis, exploring the geographic relationship between tsunami sources, ships locations, and the ship network's detection of the hazard.

20 years of ground deformation patterns along Koa’e fault zone on Kīlauea volcano

Bruce Thomas, James Foster

Extreme long-term extensions are experienced along the Koa’e fault zone, a structural link between the East Rift zone and the Southwest Rift Zone on Kīlauea volcano. Both tectonic motions of the south flank of the volcano, as well as magma storage and transport at the summit and along the rift zones create stresses and ground motion patterns across this fault zone. To assess the role of Koa’e structure in these processes, and its contribution to hazard potential, this study investigates 20 years of survey GNSS data along a benchmark line running from south of Kīlauea’s caldera through the Koa’e fault zone. This survey was realized by Bruce Thomas with the help of James Foster and Jon Avery (University of Hawai’i) in 2017, late 2021 and late 2022 (Figure 7). We would also like to acknowledge the contribution during this project of Andi Ellis and David Phillips from the Hawaiian Volcano Observatory, as well as the help given by the Hawai’i Volcanoes National Park.

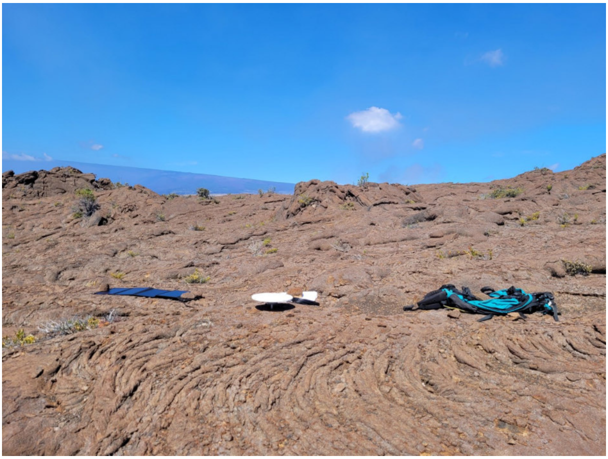

Figure 7: Fieldwork in progress on Kīlauea volcano.

First results of the deformation data capture trends of inflation/deflation from the summit magma chambers during eruptive events, as well as transient local signals from both tectonic and magmatic processes, highlighting the complexity of the volcanotectonic processes active in and around the Koa’e fault zone. Mapping the cumulative displacement over the last 20 years captures the response to the constant southeast seaward slip of the south flank which results in earthquake swarms, open fractures, intrusion of magma through shallow paths and the possible risk of eruptive fissures. This dataset is being used to guide numerical models of the kinematic deformation of this area.

A fast and low-cost method for evaluating population and infrastructure exposed to natural hazards

Bruce Thomas

Coastal communities are highly exposed to ocean-related hazards but often lack an accurate population and infrastructure database. On January 15, 2022 and for many days thereafter, the Kingdom of Tonga was cut off from the rest of the world by a destructive tsunami associated with the Hunga Tonga Hunga Ha'apai volcanic eruption. This situation was made worse by COVID-19-related lockdowns and no precise idea of the magnitude and pattern of destruction incurred.

The occurrence of such events in remote island communities highlights the need for (1) precisely knowing the distribution of buildings, and (2) evaluating what proportion of those would be vulnerable to a tsunami. A GIS-based dasymetric mapping method, previously tested in New Caledonia for assessing and calibrating population distribution at high resolution, is improved and implemented in less than a day to jointly map population clusters and critical elevation contours based on runup scenarios, and is tested against destruction patterns independently recorded in Tonga after the two recent tsunamis of 2009 and 2022 (Figure 8). This project is the result of an active contribution with Jean Roger (GNS Science), Yanni Gunnell (University Lumière Lyon 2), and Salman Ashraf (GNS Science).

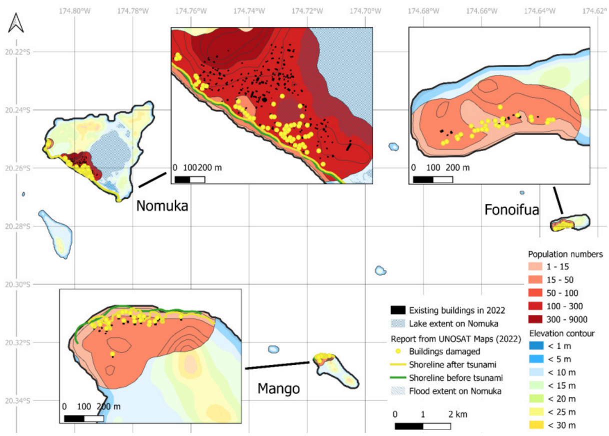

Figure 8: Overview of buildings damaged by the 2022 tsunami on Nomuka, Mango and Fonoifua islands.

Results show that 62 % of the population of Tonga lives in well-defined clusters between sea level and the 15 m elevation contour. The patterns of vulnerability thus obtained for each island of the archipelago allow exposure and potential for cumulative damage to be ranked as a function of tsunami magnitude and source area. By relying on low-cost tools and incomplete datasets for rapid implementation in the context of natural disasters, this approach works for all types of natural hazards, is easily transferable to other insular settings, can assist in guiding emergency rescue targets, and can help to elaborate future land-use planning priorities for disaster risk reduction purposes.

Recovering seafloor geodetic networks with GEOMAR team on board of RV Sonne

Bruce Thomas

The main objective of the COMBO project was the recovery of three seafloor geodetic networks of the GeoSEA array which were installed on the continental margin and outer rise offshore Iquique in northern Chile during RV SONNE cruise SO244 (Figure 9). Bruce Thomas was an invited guest on board in an international team led by Prof. Dr. Heidrun Kopp and Dr. Dietrich Lange.

Figure 9: Recovery of one tripod on board of RV Sonne.

The three seafloor geodetic networks measure the change in the position of a set of points as a function of time (the displacement due to an earthquake), thus identifying *deformation hotspots* on the seafloor, which then need to be linked to defined geological features. This requires high-frequency seismic profiling to complement the punctual observations of the mm- to cm-scale displacement achieved through the geodetic surveying. This work is flanked by seismic surveys to have more info on subsurface structures, using high resolution multichannel profiling with GI-guns and a $175\,\mathrm{m}$ long streamer. Information on the seismic velocity structure and thus on the structure of the bedrock is obtained from wide angle seismic surveying employing ocean bottom seismometers (OBS).

Data-driven identification of reduced-order rainfall-runoff models from GRACE and in-situ data

Karim Douch

By mapping on a regular basis the time-variable gravity field of the Earth, GRACE and now GRACE Follow-On permit to monitor variations of Terrestrial Water Storage (TWS) at a regional scale. In the case of large drainage basins, previous studies have shown that the time evolution of TWS and discharge at the basin's outlet can clearly reveal the underlying global drainage dynamics. We further develop this observation for specific catchments where linear models in the form of differential equations can reasonably well approximate the TWS-discharge relationship. The identification of such continuous-time models from discrete data, although challenging, allows part of the model parameters to be interpreted physically (e.g. time constant, damping ratio) and therefore gives new insight into the dynamics. One important parameter of the TWS-discharge model is the temporal mean of the total drainable water storage, which represents the total volume of water dynamically connected to the drainage system in the catchment. For instance, we estimate it to be $1925\,\mathrm{km}^3$ for the catchment upstream Óbidos, covering almost 80 % of the whole Amazon basin.

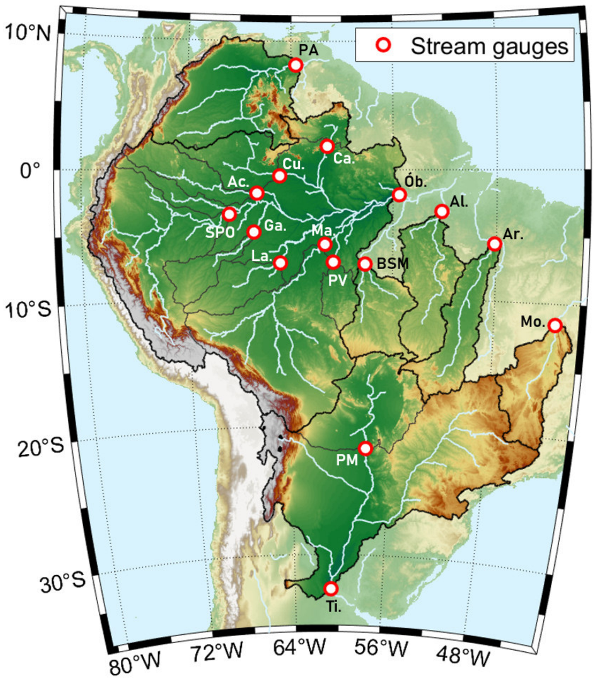

Figure 10: Delineation and location of the 16 South-American catchments investigated.

Once the linear TWS-discharge model is identified and reformulated in a state-space representation, we couple it with the water mass balance equation to form a mass-conserving rainfall-storage-discharge model of the catchment. A major advantage of this approach is that the resulting model is calibrated independently of the system input data, namely the precipitation and evapotranspiration. In the classical calibration process, the estimated model parameters would strongly dependent on the choice of an estimate of these fluxes, which usually suffer from large discrepancies from one data set to another. Conversely, the rainfall-storage-discharge model can be used to evaluate the accuracy of different input data set by comparing their ability to simulate correctly the observed output. The identification of linear rainfall-storage-discharge models, when possible, has been carried out on 16 south-American catchments (see their distribution on Figure 10) with the aim of reconstructing continuous time series of monthly TWS and discharge from 1980 to 2022 via a Kalman smoother. The results are shown for 2 Amazonian sub-catchments in Figure 11. In most cases, we find that ERA-5 precipitation reanalysis yields the best simulation results.

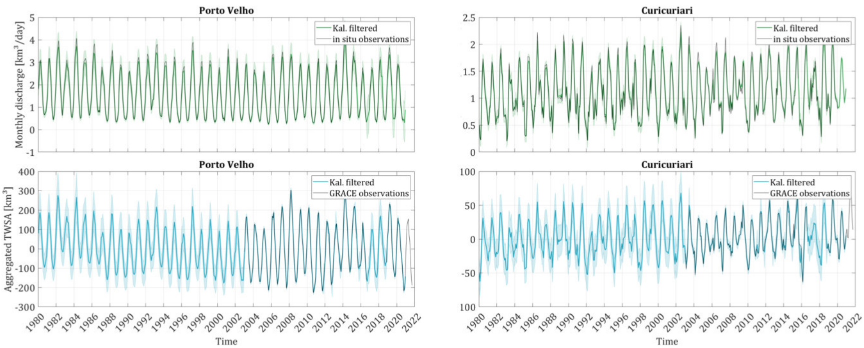

Figure 11: Reconstructued time series for two sub-catchments of the Amazon upstream Porto Velho and Curicuriari, respectively. While the discharge time series spans almost the entire period from 1980 to 2022 for both catchments, it is not the case for the GRACE-like TWS anomaly, which only starts in 2003. The spread around the curves indicate the 1σ uncertainty.

Current availability and distribution of Congo Basin's freshwater resources

Mohammad Tourian

The Congo Basin (Figure 12) is of global significance for biodiversity and the water and carbon cycles. However, its freshwater availability remains highly unknown. Here, we leverage two decades of satellite and in situ observations to develop a new method that characterizes the relationship between Drainable Water Storage Anomaly (DWSA) and river discharge across the entire basin. We obtain DWSA by subtracting spaceborne estimates of the Lake Water Storage Anomaly (LWSA) and the Wetland Water Storage Anomaly (WWSA) from the

Total Water Storage Anomaly (TWSA) of GRACE. We determine the TDWS of the Congo Basin to be only 476 ± 10 km^3 (Figure 13).

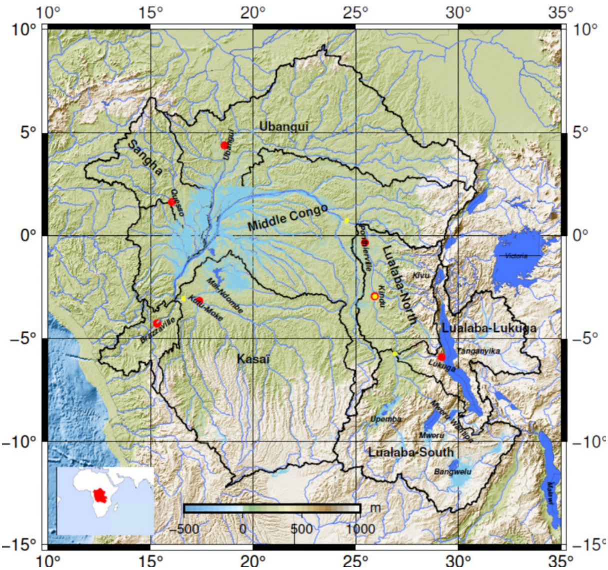

Figure 12: The Congo Basin and its sub-basins: Kasaï, Middle-Congo, Ubangui, Sangha, Lualaba-North, Lualaba-South and Lualaba-Lukuga covering a total area of 3.7×10^6 km^2. Red dots represent the discharge gauging stations and yellow dots shows the location of selected satellite altimetric virtual stations. Wetlands are shown in light blue color and lakes are depicted in dark blue color. Five wetlands around lakes Mai-Ndombe, Bangwelu, Mweru, Mweru Wantipa, and Upemba are considered for quantifying water storage in wetlands.

This water amount corresponds to 133 ± 3 mm of equivalent drainable water height, i.e., the level at which the discharge in Figure 13 reaches zero. Our results show that currently the Congo Basin's Total Drainable Water Storage lies within a range of 476 km^3 to 502 km^3, unevenly distributed throughout the region, with 63 % being stored in the southernmost sub-basins, Kasaï (220–228 km^3) and Lualaba (109–169 km^3), while the northern sub-basins contribute only 173 ± 8 km^3. We further estimate the hydraulic time constant for draining its entire water storage to be 4.3 ± 0.1 months, but, regionally, permanent wetlands and large lakes act as resistors resulting in greater time constants of up to 105 ± 3 months. Our estimate provides a robust basis to address the challenges of water demand for 120 million inhabitants, a population expected to double in a few decades.

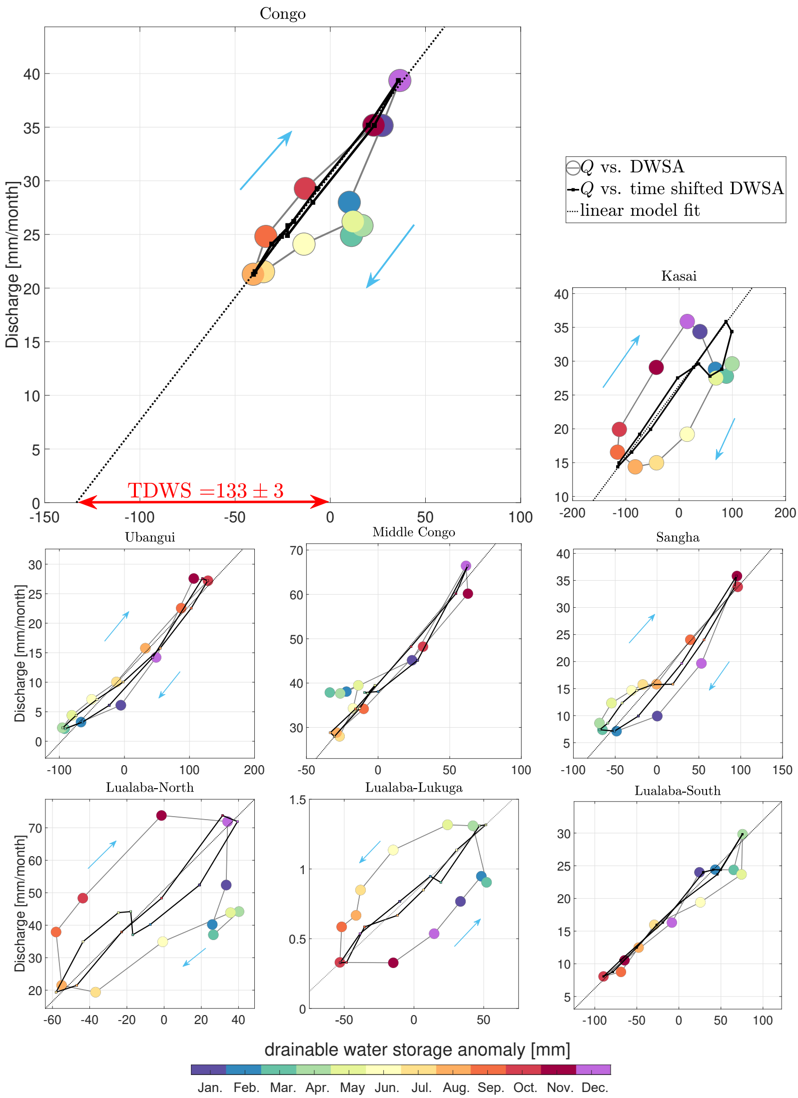

Figure 13: Mean monthly river discharge Q against mean monthly drainable water storage anomaly (DWSA = TWSA − WWSA − LWSA) (thin gray curve with colored disks) and time shifted drainable water storage anomaly (thicker black curve). Mean monthly discharge values are obtained from discharge time series available over different time periods. DWSA mean monthly values were obtained from time series from 2002 to 2015 for Kasaï, Lualaba South, and Congo, and 2002 to 2017 for the other sub-basins. The arrows represent the annual behavior of the runoff-storage relationship.

Long-term Total Water Storage Anomalies Over Land: leveraging GRACE observations, Models, and data-driven method

Peyman Saemian

The gravity recovery and climate experiment (GRACE) satellite mission revolutionized remote measurement of total water storage (TWS) anomalies, providing comprehensive insights at regional to continental scales. With a wealth of applications, GRACE data has been leveraged for monitoring ice sheets and glaciers, uncovering anthropogenic groundwater depletion, tracking droughts, and predicting floods, among others. Its legacy continues with the launch of GRACE Follow-On (GRACE-FO) on 22 May 2018. However, the time span of GRACE(-FO) observations (covers so far), limited to 20 years of monthly data with a year gap between GRACE and GRACE-FO, hinders capturing long-term climate projections. A short record may not accurately reflect the changes in climate and its impacts on various aspects of the environment, such as water resources, agriculture, and ecosystems. Additionally, the shortage of data from the last decades of the 20th century may lead to inaccurate results (underestimation or overestimation) in various GRACE(-FO) applications, such as characterizing droughts. To accurately assess global and regional climates, continuous observations for at least 30 years (more favorably 60 years) are highly recommended.

To overcome the limitations of the short record of GRACE data, we have employed a hindcasting approach using state-of-the-art datasets from Global Hydrological Models (GHMs), Land Surface Models (LSMs), and atmospheric reanalysis models. The intersected period between GRACE and these models was divided into training and validation periods. A Gaussian Process Regression (GPR) was trained using the model's total water storage anomalies (TWSA) as features and GRACE TWSA as target values, at a global land scale, for each grid cell. The trained model then hindcasted TWSA back to 1980. The results before 2002 were compared with key hydrological fluxes, such as precipitation, evapotranspiration, and runoff, at both the pixel and basin scales. The newly obtained long-term dataset of TWSA can be utilized for climate-related research and to enhance extremes monitoring within the GRACE period. This approach offers a valuable solution to the problem of the limited record of GRACE data, allowing for more accurate and comprehensive analysis of global and regional climates.

Figure 14 presents the results from the hindcasted total water storage anomalies (GRACE-H) over four selected basins. The performance of the GPR is compared against the ensemble mean of the models. Our proposed method has significantly improved the results in terms of the Nash-Sutcliffe Efficiency (NSE), with an increase from 12 % in the Yangtze basin to 30 % in the Amazonas basin. The Normalized Root-Mean-Squared-Error (NRMSE) also demonstrates significant improvement, ranging from 50 % in the Yangtze basin to 70 % in the Amazonas basin. The same evaluation conducted at the global scale indicated general enhancement in the reconstruction of GRACE TWSA from the models, with improvements ranging from 5–90 % for NSE and 10–100 % for NRMSE.

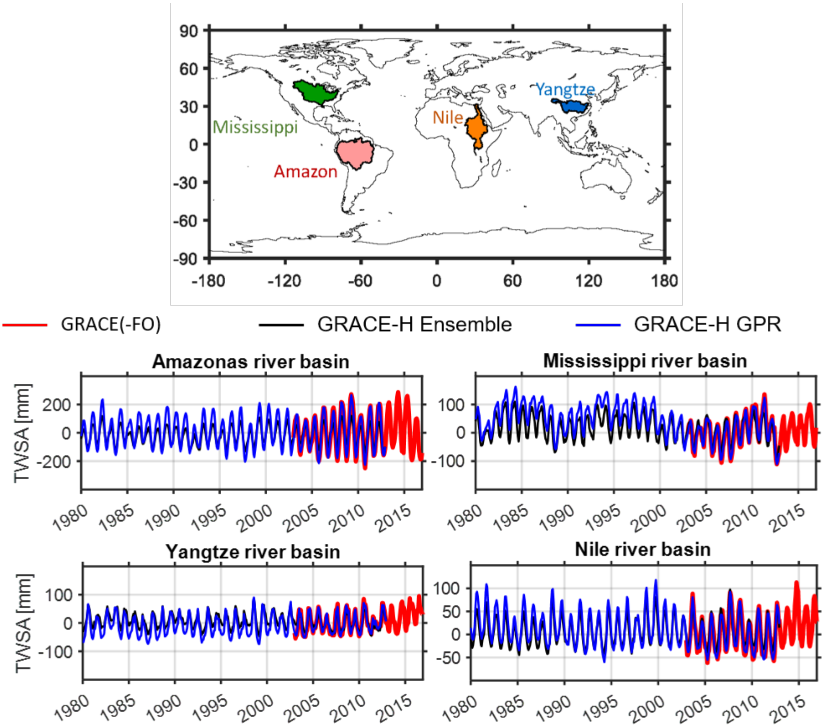

Figure 14: Comparison of the TWSA from GRACE with the hindcasted time series from the ensemble mean of the models and the GPR approach over selected basins. The distribution of the selected basins is shown in the top figure.

Monitoring the water volume anomaly of global lakes and reservoirs

Omid Elmi

Continental water storage is an essential part of the global hydrological cycle. Among the Earth's water storage components, terrestrial surface water in lakes and reservoirs is essential for wildlife and human habitats as they store freshwater in the most accessible way, control seasonal floods and generate hydropower. Despite the negligible spatial coverage, lakes and reservoirs act as a buffer against climate extremes and have a crucial role in the climate system by affecting the land-atmosphere interaction processes like the global carbon and methane cycles. Despite the importance, the estimation of surface water storage variation at a global scale is usually obtained from simplified models due to the absence and lack of necessary measurements. In recent decades, the breakthrough in spaceborne geodetic techniques has enabled us to overcome the lack of comprehensive measurements of surface water variables. Satellite altimetry and imaging missions provide consistent measurements for generating dense and long time series of water level and surface water area of lakes and reservoirs. The water area-level relationship can be obtained by pairing the simultaneous water area and height measurements. Afterward, the time series water volume change is calculated benefiting from the developed model and the measurements. However, satellite altimetry missions cannot measure the water level of the majority of inland lakes and reservoirs because of the large ground track separation. To overcome this issue, the water area-height relationship and water storage variation can be obtained benefiting from water area estimates from satellite imagery and water height information extracted from Digital Elevation Models (DEM).

We developed water volume variation time series for 182 255 lakes and reservoirs larger than $1\,\text{km}^2$ from 1984 to 2018. To do so, water area time series of lakes and reservoirs are obtained from the Global Surface Water Data set provided by the Joint Research Centre of the European Commission. For more than 1000 lakes and reservoirs with available in situ or altimetric water level measurements, water volume anomaly time series are generated using the direct measurements. For the remaining water bodies, water volume anomaly time series are obtained by incorporating water area time series and the height information obtained from TanDEM-X DEM.

The annual water volume anomaly time series of 182 255 global lakes and reservoirs are plotted in Figure 15(a–f). Most of the water bodies do not show any significant variation during the 35 years monitoring. However, in each continent, there are a couple of water bodies with significant positive and negative trends and annual variations during the monitoring period. Figure 15 (top panel) presents the time series of total surface water volume anomaly for each continent. Interestingly the total surface water volume anomaly has almost the same pattern in Africa, Asia, South America and Australia. All of them have a positive trend from 1984 until 2008. After 2008, the rate of the positive trend slightly decreases in Asia, Africa and Australia. Surface water storage shows a negative trend from 2008 until 2018 in South America. The total surface water anomaly doesn't show any significant trend in Europa. After a considerable drop in the early years (1984–1988), surface water storage gradually increased and recovered the water storage lost in the early monitoring phase until 2013. Because of so many large lakes and reservoirs in North America, the magnitude of the surface water storage change is larger than in other continents. Despite the remarkable variation in the water volume change, the time series of North America does not show any clear pattern until 2014. After that, the annual surface water volume increased significantly until the end of the monitoring period, and the surface water storage increased about $5000\,\text{km}^3$ in 2018 in comparison to 1984.

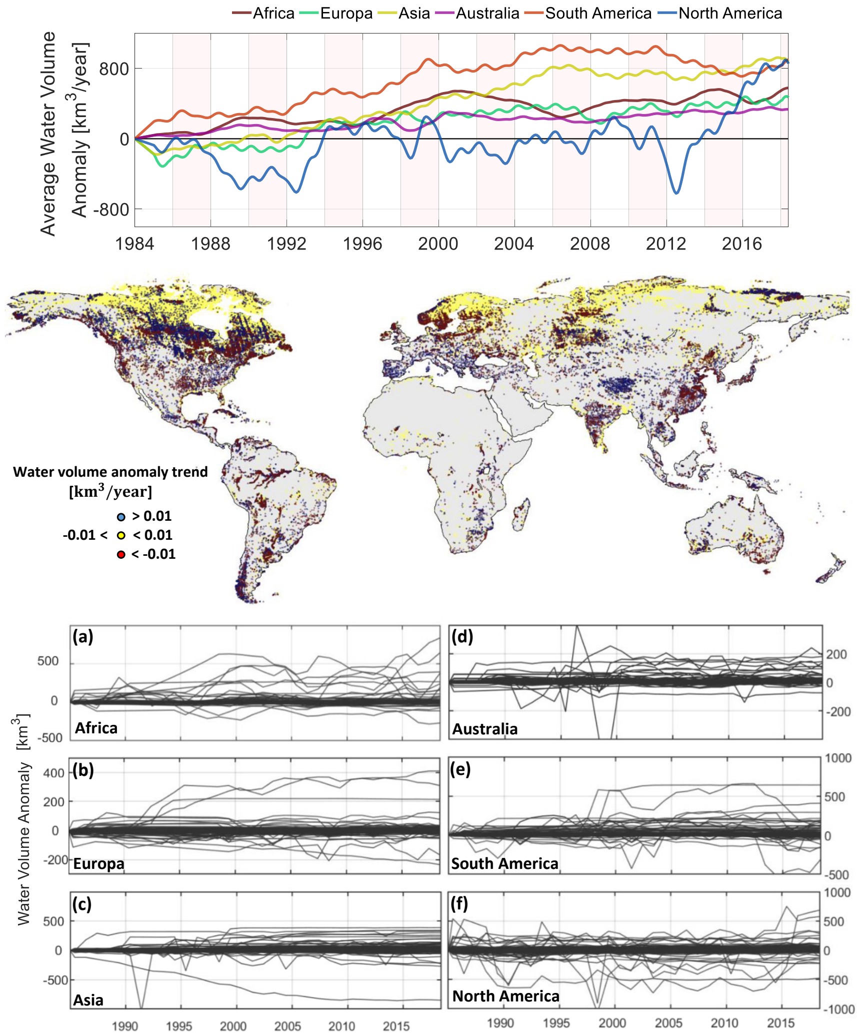

Figure 15: Time series of annual water storage change of global lakes and reservoirs for each continent is in the top panel. Map of water volume anomaly trend (1984–2018) is in the middle panel. (a–f) are water volume anomaly time series of global lakes and reservoirs.

Crossover Adjustment of ICESat-2 Satellite Altimetry for the Arctic Region

Bo Wang

The ICESat-2 mission obtains height measurements to create a global portrait of Earth's radial dimension, gathering data to monitor changes of terrain including glaciers, sea ice, forests and more. Therefore, it is important to understand the error budget of the observations, one component of which is radial orbit error. Apart from the altimetric ranging errors, radial orbit errors directly influence the precision of the measurement of sea surface height (SSH). These errors can be assessed by analyzing the difference of SSH at ground track intersections, so-called crossover differences (XO differences). An effective approach is to model the orbit error by minimizing the residual XO difference by the least-squares method. XO differences are assumed to be caused by the difference of radial orbit errors between ascending and descending arcs, the sea surface variation, mispointing, and measurement errors. Since the sea surface variation in a short time interval and measurement errors can be considered as random variable, these residuals can be reduced by the method of XO adjustment.

In general, the error function model is described as a function of time or the track length. The most popular parameterization for regional applications is a simple bias or bias-and-tilt model. The parameters (bias and tilt) for each track are determined by minimizing the residual XO differences. When the length of a track is a small fraction of one revolution, this parameterization is adequate. However, this is not always the case. For global applications, enhanced parameterizations are to represent the radial orbit error using higher-degree polynomials or Fourier series. Consequently, the choice of parameterization is a balance between efficiency and simplicity. Since the orbits of altimeter satellites are almost circular, at least locally the orbit can be described as a Keplerian orbit. We describe the XO adjustment with Keplerian orbit model in the Arctic region. One reason for our choice of the Arctic region is the fact that ICESat-2 focuses on arctic ocean regions. A second reason is that previous XO analyses chose rectangular and/or diamond shaped regions. Consequently, XO analysis for the Arctic region will help to understand the performance of the LS adjustment over spherical cap geometry. A mathematical function of the radial orbit error is created after linearizing the Keplerian orbit model. One problem of XO adjustment is the existence of singular solutions, which belong to a so-called null space of the normal equations. The situation is comparable to that of a leveling network. Networks of height difference observations are derived by the differential leveling method. A closed leveling network is a loop that begins and ends at one point. Theoretically, the misclosure should be zero, but in fact random errors cannot be avoided, which can be subjected to a least squares adjustment. There will be a datum problem when adjusting the errors, i.e. heights of points can only be determined by fixing the height of one arbitrary point. When a point is fixed, absolute constraints are applied in the adjustment by setting the corresponding parameters to zero. The same holds true here; therefore, we fix parameters falling inside the null space of the XO minimization problem.

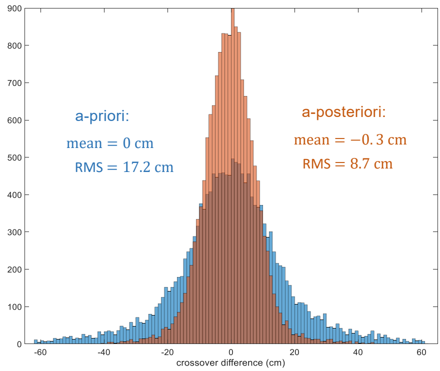

Figure 16: a-priori/a-posteriori histogram of XO differences

The histograms of XO differences before and after adjustment are demonstrated in Figure 16. The RMS is reduced from 17.2 cm to 8.7 cm using the method of the XO adjustment. Assuming the residual errors are independent in the XO difference function, 8.7 cm divided by $\sqrt{2}$ gives a value of 6.1 cm. That means the orbit error and mispointing error level of ICESat-2 in the Arctic region is generally 6.1 cm.

From Figure 17 we can see XO differences at different latitudes before and after adjustment. At the XOs closest to the North Pole, the differences are reduced to about 6 cm to 7 cm. The reduced value of XO difference divided by $\sqrt{2}$ gives an approximate value of 4 cm to 5 cm. However, parts of the XO differences are not significantly reduced, which may be caused by the boundaries of sea-ice-land. For this reason, the altimetry will have large measurement errors influenced by these boundaries.

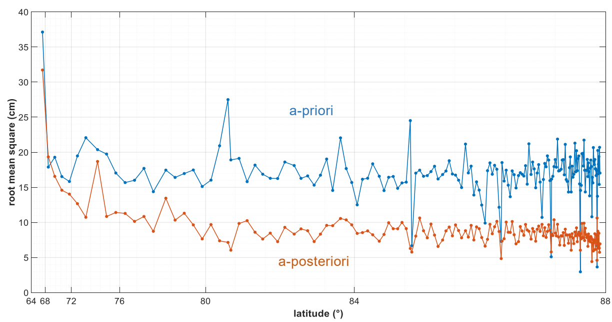

Figure 17: Comparison of XO differences at different latitudes before and after adjustment

Publications

(https://www.gis.uni-stuttgart.de/en/research/publications/index.html)

Refereed Journal Publications

Antoni, M. (2022): A review of different mascon approaches for regional gravity field modelling since 1968. In: *History of Geo- and Space Sciences* 13.2, pp. 205–217. DOI: 10.5194/hgss-13-205-2022.

Behling, R., S. Roessner, S. Foerster, P. Saemian, M. J. Tourian, T. C. Portele, and C. Lorenz (2022): Interrelations of vegetation growth and water scarcity in Iran revealed by satellite time series. In: *Scientific Reports* 12.1, pp. 20784–. ISSN: 20452322. DOI: 10.1038/s41598-022-24712-6.

Camici, S., G. Giuliani, L. Brocca, C. Massari, A. Tarpanelli, H. Hashemi Farahani, N. Sneeuw, M. Restano, and J. Benveniste (2022a): Synergy between satellite observations of soil moisture and water storage anomalies for runoff estimation. In: *Geoscientific Model Development* 15, pp. 6935–6956. DOI: 10.5194/gmd-15-6935-2022.

Ghajarnia, N., M. Akbari, P. Saemian, M. R. Ehsani, S.-M. Hosseini-Moghari, A. Azizian, Z. Kalantari, A. Behrangi, M. J. Tourian, B. Klöve, and A. T. Haghighi (2022): Evaluating the Evolution of ECMWF Precipitation Products Using Observational Data for Iran: From ERA40 to ERA5. In: *Earth and Space Science* 9.10, e2022EA002352. DOI: 10.1029/2022EA002352.

Ghorbanpour, A. K., I. Kisekka, A. Afshar, T. Hessels, M. Taraghi, B. Hessari, M. J. Tourian, and Z. Duan (2022): Crop Water Productivity Mapping and Benchmarking Using Remote Sensing and Google Earth Engine Cloud Computing. In: *Remote Sensing* 14.19. ISSN: 2072-4292. DOI: 10.3390/rs14194934.

Huang, Q., N. C. Schmerr, S. D. King, D. Kim, A. Rivoldini, A.-C. Plesa, H. Samuel, R. R. Maguire, F. Karakostas, V. Lekić, C. Charalambous, M. Collinet, R. Myhill, D. Antonangeli, M. Drilleau, M. Bystricky, C. Bollinger, C. Michaut, T. Gudkova, J. C. E. Irving, A. Horleston, B. Fernando, K. Leng, T. Nissen-Meyer, F. Bejina, E. Bozdağ, C. Beghein, L. Waszek, N. C. Siersch, J.-R. Scholz, P. M. Davis, P. Lognonné, B. Pinot, R. Widmer-Schnidrig, M. P. Panning, S. E. Smrekar, T. Spohn, W. T. Pike, D. Giardini, and W. B. Banerdt (2022): Seismic detection of a deep mantle discontinuity within Mars by InSight. In: *Proceedings of the National Academy of Sciences* 119.42. DOI: 10.1073/pnas.2204474119.

Kitambo, B., F. Papa, A. Paris, R. M. Tshimanga, S. Calmant, A. S. Fleischmann, F. Frappart, M. Becker, M. J. Tourian, C. Prigent, and J. Andriambeloson (2022): A combined use of in situ and satellite-derived observations to characterize surface hydrology and its variability in the Congo River basin. In: *Hydrology and Earth System Sciences* 26.7, pp. 1857–1882. DOI: 10.5194/hess-26-1857-2022.

Lagacherie, P., C. Dagès, E. Zadonina, J. C. Fabre, J. Molénat, H. Squividant, and B. Thomas (2022): A fully automated and generic spatial discretization procedure for cultivated landscapes with human-made landscape elements. In: *Journal of Hydroinformatics* 24.4, pp. 917–931. ISSN: 1464-7141, 1465-1734. DOI: 10.2166/hydro.2022.048.

Liu, B., X. Zou, S. Yi, N. Sneeuw, J. Li, and J. Cai (2022): Reconstructing GRACE-like time series of high mountain glacier mass anomalies. In: *Remote Sensing of Environment* 280, pp. 1–22. DOI: 10.1016/j.rse.2022.113177.

Pirooznia, M., M. Raoofian Naeeni, A. Atabati, and M. J. Tourian (2022): Improving the Modeling of Sea Surface Currents in the Persian Gulf and the Oman Sea Using Data Assimilation of Satellite Altimetry and Hydrographic Observations. In: *Remote Sensing* 14.19. ISSN: 2072-4292. DOI: 10.3390/rs14194901.

Saemian, P., M. J. Tourian, A. AghaKouchak, K. Madani, and N. Sneeuw (2022a): How much water did Iran lose over the last two decades? In: *Journal of Hydrology: Regional Studies* 41, p. 101095. ISSN: 2214-5818. DOI: 10.1016/j.ejrh.2022.101095.

Tourian, M. J., O. Elmi, Y. Shafaghi, S. Behnia, P. Saemian, R. Schlesinger, and N. Sneeuw (2022b): HydroSat: geometric quantities of the global water cycle from geodetic satellites. In: *Earth System Science Data* 14, pp. 2463–2486. DOI: 10.5194/essd-14-2463-2022.

Yi, S. and N. Sneeuw (2022a): A novel spatial filter to reduce north–south striping noise in GRACE spherical harmonic coefficients. In: *Journal of Geodesy* 96.4, p. 23. ISSN: 1432-1394. DOI: 10.1007/s00190-022-01614-z.

Books & Miscellaneous

Delage, P., E. Marteau, C. Vrettos, M. Golombek, V. Ansan, W. B. Banerdt, M. Grott, K. Hurst, P. Lognonné, N. Murdoch, S. Piqueux, C. Schmelzbach, T. Spohn, N. H. Warner, R. Widmer-Schnidrig, N. Brinkman, B. Caicedo, J.-P. Castillo Betancourt, E. P., S. Kedar, L. Lange, M. Lemmon, N. Mueller, K. Onodera, J. Robertsson, S. C. Stähler, V. Nicolas, and R. Williams (2022): "The mechanical properties of the Martian soil at the InSight landing site". In: *Proceeedings 20th International Conference on Soil Mechanics and Geotechnical Engineering, Sydney, May 2022*. Sydney, Australia. URL: https://hal.archives-ouvertes.fr/hal-03706564.

Conference Presentations

Azzola, J., N. K. Toularoud, E. Gaucher, T. Forbriger, R. Widmer-Schnidrig, F. Bögelspacher, M. Frietsch, and A. Rietbrock (2022): *Comparison between Distributed Acoustic Sensing (DAS) and strain meter measurements at the Black Forest Observatory*. EGU 2022. Vienna, Austria. DOI: 10.5194/egusphere-egu22-6976.

Behnia, S., E. Woolliams, N. Schneider, M. J. Tourian, N. Sneeuw, J.-C. Poisson, N. Picot, J.-F. Cretaux, F. Piras, and A. Tarpanelli (2022): *Satellite altimetry Cal/Val for inland waters: How to couple FDRs and TDPs to FRMs?* Metrology for Climate Action. online.

Bützler, C., K. Douch, R. Widmer-Schnidrig, and N. Sneeuw (2022a): *Realistic modeling of gravity strain due to prompt elasto-gravity signals (PEGS) - How simple can the Earth model be?* Conference on Mathematics of Wave Phenomena 2022. Karlsruhe, Germany.

Bützler, C., T. Forbriger, R. Widmer-Schnidrig, and N. Sneeuw (2022b): *Instrumental Disturbances of Superconducting Gravimeters - How much do they influence long term studies of gravity?* Arbeitskreis Geodäsie/Geophysik. Oppurg, Germany.

Camici, S., A. Tarpanelli, L. Brocca, C. Massari, P. Filippucci, K. Nielsen, N. Sneeuw, M. J. Tourian, S. Yi, M. Restano, and J. Benveniste (2022b): *Satellite-based river discharge estimation: the STREAMRIDE project*. COSPAR 2022, 44th Scientific Assembly. Athens, Greece.

Camici, S., A. Tarpanelli, L. Brocca, C. Massari, K. Nielsen, N. Sneeuw, M. J. Tourian, S. Yi, M. Restano, and J. Benveniste (2022c): *Satellite observations for runoff and river discharge estimation: STREAMRIDE approach*. EGU 2022. Vienna, Austria. DOI: `10.5194/egusphere-egu22-9234`.

Camici, S., A. Tarpanelli, C. Massari, L. Brocca, K. Nielsen, N. Sneeuw, M. J. Tourian, S. Yi, M. Restano, and J. Benveniste (2022d): *STREAMRIDE: runoff and river discharge estimation by using satellite observations*. ESA Living Planet Symposium 2022. Bonn, Germany.

Cretaux, J.-F., M. Bergé-Nguyen, and N. Sneeuw (2022): *Use of a priori mean lake surface for calibration of rolling and random errors*. SWOT Science Team Meeting. Chapel Hill, NC, USA, Toulouse, France and online.

Douch, K., P. Saemian, and N. Sneeuw (2022): *Identification of conceptual rainfall-runoff models of large drainage basins based on GRACE and in-situ data*. EGU 2022. Vienna, Austria.

Douch, K., N. Sneeuw, and P. Saemian (2022): *Identification of lumped rainfall-runoff models of large drainage basins for satellite data assimilation*. ESA Living Planet Symposium 2022. Bonn, Germany.

Elmi, O., M. J. Tourian, A. Bárdossy, and N. Sneeuw (2022): *Spaceborne river discharge from a nonparametric stochastic quantile mapping function*. ESA Living Planet Symposium 2022. Bonn, Germany.

Elmi, O. and M. J. Tourian (2022): *Global dynamic river masks from Landsat imagery*. ESA Living Planet Symposium 2022. Bonn, Germany.

Gou, J. and M. J. Tourian (2022): *RiwiSAR-SWH: A data-driven method for estimating significant wave height using Sentinel-3 SAR altimetry*. ESA Living Planet Symposium 2022. Bonn, Germany.

Nielsen, K., A. Tarpanelli, S. Camici, M. J. Tourian, M. Restano, and J. Benveniste (2022): *Reconstructing river water level time series from multi-mission satellite altimetry – reach based methods*. ESA Living Planet Symposium 2022. Bonn, Germany.

Poisson, J. C., N. Picot, H. Yésou, A. Tarpanelli, A. Paris, N. Sneeuw, S. Behnia, M. J. Tourian, R. Fjortoft, F. Boy, D. Blumstein, M. Calzas, M. Cancet, S. Lucas, M. Azzoni, B. Laignel, J.-F.

Crétaux, S. Calmant, K. Nielsen, O. B. Andersen, L. Fichen, M. Studer, J. Maxant, P. Bonnefond, S. Amzil, S. Camici, T. Ledauphin, N. Taburet, M. Vayre, and P. Férnéias (2022): *Towards the provision of operational FRM measurements for Sentinel-3 over inland water: procedures, protocols and roadmap*. ESA Living Planet Symposium 2022. Bonn, Germany.

Saemian, P., M. J. Tourian, K. Douch, and N. Sneeuw (2022b): *Long-term Total Water Storage Anomalies Over Land Using GRACE observations, Models, and data-driven method*. Frontiers of Geodetic Science. Essen, Germany.

Saemian, P., M. J. Tourian, and N. Sneeuw (2022): *A least-squares collocation approach to densifying river level from multi-mission satellite altimetry; Case study Mackenzie River basin*. EGU 2022. Vienna, Austria.

Sneeuw, N. (2022a): *Multi-mission Satellite Geodesy for the Quantification of the Water Cycle*. Tongji University, China, Guest lecture.

Sneeuw, N. (2022c): *Satellite gravimetry: how to weigh ice sheets, glaciers and the global watercycle?* Erasmus+ Project: Climate Change: open your senses. University of Stuttgart, Germany.

Sneeuw, N., M. Berge-Nguyen, and J.-F. Cretaux (2022): *Physical heights of inland lakes*. X Hotine-Marussi Symposium 2022. Milan, Italy.

Sneeuw, N., M. Bergé-Nguyen, and J.-F. Crétaux (2022): *Physical heights of inland lakes*. Frontiers of Geodetic Science. Essen, Germany.

Sneeuw, N., B. Wang, J. Bao, S. Ke, and M. J. Tourian (2022): *Constraining river streamflow determination using bathymetry and slope from ICESat-2 satellite altimetry*. EGU 2022. Vienna, Austria. DOI: 10.5194/egusphere-egu22-7475.

Thomas, B. E. O. and J. Foster (2022): *Insight in ground deformation patterns in Koa'e fault zone on Kīlauea volcano*. Heraklion, Greece.

Thomas, B. E. O., T. Louartani, and J. Foster (2022): *Ability of a cargo-ship GNSS network to detect tsunamis*. Essen, Germany. URL: https://www.intergeo.de/en/program-conference#/talk/1164200.

Thomas, B. E. O., J. Roger, and Y. Gunnell (2022a): *A rapid, low-cost, high-resolution, map-based assessment of the January 15, 2022 tsunami impact on population and buildings in the Kingdom of Tonga*. Vienna, Austria. DOI: 10.5194/egusphere-egu22-13580.

Thomas, B. E. O., J. Roger, and Y. Gunnell (2022b): *Rapid · Low-cost · High-resolution map-based assessment of tsunami impact on population in Tonga and New Caledonia*. Paris, France.

Toularoud, N. K., J. Azzola, E. Gaucher, T. Forbriger, R. Widmer-Schnidrig, F. Bögelspacher, M. Frietsch, and A. Rietbrock (2022): *PSD analysis and seismic event detectability of Distributed Acoustic Sensing (DAS) mesurements from several monitoring sites*. EGU 2022. Vienna, Austria. DOI: 10.5194/egusphere-egu22-8787.

Tourian, M. J., S. Behnia, S. Yu, O. Elmi, and N. Sneeuw (2022a): *Estimation of inter-satellite and inter-track biases of satellite altimetry missions over lakes and reservoirs using surface area from satellite imagery*. ESA Living Planet Symposium 2022. Bonn, Germany.

Wang, B. and N. Sneeuw (2022): *Crossover Adjustment of ICESat-2 Satellite Altimetry for Arctic Region*. ESA Living Planet Symposium 2022. Bonn, Germany.

Widmer-Schnidrig, R. (2022): *Observation of acoustic normal modes of the atmosphere after the 2022 Hunga-Tonga eruption.* EGU 2022. Vienna, Austria. DOI: `10.5194/egusphere-egu22-13581`.

Yi, S. and N. Sneeuw (2022b): *A novel spatial filter to reduce north-south striping noise in GRACE spherical harmonic coefficients*. X Hotine-Marussi Symposium 2022. Milan, Italy.

Master Theses

(`https://www.gis.uni-stuttgart.de/lehre/abschlussarbeiten/`)

Imanimfashe, Epiphanie: Hydrological gravitiy effect at Black Forest Observatory (BFO) - aspect of topography

Necșulescu, Edward: Performance analysis of the low-cost GNSS receivers based on the PPP techniques

Yu, Shuhua: Estimation of inter-satellite and inter-track biases of satellite altimetry missions over lakes and reservoirs using surface area from satellite imagery

Bachelor Theses

(`https://www.gis.uni-stuttgart.de/lehre/abschlussarbeiten/`)

Bao, Jingyi: Analysis of river surface slope using ICESat-2 satellite altimetry

Liu, Jiaxin: Dealing with challenges of altimetry-based surface water height derivation over boreal catchments : case study of Mackenzie River

Peng, Miao: Lakes' response within drought periods

Activities in National and International Organizations

Keller W.

Doctorate honoris causa, Wrocław University of Environmental and Life Sciences, Wrocław, Poland

Sneeuw N.

Member of ESA Advisory Committee for Earth Observation (ACEO), 2019-2022

Distinguished Professor, Land Satellite Remote Sensing Application Center (LASAC), China

Professor h.c. (Luojia chair), Wuhan University, China
Adjunct Professor of the College of Engineering, University of Tehran, since 2015
Fellow International Association of Geodesy (IAG)
Full Member Deutsche Geodätische Kommission (DGK)
Member of Gauss-Gesellschaft e.V., since 2018
Member of the editorial board of Surveys in Geophysics

Research stays

Thomas B.

Visiting PhD student at GEOMAR Helmholtz-Zentrum für Ozeanforschung Kiel on board of RV SONNE. The aim was to recover seafloor geodetic networks installed on the continental margin and outer rise offshore Iquique in northern Chile to provide an innovative way to monitor crustal deformation. (01.2022–02.2022)

Visiting PhD student at University of Hawai'i to realize fieldwork of roving GNSS occupations on Kīlauea volcano with collaboration with the Hawai'i Volcano Observatory. (11.2022–12.2022)

Courses – Lecture/Lab/Seminar

Bachelor Geodesy and Geoinformatics (German):

Amtliches Vermessungswesen und Liegenschaftskataster (Grams)	2/0/0/0
Einführung Geodäsie und Geoinformatik (Sneeuw)	2/2/0/0
Integriertes Praktikum/Integrated Field Work (Sneeuw, Foster)	10 days
Landesvermessung (Foster, Bützler)	2/2/0/0
Physikalische Geodäsie (Sneeuw, Bützler)	2/2/0/0
Referenzsysteme (Sneeuw, Antoni)	2/2/0/0
Satellitengeodäsie (Sneeuw, Antoni)	2/2/0/0

Master Geodesy and Geoinformatics (German):

Aktuelle Geodätische Satellitenmissionen (Sneeuw)	2/2/0/0
Amtliche Geoinformation (Heß)	2/0/0/0
Ausgewählte Kapitel der Parameterschätzung (Tourian, Douch)	2/2/0/0
Geodätische Erdbeobachtungen (Tourian)	2/0/0/0
Geodynamische Modelle (Engels, Bützler)	2/2/0/0
Hydrogeodäsie (Tourian, Saemian)	2/2/0/0
Koordinaten- und Zeitsysteme in der Geodäsie (Sneeuw)	2/0/0/0
Marine-Geodäsie (Foster, Thomas)	2/2/0/0
Physikalische Geodäsie (Engels, Bützler)	2/1/0/0
Satellitengeodäsie (Tourian, Douch)	2/1/0/0

Master Umweltschutz (German):

Fernerkundung der Hydrologie und Wasserwirtschaft (Tourian)	2/2/0/0

Master GeoEngine (English):

Advanced Mathematics (Foster, Thomas)	3/2/0/0
Foundations of Satellite Geodesy (Sneeuw, Antoni)	2/1/0/0
Integriertes Praktikum/Integrated Field Work (Sneeuw, Foster)	10 days
Map Projections and Geodetic Coordinate Systems (Foster, Thomas)	2/1/0/0
Physical Geodesy (Sneeuw, Saemian)	2/1/0/0
Satellite Geodesy Observation Techniques (Foster, Thomas)	2/1/0/0
Statistical Inference (Tourian, Douch)	2/1/0/0

Institute of Navigation

Breitscheidstraße 2
D-70174 Stuttgart
Tel.: +49 711 685 83400
Fax: +49 711 685 82755
ins@ins.uni-stuttgart.de
http://www.ins.uni-stuttgart.de

Head of Institute

Prof. Dr. techn. Thomas Hobiger, Dean of Studies (since Oct. 2021)

Deputy:	Dr.-Ing. Aloysius Wehr
Secretary:	M.A. Dagmar Epple (until Feb. 2022)
	Mina Sungur (from July 2022)
Retired Professor:	Prof. i.R. Dr.-Ing. Alfred Kleusberg

Academic Staff

Dipl.-Ing. Doris Becker	Navigation Systems
Dipl.-Ing. (FH) Martin Thomas	Digital Electronics and Hardware Programming
Dr.-Ing. Aloysius Wehr	Optical and Wireless Communication

PhD students

M.Sc. Kevin Gutsche	Precise orbit determination
M.Sc. Shengping He	GNSS troposphere & PPP
M.Sc. Tomke Jantje Hobiger	Parameter Estimation in Dynamic Systems
M.Sc. Daniel Klink	FPGA design, autonomous flight
M.Sc. Marcel Maier	Navigation Software Development
M.Sc. Clemens Sonnleitner	Autonomous flight, ADS-B
M.Sc. Bayram Stucke (from May 2022)	Precise orbit determination
M.Sc. Thomas Topp	Navigation Software Development
M.Sc. Rui Wang	GNSS, RTK, PPP, integrity

IT

Regine Schlothan	Computer infrastructure and programming

Electr. and Mech. Workshop (ZLW)

Dr.-Ing. Aloysius Wehr	Head of ZLW
Michael Pfeiffer	Mechanician Master
Sebastian Schneider	Electrician
Dipl.-Ing. (FH) Martin Thomas	Electrical engineer

External lecturers

Dipl.-Ing. Steffen Bolenz	Stadtmessungsamt, Stuttgart
Dr. Toni Caesperlein	Dr. Koch Immobilienbewertung, Esslingen

Guests

M.Sc. Grzegorz Marut (11.7.-5.8.2022)	University of Wroclaw, Poland
Dr. Gregor Möller (12.-13.9.2022)	ETH Zürich, Schweiz

Preface

This report summarizes the activities of the Institute of Navigation (INS) in the year 2022. With COVID-19 in the past and all restrictions for teaching and office work lifted, we returned to operating like before the pandemic. Thus, meetings could be held in person, conference attendance became possible again, and social activities in our group were recommenced.

We also saw our research team grow and new projects could be acquired, paving the way for a sustainable growth of our group in the next years. We could also streamline some of our internal processes and reduce administrative burdens by making use of agile planning tools, self-hosted cloud solutions, and a flexible version control system. This system also allows us to deliver clean and well-tested code, that complies with industry standards. Research highlights, which are described in greater detail in this report, cover a wide range of topics, including GNSS, sensor fusion, precise orbit determination, airspace monitoring, robust real-time kinematic GNSS positioning, precise point positioning, troposphere estimation.

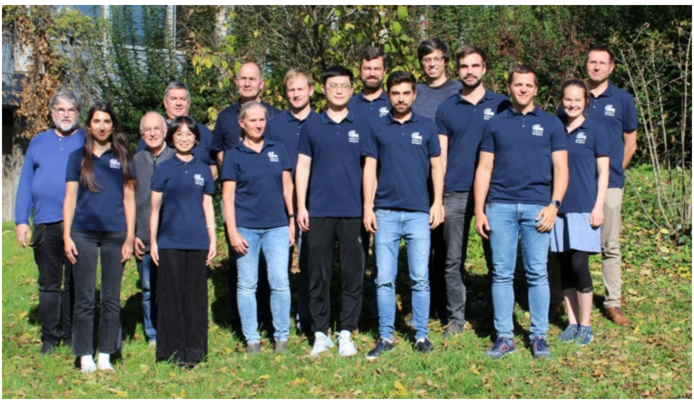

Figure 13: Group photo of almost all INS members.

GNSS simulators

The Institute of Navigation currently operates an industry-compatible hardware GNSS simulator and an additional GNSS simulator, which can be used for educational purposes or testing. While the hardware-GNSS-simulator from Spirent Communications is used heavily in research projects dealing with precise orbit determination, autonomous flight, and GNSS studies dealing with the atmosphere, the Skydel simulator, which is provided under the Orolia Academic Partnership Program (OAPP), is mostly being used for educational purposes.

In order to intensify the cooperation with the manufacturer of the hardware simulator, the Institute of Navigation has joined the Spirent Academia Programme in 2022 under which both partners will cooperate on research and educational topics related to the simulation of real-world GNSS scenarios. The program will provide PhD students and researchers from the Institute of Navigation exclusive insights into Spirent's simulation tools and algorithms while providing feedback to Spirent engineers to further enhance their software and hardware suites. Figure 14 shows the usage in hours of both simulators. While the Spirent hardware simulator was used in total for more than 47 days, the Orolia solution was only used for about a week of computation time. The heavy load of the first can be explained by very extensive simulations of LEO spacecrafts and unmanned aerial vehicles, whereas the Skydel simulator was only used in smaller students' projects and bachelor or master thesis projects.

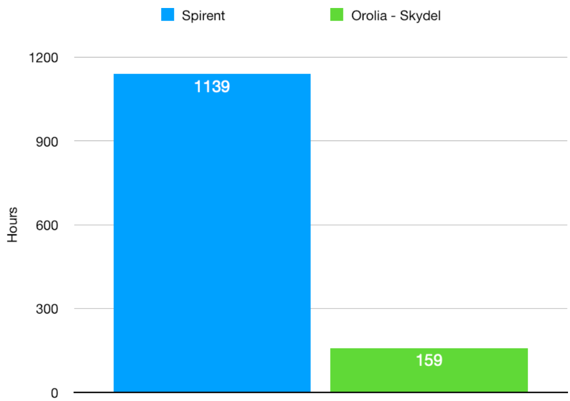

Figure 14: Usage (in hours) of the two GNSS simulators in 2022.

Research

The INS identifies new fields of applications, develops and tests navigation solutions, and assigns research projects according to four "focus areas", which were originally defined in 2018. Considering the way the institute is organized and its participation in different research projects, those areas reflect most of the activities of the INS. Moreover, the teaching activities, which are described later in this report, also reflect the research activities that the INS is involved in. Figure 15 depicts those focus areas, which are grouped around the topics of "positioning, navigation, and timing".

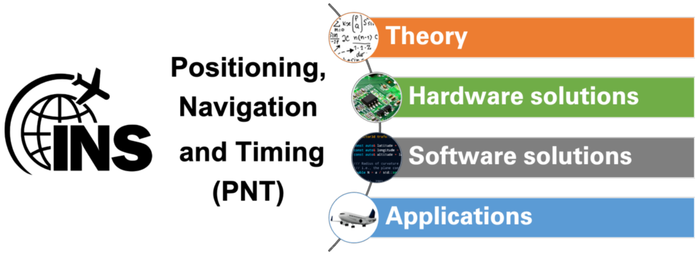

Figure 15: INS focus areas to which the institute is actively contributing in the form of research projects.

While most of the current research projects can be clearly assigned to one or two focus areas shown in the figure, larger research projects, described later in this report, usually fall under the category "applications" but require intense input from the other three research areas. In the following, the purpose and vision for each research area are presented alongside examples of ongoing research projects.

Research focus: Theory

The following sections describe theoretical work that was conducted in 2022.

ADS-B

Since the end of the year 2020, a large portion of commercial aircraft operating in the European sky airspace have to be equipped with an Automatic Dependent Surveillance - Broadcast (ADS-B) transponder. This obligation has pushed forward the amount of performed flights during which ADS-B messages were broadcasted to about 94 % at the end of 2022. Besides professional dedicated receivers, these signals can be detected and decoded by low-cost general-purpose hardware as installed on the roof of the institute[1]. The institute and many others feed the gathered data into the OpenSky Network database, building up an immense open-access dataset of real-world air traffic control data.

[1] https://opensky-network.org/receiver-profile?s=-1408232197

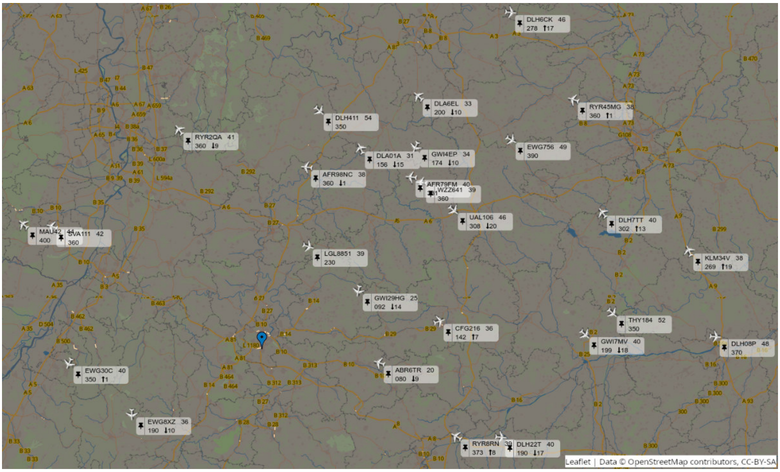

Figure 16: Snapshot of the airspace around Stuttgart monitored by the ADS-B receiver on the roof of the institute and fed into the open-access OpenSky Network database.

This data can be used for a large variety of research purposes. At the institute, it is used as a basis for in-depth performance analysis of a Time-Differential-Of-Arrival (TDOA) localization system built upon the emitted ADS-B messages of aircraft. One of the research focuses is the low-cost clock synchronization of the receiver network. Another focus is the development of a precise, reliable solution that can detect and mitigate attempts of spoofing.

Stochastic modeling with a robust Kalman filter for RTK positioning

In standard Real-Time Kinematic (RTK) processing, the measurement noise Variance-Covariance (VC) matrix is based on the satellite elevation-dependent function. However, this stochastic model cannot always be appropriate in challenging environments, such as urban areas. To improve the reliability of ambiguity resolution and the positioning accuracy in dynamics, the adaptation of the measurement noise VC matrix is applied by choosing a moving estimation window. Besides, the performance of Kalman filtering is prone to degrade when measurements are contaminated by outliers. To resist such effects, the Institute of Geodesy and Geophysics (IGG) III scheme is utilized. In both simulated and practical tests, this proposed approach can enhance the robustness of filtering, as well as achieve higher ambiguity fixing rates. The relevant research paper has been submitted to an academic journal and is currently undergoing review.

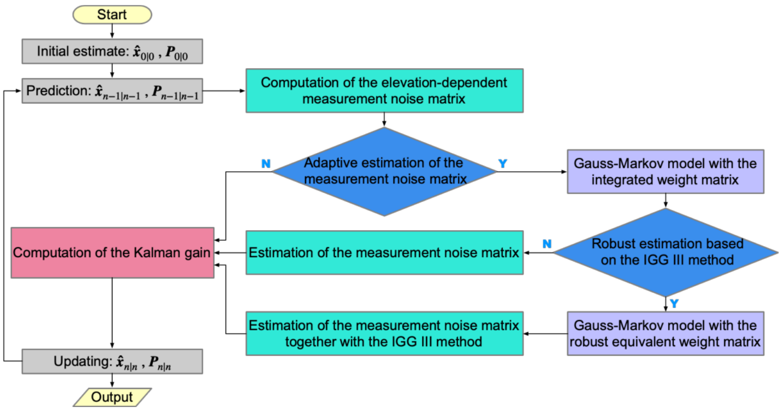

Figure 17: Filter flowchart with three different measurement noise VC matrices

Multi-Receiver Fusion for Improved Tropospheric Modeling

In the STEPPP project, a Precise Point Positioning (PPP) algorithm based on an Extended Kalman Filter (EKF) has been implemented. The EKF can achieve millimeter-accurate positioning results, as well as provide time series of Zenith Wet Delay (ZWD) for meteorologic applications. However, either the precision or accuracy of such ZWD estimates is limited due to receiver noise and system characteristics like cycle slips. Thus, the INS developed a novel approach that combines observations from multiple receivers to estimate a common ZWD parameter, which is superior compared to single receiver estimates in terms of precision and accuracy. This approach can be extended to larger networks and also have broader implications for GNSS analysis, such as improving positioning accuracy and precision in challenging environments. More research on this topic is undergoing.

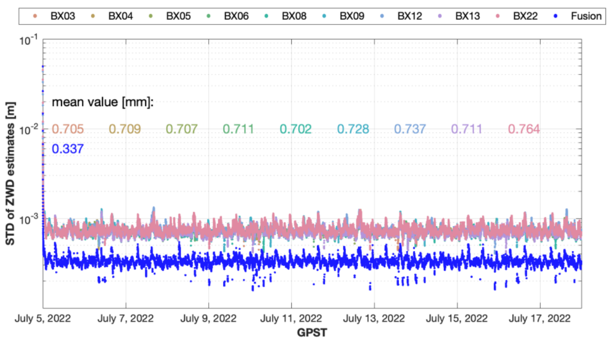

Figure 18: Standard Deviations (STD) of ZWD estimates from PPP and Fusion solutions for multiple low-cost receivers

Research focus: Hardware development

The following sections describe the institute’s hardware development activities in the year 2022.

Development of a ground-based landing aid for unmanned air vehicles

The development of a subsystem to aid in the autonomous landing, which is a requirement for the project CNSAlpha, was continued with hardware improvements and simulation tests. In 2022 the demonstration hardware was completed comprising the RF- input/output module, the IF- and digitizer board, and the logic board (see Figure 19). Both the RF- input/output module and the digitizer board were developed and manufactured by the INS, whereas the logic board is the commercial FPGA development board Arty Z7 with Xlinx ZYNQ XC7Z020. Signal processing algorithms were implemented in the logic board’s FPGA and tested.

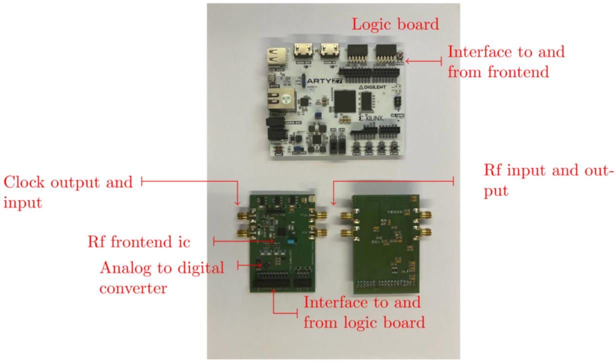

Figure 19: Demonstration hardware, comprising the RF- input/output module, the IF- and digitizer board, and the logic board.

Parallel to this work, various direct and iterative algorithms for the position calculation were studied by running simulations concerning the achievable positioning accuracy. Simulations evidenced that both, the geometric placement of the transmitters and the slant range measurement accuracy, primarily determine the system positioning performance. To underline the simulation results, experiments will be conducted with the hardware shown in Figure 19 in the year 2023. A one-way slant ranging testbed for a free space signal transmission will be set up. Here the receiver and its antenna will be mounted on a linear motion unit and moved with a resolution better than a tenth of a millimeter, whereas the antenna of the transmitter remains at a fixed position. Measured phase differences between the transmitted and received signal, together with moving steps of the linear motion unit, will be logged in a file. This data will be used to determine the ranging performance achieved by the hardware and the software programming of the FPGA of the logic board. After successfully completing the laboratory tests, field tests will be carried out with a multiple transmitter setup.

Time synchronization of different independent IMUs using GPS time

Setting up multi sensor systems on mobile platforms requires accurate time synchronization for accurate measurements. Therefore, the INS developed a software-based synchronization using a microcontroller and a GNSS receiver. The GNSS receiver provides a GPS time that is very accurate, but only available once a second. In contrast, the sensors offer much higher sampling rates of more than 100 kHz but do not exhibit any timing as accurate as GPS time. The developed very sophisticated time synchronization concept is exemplified based on a cluster of five Inertial Measurement Units (IMUs), each set up in micro-electro-mechanical systems technology (MEMS technology). The synchronization problem is solved by using a fast hardware counter for generating the time stamps of the sensor measurements. The values of the counter are synchronized to the GPS time by the pulse per second pulses (PPS) output by the GPS receiver. As PPS is directly linked to GPS time, the user now obtains measurement data in the GPS timeframe. This synchronization works either online or offline. In the offline case, the datasets' counter values of the measurements and the measurements themselves, as well as the counter values of the PPS pulses and the associated GPS time can be stored in separate files. The synchronization is carried out offline by the same algorithm used in the online case, i.e. by linking the counter values of the measurements to the PPS and by that also to GPS time. Figure 20 shows an experimental setup comprising five IMUs (MPU 6050, TDK InvenSense), a GPS receiver (LEA 6T, ublox) with antenna, as well as the microcontroller board Arduino MEGA 2560 based on the ATmega2560 with Arduino shield and with interfaces to the IMUs and the GPS receiver. Figure 21 shows a typical synchronized data output of an IMU.

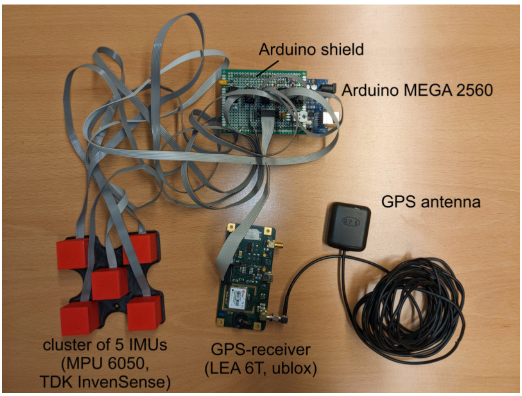

Figure 20: Experimental setup for the verification of the synchronization method

```
PPS 1000408
62899.019531 ACX 1.205 ACY 0.129 ACZ 10.802 GyX -507.000 GyY 315.000 GyZ -53.000
62899.070312 ACX 1.174 ACY 0.139 ACZ 10.556 GyX -504.000 GyY 278.000 GyZ 12.000
GPGGA,172819.00,4854.00945,N,00912.28280,E,1,09,1.15,323.0,M,47.6,M,,*5C
gps-sekunden  62899
62899.121093 ACX 1.154 ACY 0.117 ACZ 10.656 GyX -501.000 GyY 289.000 GyZ -82.000
62899.171875 ACX 1.157 ACY 0.081 ACZ 10.719 GyX -511.000 GyY 306.000 GyZ -10.000
62899.218750 ACX 1.166 ACY 0.151 ACZ 10.671 GyX -517.000 GyY 309.000 GyZ -59.000
62899.269531 ACX 1.107 ACY 0.122 ACZ 10.592 GyX -504.000 GyY 299.000 GyZ -7.000
62899.320312 ACX 1.186 ACY 0.115 ACZ 10.692 GyX -513.000 GyY 301.000 GyZ -67.000
62899.371093 ACX 1.140 ACY 0.069 ACZ 10.731 GyX -538.000 GyY 305.000 GyZ -3.000
62899.421875 ACX 1.164 ACY 0.125 ACZ 10.702 GyX -498.000 GyY 305.000 GyZ -47.000
62899.468750 ACX 1.150 ACY 0.115 ACZ 10.632 GyX -519.000 GyY 306.000 GyZ -28.000
62899.519531 ACX 1.164 ACY 0.081 ACZ 10.738 GyX -511.000 GyY 309.000 GyZ 4.000
62899.570312 ACX 1.162 ACY 0.132 ACZ 10.707 GyX -520.000 GyY 309.000 GyZ -43.000
62899.621093 ACX 1.128 ACY 0.134 ACZ 10.690 GyX -501.000 GyY 302.000 GyZ -14.000
62899.671875 ACX 1.219 ACY 0.125 ACZ 10.750 GyX -534.000 GyY 318.000 GyZ -29.000
62899.718750 ACX 1.071 ACY 0.050 ACZ 10.723 GyX -493.000 GyY 273.000 GyZ -10.000
62899.769531 ACX 1.162 ACY 0.115 ACZ 10.769 GyX -508.000 GyY 326.000 GyZ -67.000
62899.820312 ACX 1.131 ACY 0.091 ACZ 10.654 GyX -527.000 GyY 307.000 GyZ 6.000
62899.871093 ACX 1.138 ACY 0.137 ACZ 10.695 GyX -531.000 GyY 304.000 GyZ -55.000
62899.921875 ACX 1.133 ACY 0.149 ACZ 10.695 GyX -520.000 GyY 301.000 GyZ -2.000
62899.968750 ACX 1.147 ACY 0.105 ACZ 10.690 GyX -516.000 GyY 297.000 GyZ -40.000
synchr. time      accelerations                      angular rates
```

Figure 21: Typical synchronized data output

Research focus: Software development

The following sections describe the institute's software development activities in the year 2022.

INSTINCT - INS Toolkit for Integrated Navigation Concepts and Training

The in-house navigation software framework INSTINCT continues to improve. The focus of last year's efforts was reliability, extensibility, and performance. To achieve this, INSTINCT utilizes the "Flow-based Programming" paradigm (FBP). The paradigm is described in more detail in older annual reports of the institute. In short, functionality is bundled into modules, so-called nodes, which communicate over links between each other. Data flowing over the links trigger calculations in the nodes, which is the reason why it is called flow-based programming. FBP was used inside INSTINCT from the start, but now we completely utilize its benefits. The additional abstraction layer of FBP enables us to run all nodes in parallel. This is especially useful when running INSTINCT on Single-board Computers like a Raspberry Pi, which has multiple but slow CPU cores. Now we can read data from sensors, pre-process them, and run the final sensor fusion algorithm in parallel. This increases the performance depending on the used nodes by more than a factor of 2.

Moreover, INSTINCT was finally publicly released on the institute's GitHub (`https://github.com/UniStuttgart-INS/INSTINCT`). There, information on how to build the software and also its documentation can be found. The institute will continue to maintain the repository and update it with new functionality such as RTK, tightly-coupled INS/GNSS, and multi-IMU sensor fusion algorithms, which are already available on our internal development version but not yet publicly available. Further, with the publicly available GitHub repository, we hope to enable future collaboration and attract developers who make pull requests to fix bugs and/or to add new functionality.

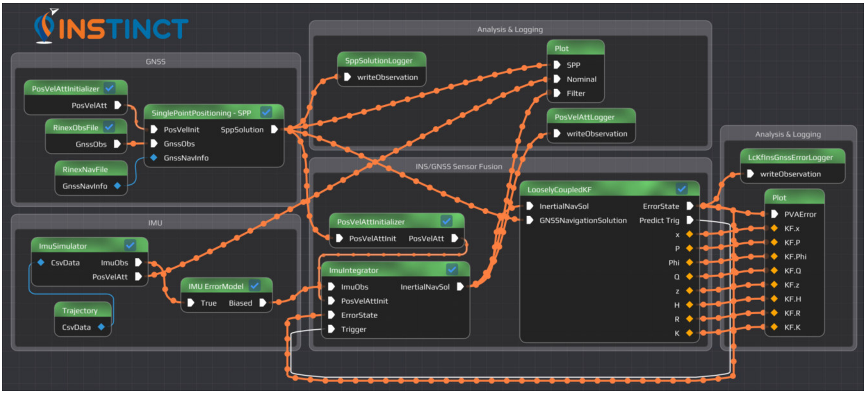

Figure 22: An example flow inside INSTINCT of an INS/GNSS loosely-coupled sensor fusion algorithm

PODCAST - Precise Orbit Determination for Complex and Agile Satellite Technology

In the previous year, the Precise Orbit Determination (POD) capabilities of PODCAST have been significantly improved. The main progress with respect to the previous year was the incorporation of carrier-phase measurements. To utilize these highly precise measurements, PODCAST now features all measurement models needed for this type of measurement. Additionally, the associated carrier-phase ambiguities can be estimated in the orbit determination process as float values. The precise GNSS products from the International GNSS Service (IGS) can now also be used within PODCAST to further improve the POD performance. To validate the POD within PODCAST, we used a Sentinel-3A trajectory and simulated corresponding measurements using our Spirent simulator. The resulting POD accuracy based on the ionosphere-free combination of these simulated pseudorange and carrier-phase measurements is depicted in Figure 23. A second POD solution based on in-orbit measurements is displayed in Figure 24. Further improvements that are expected to benefit the POD performance are planned for the coming year. These include a robust outlier detection, cycle slip detection, as well as an investigation of POD for agile satellite missions.

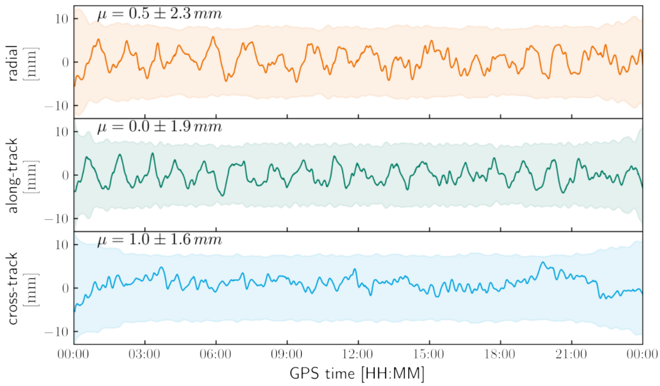

Figure 23: POD accuracy and 3-sigma bounds (shaded area) in radial, along-track, and cross-track direction for simulated pseudorange and carrier-phase measurements based on a Sentinel-3A trajectory.

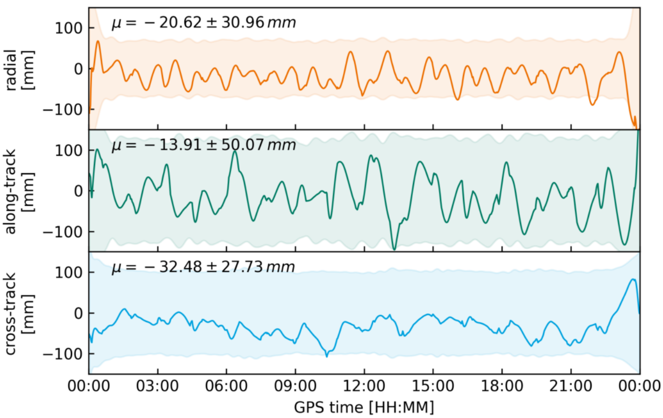

Figure 24: POD accuracy and 3-sigma bounds (shaded area) in radial, along-track, and cross-track direction for in-orbit pseudorange and carrier-phase measurements of Sentinel-3A.

PBD - Precise Baseline Determination

As a new functional aspect of PODCAST, the topic of Precise Baseline Determination (PBD) was introduced. PBD refers to the estimation of the 3D relative position of a rover spacecraft with respect to a base spacecraft with the utmost precision. The precise determination of inter-spacecraft baselines is a key technology for Low Earth Orbiting (LEO) satellite missions featuring formation flying satellites. These formations allow for advanced mission profiles that would not be possible with a single spacecraft. Applications are gravimetry and Synthetic Aperture Radar (SAR) missions, such as along-track interferometry for traffic monitoring, and cross-track interferometry for deriving accurate Digitial Elevation Models (DEM). One example is the German mission TanDEM-X, where the twin satellites TerraSAR-X and TanDEM-X perform measurements of the digital elevation of the Earth's surface. In contrast to gravimetry missions, SAR missions do not feature an inter-satellite laser ranging system but rely solely on GNSS-based baseline determination. The TanDEM-X mission requires a precision of 1 mm with the confidence of 68% for the projected baseline in the cross-track direction. The latest available advancements in PBD are utilized to achieve the necessary estimation quality and it is aimed to also reach these precisions within the in-house software PODCAST.

While state-of-the-art PBD techniques are suitable for meeting the current requirements, future SAR missions will demand higher baseline precisions for more challenging mission profiles. Especially the upcoming trend for agile missions holds multiple challenges that have to be overcome. Therefore, PODCAST takes a significant step to improve the PBD precision of inter-spacecraft baselines for future agile and non-agile formation flying spacecraft missions.

Within the last year, the software framework for PBD was implemented within PODCAST. The implementation obeys the overall concept of PODCAST, enabling flexible testing of the software for novel approaches related to Precise Orbit Determination. Topics related to PBD that were finalized were the detection of cycle slips of GNSS carrier phase observations, algorithms to recover the integerness of the ambiguities of said carrier phase observations, and the overall estimation tool chain. A Kalman-Filter-based approach was selected for the PBD estimation. As the Kalman Filter profits considerably from a good initialization, a least squares estimate is calculated before the start of the actual estimation loop. The following Kalman Filter estimation consists of the smoothed result of a forward and a backward Kalman Filter estimate.

In test scenarios, the state-of-the-art precision of 1 mm could be reached. The results can be seen in Figure 25. The continuous line indicates the errors in the radial, along-track, and cross-track direction of the satellites and the dashed lines indicate the confidence of different levels. The grey dashed lines indicate the estimated 3-sigma confidence of the filter, while the blue and green dashed lines indicate the empirical 1- and 3-sigma bounds, recovered from the knowledge of the true error. Moreover, it was possible to verify the capabilities of PODCAST regarding PBD by processing observations from a low-cost off-the-shelf GNSS receiver. The test setup consisted of the aforementioned receiver, which was plugged into a GNSS signal stimulator. The orbit for the simulated scenario was propagated by the in-house Precise Orbit Propagator (PrOP). The PBD scenario consisted of two spacecraft that were simulated consecutively, which resulted in asynchronous observations of the GNSS satellites. After the re-synchronization of the observed signals, the former claimed precision of 1 mm could again be reached, as shown in Figure 26. Upcoming challenges are the introduction of agility, the mitigation of the ionospheric influence, and the improvement of robustness. Furthermore, tests for in-orbit satellite observations are still pending.

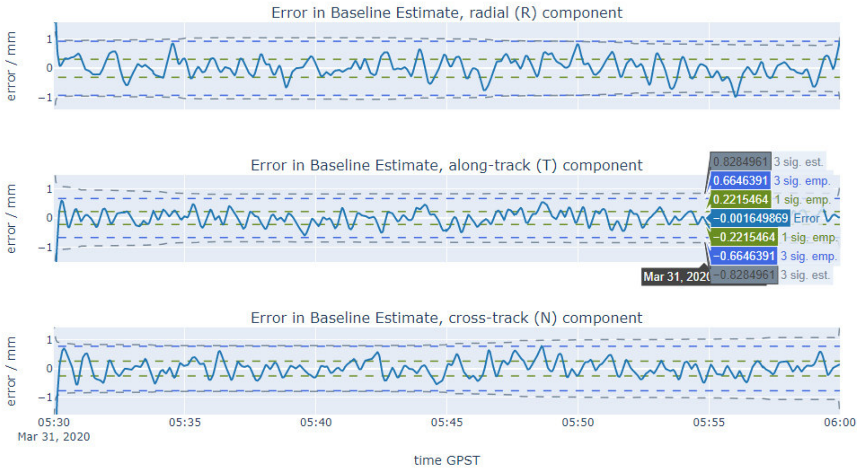

Figure 25: PBD accuracy, estimated 3-sigma bounds (grey dashed line), and empirical 1- and 3-sigma bounds (blue and green dashed lines) in radial, along-track, and cross-track direction for simulated pseudorange and carrier-phase measurements of two chasing satellites with a baseline length of about 7 km.

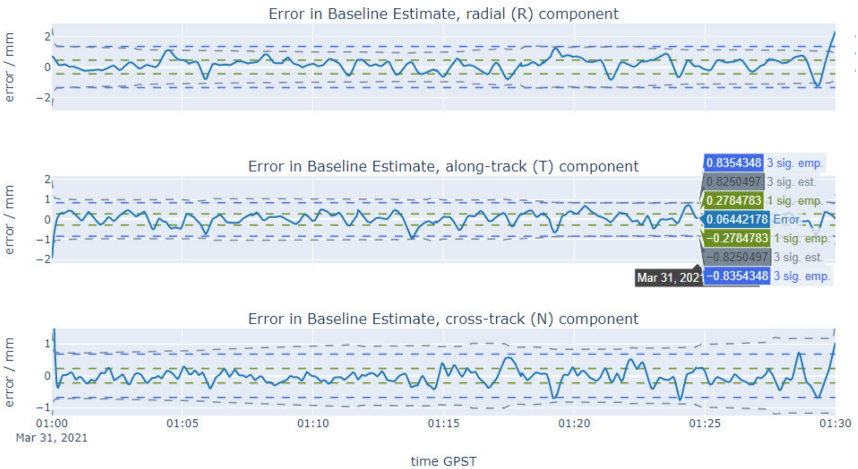

Figure 26: PBD accuracy, estimated 3-sigma bounds (grey dashed line), and empirical 1- and 3-sigma bounds (blue and green dashed lines) in radial, along-track, and cross-track direction for simulated and hardware received pseudorange and carrier-phase signals of two chasing satellites with a baseline length of about 7 km.

Development of a PPP Software for Troposphere Studies

Troposphere delays are usually regarded as isotropic in PPP applications. However, in reality, the troposphere is inhomogeneous and can cause considerable errors in extreme weather and terrain conditions, sometimes up to ten centimeters. Researchers proposed two-axis gradient models to compensate for this disparity, but the model does not have such a good performance concerning accuracy and flexibility. In order to overcome the shortcomings in existing models, we proposed a new troposphere model based on B-splines. In this model, the troposphere delays at specific elevations are modeled as a circular B-spline curve, so that we can get the troposphere information at random azimuth angles.

The new model has benefits in the following points:

- Better coordinate repeatability. We compare the estimated coordinates with ITRF20 and the results show that the new model brings a significant improvement compared to traditional models: up to 30 %.
- More accurate and flexible. The new model is more capable in modeling real troposphere wet delays. The post-fit residuals in the EKF show that the new model has 10 % improvement compared to traditional models.
- More realistic. The new model can get more realistic troposphere results because the B-spline can fit the real troposphere delay better.

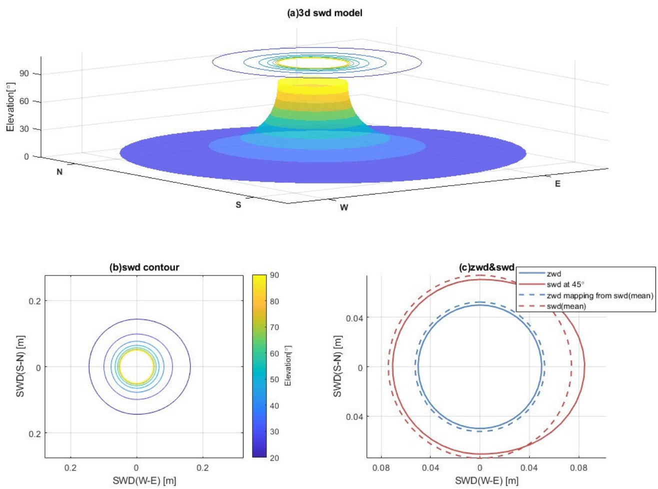

Figure 27: Figures (a) and (b) show daily averages of the troposphere wet delay around the IGS geodetic station at Wettzell (WTZR) on January 1st 2022. The contours are constructed by the B-spline model. (c) shows a simulated B-spline curve and reveals the relation between the SWD and ZWD.

Navigation Algorithms for Micro Launcher

The growing market for putting large numbers of small satellites into orbit requires new concepts for launch systems. The cost for those transportation systems should be significantly lowered with respect to today's launchers. In recent years, the industry has identified that micro launchers may satisfy this task. Micro launchers are small rockets carrying about 500 kg of payload into Low-Earth orbit. To achieve the objective of low cost, the rocket design is focused on modularity and reuse. This results in modular design not only for engines and the structure, but also for sensors, actuators, and software. Concerning the guidance and the navigation software, advanced development concepts have to be set up for underlining the modular designs in this area, too. Therefore, ESA initiated a project called "Generic Guidance and Navigation Onboard Software for Microlauncher" with ASTOS Solutions GmbH as the contractor. Here, a software library with guidance and navigation algorithms has to be established that makes a flexible software implementation possible and can be optimized to the particular launcher by auto coding. As a subcontractor, the INS is concerned with the navigation part and develops off-the-shelf navigation algorithms. The integrated navigation algorithm implemented in 2021 was finalized, verified and extensively tested by ASTOS's multi-purpose tool for space applications. The navigation is limited to the three-dimensional positioning and the orientation in three axes. The algorithm computes integrated navigation estimates in real-time by reading the outputs of GNSS receivers and several IMUs distributed in the launcher in parallel. The company ASTOS verified the auto coding performance using the Matlab/Simulink script of the INS. Figure 28 shows deviations in position and orientation during lift-off between the simulated trajectory and the computed trajectory using dedicated simulated GNSS and IMU data. The accuracy of the filter is within the requirements specified within the project for a nominal injection accuracy.

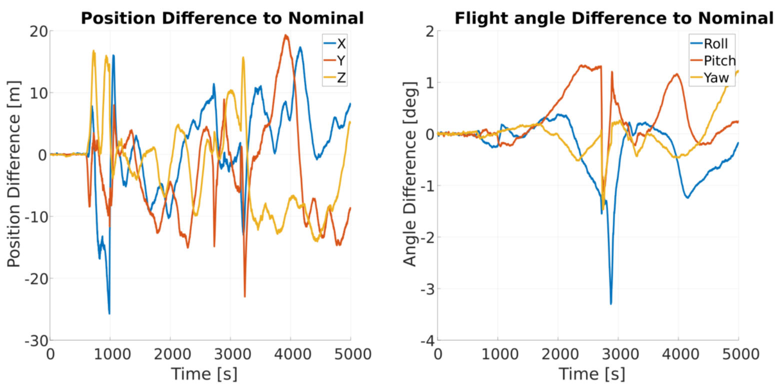

Figure 28: Filter performance

Sensor fusion of different independent IMUs

The combination of multiple IMUs yields redundancy and increased accuracy compared to a single IMU. For the use on a mobile platform, a sensor fusion algorithm was implemented in INSTINCT and subsequently tested on the experimental setup shown in Figure 20. The algorithm reads the data output as shown in Figure 21 and sorts each sensor's measurements before they are fused. The principle behind the fusion algorithm is shown in Figure 29. The IMUs measurements have a common time base realized through the GPS module. A Kalman filter then combines the measurements and provides a measurement from a virtual single IMU. This combined output can then be fed into further INS-/GNSS-fusion. In comparison to simple averaging of the IMUs measurements, the Kalman filter is capable of considering the IMUs dynamics. These are modeled by integrated random walk on the accelerometer and gyro measurements, respectively. Results from a static test are shown in the Allan deviation plot in Figure 30 (here, only the angular rate's vertical component is shown as the other components, and the accelerations are similar). The Allan deviation is reduced significantly for small averaging periods τ. For rising τ, the combined solution converges into IMU 1, which acts as the reference sensor in the tested configuration, because of effects that are not modeled by the Kalman filter. In conclusion, the lowered Allan deviation implies that the accuracy of IMU measurements can be improved when combining multiple IMUs measurements.

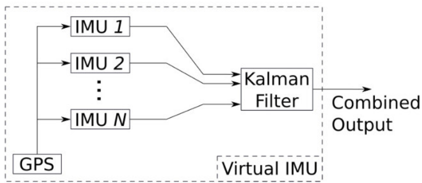

Figure 29: Sensor fusion principle

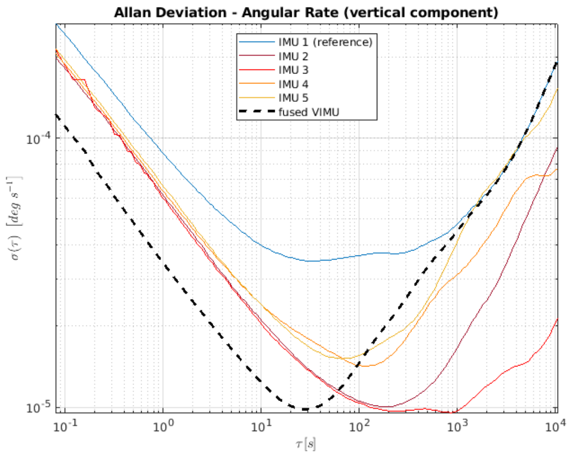

Figure 30: Allan deviation of gyroscope measurements of the single IMUs and the combined virtual IMU (VIMU)

Research focus: Applications

The following sections describe applications on which the INS worked on in the year 2022.

Testfeld eFliegen BW

The INS is one of the institutes of the University of Stuttgart that is building up the "Testfeld für energieeffizientes, elektrisches und autonomes Fliegen" (short: "Testfeld eFliegen BW") alongside partners from industry under the lead of the iFR (Institut für Flugmechanik und Flugregelung der Universität Stuttgart). All information on the operation, tests, and other news can be found on the homepage `https://area-bw.de/`, which is maintained by the institute.

Customized research platform Prism Coaxial X8

In 2022 the institute purchased a Prism Coaxial X8 drone from Watts Innovations and customized it for the usage as a research platform for navigation solutions. Figure 31 shows the drone after its first flight, which was conducted at "Ihinger Hof", one of the institute's primary testing sites. This addition to the institute's fleet of drones provides much more capacity regarding mass (up to 11 kg) and space for sensors, compared to the other available drones. Therefore, we are now able to test multiple sensors simultaneously and thereby compare measurements of the same flight trajectory. The institute's mechanical workshop has constructed an adapter plate that can carry a range of sensors and equipment as shown in Figure 32. This adapter plate can be mounted on top of the drone using the four grey screws as shown in Figure 33.

Figure 31: Prism Coaxial X8 after its first flight

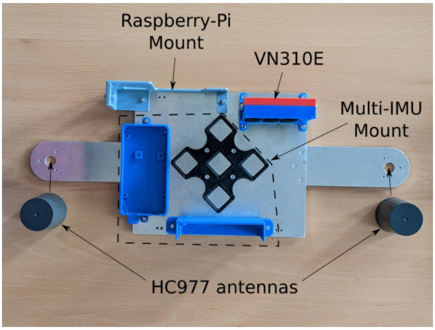

Figure 32: Adapter plate for the Prism Coaxial X8, constructed at the institute's mechanical workshop

Figure 33: Mounting points for the adapter plate of the Prism Coaxial X8

List of Publications

Gutsche K., Hobiger T., Winkler S., Stucke B.: PODCAST: Precise Orbit Determination Software for LEO Satellites, Proceedings of the 35th International Technical Meeting of the Satellite Division of the Institute of Navigation (ION GNSS+ 2022), 3707–3719, Denver, USA.

Topp T., Hobiger T.: Flow-Based Programming for Real-Time Multi-Sensor Data Fusion, Proceedings of the 35th International Technical Meeting of the Satellite Division of the Institute of Navigation (ION GNSS+ 2022), 2492–2502, Denver, USA.

List of Poster Presentations

He S., Becker D., Hobiger T.: The impact of GNSS multipath errors on ZTD estimates based on PPP, 2nd IAG Commission 4 Symposium (IAG C4 Symp 2022), Potsdam, Germany, https://doi.org/10.5281/zenodo.7326315.

Gutsche K., Hobiger T., Winkler S.: Adaptive Extended Kalman Filtering for Precise Orbit Determination, Poster presented at the 8th International Colloquium on Scientific and Fundamental Aspects of GNSS, Sofia, Bulgaria.

Research Stays

Wang, Rui (20.5.2022 – 18.6.2022)

Visiting PhD student at Wrocław University of Environmental and Life Sciences, Poland, to work on the implementation of PPP algorithms and the development of a mathematical framework that includes functional and stochastic models. This research stay allowed for close collaboration with researchers at the host institution, the exchange of different research approaches, and a deeper understanding of various error sources in GNSS positioning, which expanded the PPP applications based on EKF, especially in the field of improved tropospheric modeling.

Activities in National and International Organizations

Prof. Hobiger

Editorial board member "Acta Geodaetica et Geophysica"
Member of the German Geodetic Commission
Corresponding member of the Austrian Geodetic Commission
Fellow of the International Association of the Geodesy
Member of the Institute of Navigation
Member of the Royal Institute of Navigation
Member of the German Institute of Navigation
Member of the American Geophysical Union

Prof. Kleusberg
Fellow of the International Association of the Geodesy
Member of the Institute of Navigation
Member of the Royal Institute of Navigation
Member of the German Institute of Navigation

Teaching and Supervision

With the COVID-19 restrictions on lectures and exercises completely lifted, we saw an almost normal year in all our educational activities. A smaller number of students in elective courses posed certain challenges so that exercise formats had to be slightly adapted to accommodate smaller groups and achieve the learning objectives that are based on problem based learning or group work. The availability of two GNSS simulators allows us to implement realistic GNSS scenarios and even deal with threats like jamming or spoofing without the need to transmit signals over the air. Through Spirent's Academia Programme and Orolia's Academic Partnership Program, we have access to industry-standard GNSS simulation tools in undergraduate and graduate courses and train our students with the tools they might encounter at their future workplaces. We also saw an increasing number of master's students from different curricula at the University of Stuttgart, who carry out their projects with several of our industry partners. This turned out to be mutually beneficial - students can get in close contact with potential employers and present themselves, and companies might find the right well-educated and trained employees.

Bachelor Thesis

Ertmann, Richard: Nachweis der dynamischen Leistungsfähigkeit verschiedener GNSS-Empfänger durch Simulation (Supervisor: D. Becker)

Master Thesis

Stucke, Bayram: Development of a Satellite Trajectory Generator for Precise Orbit Determination (Supervisor: Y. Enginger (Airbus))

Education - Lectures/Exercises

Bachelor Geodesy & Geoinformatics

Adjustment Theory I (Hobiger, Becker)	2/1
Adjustment Theory II (Hobiger, Becker)	2/1
Fundamentals of Navigation (Hobiger, Becker)	2/2
Integrated Fieldwork (Sonnleitner, Topp)	10 days
Introduction of Geodesy and Geoinformatic (Hobiger, Becker)	2/2
Measurement Techniques II (Wehr, Sonnleitner, Klink)	2/2
Valuation (Caesperlein)	1/0

Master Geodesy & Geoinformatics

Filtering Techniques (Hobiger, Topp)	1/1
Inertial Navigation (Hobiger, Topp)	1/1
Inertial Sensors (Hobiger)	1/0
Integrated Navigation (Hobiger, Topp)	1/1
Measurement Techniques in Navigation (Wehr, Klink)	1/3
Satellite Navigation (Hobiger, Becker)	1/1
Signal Propagation and Antenna Theory (Hobiger, Becker)	1/1
State Estimation in Dynamic Systems (Hobiger, Sonnleitner, Maier)	2/1
Object-oriented Programming in C++ (Hobiger, Sonnleitner, Topp)	1/3
Project (Sonnleitner)	6/0
Property Valuation (Caesperlein)	1/0
Simultaneous Localization and Mapping (Hobiger, Maier, Klink)	1/1

Master GeoEngine

Dynamic System Estimation (Hobiger, Wang, Maier)	2/1
Integrated Positioning and Navigation (Hobiger, Topp, Maier)	2/1
Satellite Navigation (Hobiger, Becker, Stucke)	2/1

Master Aerospace Engineering

Inertial Navigation (Hobiger)	2/0
Satellite Navigation (Hobiger)	2/0

Master Electromobility

Navigation of Surface Vehicles (Becker)	2/0
Satellite Navigation (Hobiger)	2/0

Institute for Photogrammetry

Geschwister-Scholl-Str. 24D
D-70174 Stuttgart
Tel.: +49 711 685 83336
Fax: +49 711 685 83297
info@ifp.uni-stuttgart.de
http://www.ifp.uni-stuttgart.de

Head of Institute

Prof. Dr.-Ing. Uwe Sörgel

Deputy:	apl. Prof. Dr.-Ing. Norbert Haala
Personal Assistants:	Carmen Kaspar
	Ute Schinzel
Emeritus Professor:	Prof. Dr.-Ing. Dieter Fritsch

Academic Staff

M.Sc. Tobias Bolz	Object Reconstruction from SAR Images
M.Sc. David Collmar	Crowd-based Data Collection
Dr.-Ing. Michael Cramer	Photogrammetric Systems
Dipl.-Ing.(FH) Markus Englich	Laboratory, Computing Facilities
apl. Prof. Dr.-Ing. Norbert Haala	Photogrammetric Computer Vision
M.Sc. Lena Joachim	Integrative Computational Design
M.Sc. Michael Kölle	Crowd-based Data Collection
M.Sc. Dominik Laupheimer	Classification in Remote Sensing
M.Sc. Stefan Schmohl	Deep Learning in 3D Remote Sensing
M.Sc. Philipp Schneider	SAR Interferometrie
Dr.-Ing. Volker Walter	Geoinformatics

Stipendiaries and external PhD Students

M.Sc. Jonathan G. Santiago	Multimodal Representation Learning
Dipl.-Phys. Hendrik Schilling	Classification of Hyperspectral Data
M.Sc. David Skuddis	LiDAR-based Mobile Mapping
M.Sc. Wei Zhang	Visual SLAM for Augmented Reality
M.Sc. Xinlong Zhang	Object Recognition from LiDAR Data

Guest Scientists

M.Sc. Grzegorz Gabara	3D Object Reconstruction

External Teaching Staff

Dipl.-Ing. Stefan Dvorak, Amt für Stadtentwicklung und Vermessung, Reutlingen

Research Activities in ifp organized in four thematic Groups

Geoinformatics	Dr.-Ing. Volker Walter
Photogrammetric Computer Vision	apl. Prof. Dr.-Ing. Norbert Haala
Photogrammetric Systems	Dr.-Ing. Michael Cramer
Remote Sensing	Prof. Dr.-Ing. Uwe Sörgel

Research Projects

Crowd-driven Active Transfer Learning for Semantic Segmentation of Multi-Temporal 3D Point Clouds

The main bottleneck of machine learning systems, such as convolutional neural networks, is the availability of labeled training data. Hence, much effort (and thus cost) is caused by setting up proper training data sets. However, models trained on specific data sets often perform unsatisfactorily when used to derive predictions for another (yet related) data set. We aim to overcome this problem by employing active learning (AL) to iteratively adapt an existing classifier to another domain. Precisely, we are concerned with semantic segmentation of 3D airborne laser scanning point clouds of multiple epochs.

Our basic workflow is depicted in Figure 1. Our means to minimize labeling costs is in the first place AL to actively sample only the subset of points worth labeling by human operators. To initialize our pipeline, we first present a completely unlabeled point cloud to the crowd and ask crowdworkers to indicate one point for each of our desired classes. Received points are then checked by a second group of crowdworkers to form the initialization training set. This can then be used for training a first machine learning model, which can be a feature-driven or data-driven classification approach (e.g. a Random Forest classifier and a CNN classifier, respectively). This initial model is then utilized for inference on the remaining unlabeled data points to determine most informative samples, which can then be presented to the crowd oracle for labeling. Based on the enhanced training pool, a new classification model is trained and the loop is repeated for n iteration steps. Identification of most informative points is achieved by entropy of a posteriori probabilities.

This approach however implies that no samples from a source domain are available, so that the iteration needs to be performed from scratch. Since we expect that in many applications such a data set exists, we would like it to contribute for learning our model. AL is well suitable

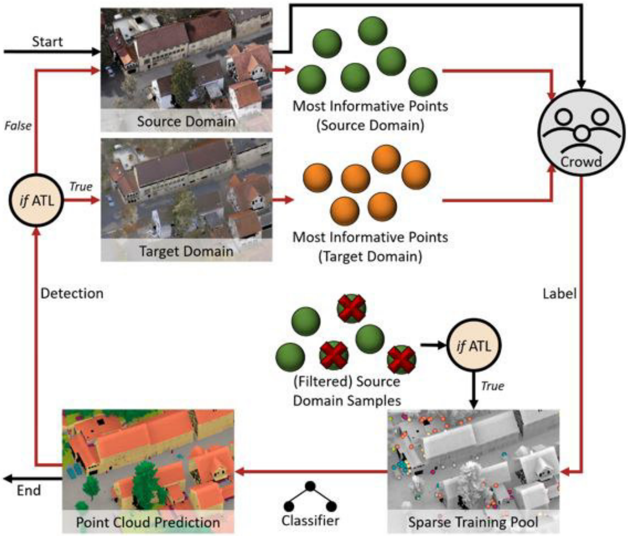

Figure 1: Crowd-powered pipeline for Domain Adaption.

for such Domain Adaptation (DA) tasks by design (if labels can be obtained in the target domain) by simply changing the pool of instances where the query function operates from the source to the target domain. The comprehensive training pool is then obtained by merging the training set sampled in the source domain with the newly sampled and labeled points of the target domain. We refer to this procedure as active transfer learning (ATL). This DA technique will work well when the source and target domain are sufficiently similar, but might also result in even more labeling effort when the domain gap is considerable.

If source domain samples used for training the classification model are not representative for the target domain, the selection of points in the target domain is suboptimal since the assumed class borders (in the vicinity of which samples are drawn) differ from the ones truly inherent in the target domain. Consequently, more iteration steps might be necessary to adapt the initial model to the new distribution and starting the iteration from scratch would be more cost-efficient. However, it is often difficult to decide whether two domains are similar enough for adaptation, i.e., whether re-using samples of a source domain is beneficial or harmful. Hence, an additional procedure is required where samples of the source domain can be included to optimally boost convergence or at least ensuring that the effect of conflicting samples is neutralized in case of a too large domain gap.

For this to achieve, we remove samples of the source domain which are most inconsistent with the target domain by measuring the disagreement between a model trained by samples of the source domain only and another model trained by the combined training set from the source and target domain. This means that we check which samples of the source domain disagree most with samples of the target domain and remove those before re-training our current classifier on samples from both the source and target domain.

The proposed methodology is applied to the newly introduced Hessigheim 3D benchmark data set comprising temporally disjoint point clouds of the same but extended area (cf. Figure 2). The point clouds incorporate different characteristics with respect to the acquisition date and sensor configuration. We demonstrate that our workflow for DA is designed in such a way that it i) offers the possibility to greatly reduce labeling effort compared to a passive learning baseline or to an AL baseline trained from scratch, if the domain gap is small enough and ii) at least does not cause more expenses (compared to a newly initialized AL loop), if the domain gap is severe. The latter is especially beneficial in scenarios where the similarity of two different domains is hard to assess.

(a) H3D - Epoch March 2018

(b) H3D - Epoch November 2018

(c) H3D - Epoch March 2016

Figure 2: Compilation of our data sets/epochs used for testing our approach. Each visualization depicts an overview of the complete data set, where the training set is colored according to available RGB data while the test set is presented as shading (left). Respective close-ups are colorized according to the number of returns of an emitted laser pulse (right).

Raster Integration of Polygons for Use as Training Data in CNNs

Convolutional Neural Networks (CNNs) are widely used in various applications in the field of remote sensing. CNNs require large amounts of training data during their training phase. Additionally, the performance of CNNs heavily depends on the quality of the training data . Paid crowdsourcing can be used for the data acquisition of such training data for CNNs. Although paid crowdsourcing has many advantages, one of the biggest problems is the poor quality of the data obtained. A common approach to improve data quality is to have different crowdworkers collect the same objects multiple times, followed by an integration using majority voting. While majority voting can be easily used for tasks such as labelling, it is not suitable for integrating complex geometric objects such as irregular polygons.

This limitation only applies to vector data. For raster data a majority vote can easily be performed on pixel-basis. Vector polygons can be integrated when converting them first from vector to raster and then performing a majority vote at pixel level, which only requires one threshold parameter. The threshold parameter determines the number of pixels needed for a successful majority vote. Figure 3 visualizes a pixel-level integration with a majority vote on the example of a tree outline. The raster-based integration led to an improvement of about 14 percentage points for the mean intersection over union (IoU). Figure 4 illustrates the integration for a polygon with 15-fold acquisition.

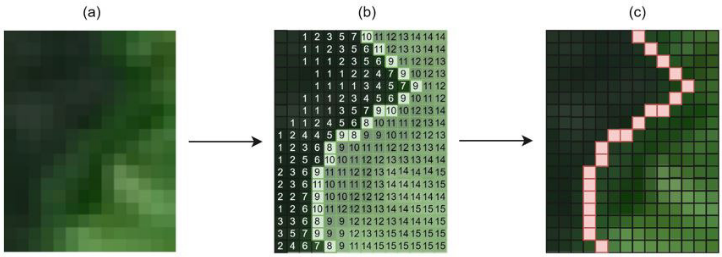

Figure 3: Visualization of raster integration. (a) Section of image tile, (b) Majority vote on pixel basis with highlighted threshold areas, (c) Integrated polygon outline.

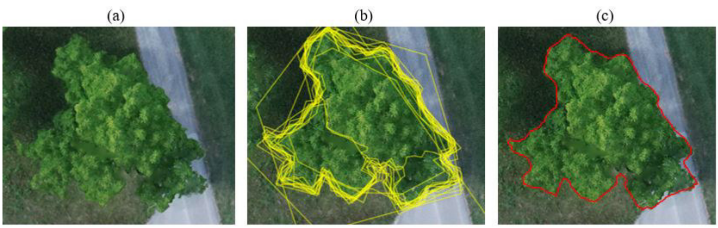

Figure 4: Integration steps. (a) Raw image, (b) 15 Crowd acquisitions, (c) Integrated result.

IntCDC: Real-Time Environment Mapping for a Cyber-Physical Construction Platform

The Cluster of Excellence IntCDC (Integrative Computational Design and Construction for Architecture) of the University of Stuttgart aims to rethink design, fabrication and construction in order to tackle the current challenges of the building industry, such as the lack of sustainability and productivity. IntCDC is funded by the German Research Foundation (DFG).

One of the research activities within this interdisciplinary project is the development of a cyber-physical construction platform, namely a tower crane, for automated on-site assembly of prefabricated building elements. In cooperation with the Institute for System Dynamics, we are developing the control for the automated tower crane and the corresponding monitoring system. The goal is to enable a fully automated load handling including the pick and place processes and the transportation in between. Therefore, task scheduling, path planning and an online feedback for collision avoidance during transportation are needed.

As main data source for solving these tasks, we investigate an array of crane-mounted cameras, which take overlapping images of the workspace of the crane. We installed such a system at the IntCDC test site to be able to test different approaches for 3D reconstruction of the workspace and the integration of the generated data into the crane control. The goal is to derive an up-to-date DEM (Digital Elevation Model), which is the basis for autonomous path planning. A popular vision-based approach to realize the real-time 3D reconstruction is Visual SLAM (Simultaneous Localization and Mapping), although the focus of its applications so far has often been localization. Thus, we performed a study to evaluate the mapping quality of four state-of-the-art Visual SLAM solutions for our specific use case, because the quality of the DEM is important for this safety critical application.

The results (see Figure 5) show that all tested methods work with the crane camera dataset. They can even compete with the offline photogrammetric result from Agisoft Metashape in terms of accuracy. However, there is still room for improvement in the completeness of the real-time data, which is due to the sparsity of the SLAM methods. Within our future work, we aim to extend the SLAM solution to a dense multi-camera approach and integrate further improvements like e.g. the consideration of the crane sensor measurements within the reconstruction process.

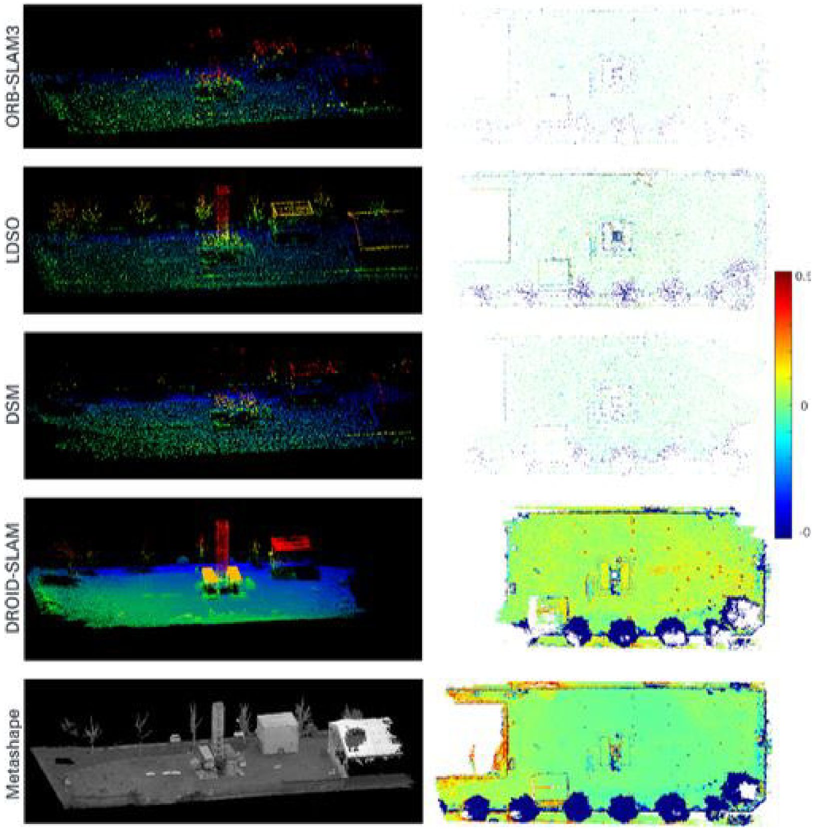

Figure 5: 3D point clouds (left) and differences between DEM and reference (right) for four Visual SLAM solutions (row 1-4) compared to the offline photogrammetric result generated with Agisoft Metashape (row 5). The input to all solutions were images taken by one crane camera during a full rotation of the jib.

LiDAR-based Trajectory Optimization for SLAM

LiDAR-based SLAM (Simultaneous Localization and Mapping) is a popular technique used in mapping applications as well as in autonomous systems for building maps and localizing the position of robots in real-time. LiDAR sensors can provide an accurate point cloud of the environment. SLAM algorithms focus on the derivation of movement information from point clouds of different points in time. The three main steps in der derivation of movement information are: 1. Assume correspondences between LiDAR scans from different points in time 2. Model the discrepancy of the scans by a target function 3. Minimize the target functional.

Within the framework of this project, an IMU-supported SLAM method is being developed. The use of an IMU increases the robustness as well as the accuracy especially at high accelerations and rotation rate changes. The goal of the method is to achieve a very high accuracy in trajectory estimation.

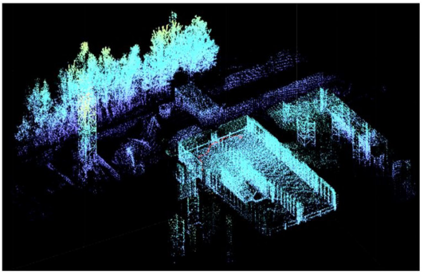

Figure 6: Resulting exemplary point cloud after SLAM

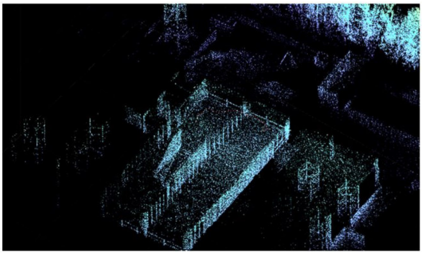

Figure 7: Resulting exemplary point cloud, close view

Towards robust indoor visual SLAM and dense Reconstruction for mobile Robots

Mobile robots are being increasingly employed in various indoor scenarios. The fundamental prerequisite is that the robot can reconstruct an accurate and complete map of the observed environment and estimate the track of its movements in this map. Current visual SLAM methods can perform this task reasonably well, but mostly in small spaces, such as a single room, and often tested in well-textured environments. In real-world applications of large indoor scenes, they lack robustness and fail to build a globally consistent map. To this end, we propose a novel system that can robustly solve the problem encountered by existing visual SLAM methods, such as weak texture and long-term drift. By combining information from a wheel odometer, the robot poses can be predicted smoothly in the absence of texture. The geometric cues are leveraged by aligning Truncated Signed Distance Function (TSDF) based submaps to minimize the long-term drift. To reconstruct a more complete and accurate dense map, we refine the sensor depth maps by taking advantage of color information and the optimization result of global bundle adjustment.

Figure 8: a) Failed camera tracking in front of a white wall; b) Smooth tracking after fusing with wheel odometer measurements; c) Reconstructed map contaminated by the misalignment due to missed large-baseline loop closure; d) Improved dense map with submap registration.

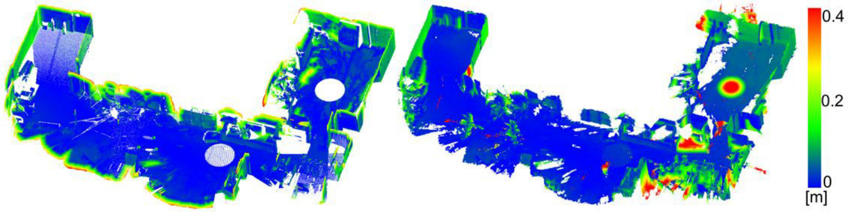

Figure 9: Evaluation on reconstructed 3D map. Left: Reference model by Faro laser scanner. Right: our reconstructed 3D map. Colors indicate the nearest neighbor distance to each other.

As a result, the system can provide precise trajectory estimation and a globally consistent map for the downstream tasks. We validate the accuracy and robustness of the proposed method on both public and self-collected datasets and show the complementary nature of each module. Evaluation results based on high precision ground-truth show an improvement in the mean Absolute Trajectory Error (ATE) from 21 cm to 2 cm for the trajectory estimation, and the reconstructed map has a mean accuracy of 8 cm.

Fusion of BIM and SAR (BIMSAR) for Semantic Building Monitoring

According to the announcement of German Federal Ministry of Transport and Digital Infrastructure, Building Information Modeling (BIM) has become the standard digital format for the construction project of high-building and infrastructure in Germany after 2020. To contribute to the building monitoring in future, we are granted in an innovative project BIMSAR from German Federal Ministry for Economic Affairs and Energy. Our aim is to fuse BIM and SAR data to realize a semantic building monitoring at a fine scale, e.g., for change detection or deformation analysis.

Here BIM will be the reference basis for a digital building model. Via Persistent Scatterer Interferometry (PSI), PS-points are extracted from a high-resolution SAR image stack. These PS-points are regarded as pseudo-substructures, of which a building consists. Their important properties contain geographic position and deformation estimates. The PS-points will then be fused with the BIM-models and clustered to different self-contained units like façades or roofs. This step will be implemented via a novel distance metric adapted by a dimension reduction, if needed, as well as AI-based algorithms. The fused data will be finally integrated into a web- and cloud-based monitoring platform. Except visualization, this platform also contains local and expert knowledge to assist users in data analysis and decision making.

Figure 10: Proposed workflow: The PSI Points are clustered, based on their deformation time series. Than they are combined with a BIM Model, that represents the structural information of the building. Finally, the end-user can investigate in the deformations of each part of the building, via a web platform displayed on the bottom.

Building Information Modeling (BIM) can be used throughout the lifecycle of a construction project, from design to demolition or renovation. With a high level of detail and temporal modeling, decision-making processes can be more efficiently and cost-effectively carried out between the administration and the builder. Compared to traditional on-site measurement of ground movements, satellite-based InSAR technology can be applied much more cost-effectively in terms of time and space. With data from the Copernicus Sentinel-1 satellites, ground movements (in the millimeter range) can be estimated every 3 days under optimal conditions, covering an area of 250 km x 180 km. However, it is unclear which movement belongs to which object, such as ground, wall, or roof. Using the developed BIMSAR methods, a fused BIM model is created. Each building component also contains movement data in addition to its properties. The models are made available for building monitoring through an online platform via web browser. Users can use interactive tools to visualize, rotate, zoom in and out of a BIM model and examine detected movements to see if a building component or the entire building is at risk.

On the Information Transfer between Imagery, Point Clouds, and Meshes for Multi-Modal Semantics

The semantic segmentation of the huge amount of acquired 3D data has become an important task in recent years. Images and Point Clouds (PCs) are fundamental data representations, particularly in urban mapping applications. Textured meshes integrate both representations by wiring the PC and texturing the reconstructed surface elements with high-resolution imagery. Meshes are adaptive to the underlying mapped geometry due to their graph structure composed of non-uniform and non-regular entities. Hence, the mesh is a memory-efficient realistic-looking 3D map of the real world.

For these reasons, we primarily opt for semantic segmentation of meshes, which is a widely overlooked topic in photogrammetry and remote sensing yet. In particular, we head for multi-modal semantics utilizing supervised learning. However, publicly available annotated geospatial mesh data has been rare at the beginning of this research. Therefore, annotating mesh data has to be done beforehand.

We aim for a multi-modal fusion that enables multi-modal enhancement of entity descriptors and semi-automatic data annotation leveraging publicly available annotations of non-mesh data. We propose a novel holistic geometry-driven association mechanism that explicitly integrates entities of modalities imagery, PC, and mesh (see Figure 11). The established entity relationships between pixels, points, and faces enable the sharing of information across the modalities in a two-fold manner: (i) feature transfer (measured or engineered) and (ii) label transfer (predicted or annotated). The implementation follows a tile-wise strategy to facilitate scalability to large-scale data sets. At the same time, it enables parallel, distributed processing, reducing processing time. We demonstrate the effectiveness of the proposed method on the ISPRS benchmark data sets Vaihingen 3D and Hessigheim 3D.

Taken together, the proposed entity linking and subsequent information transfer inject great flexibility into the semantic segmentation of geospatial data. Imagery, PCs, and meshes can be semantically segmented with classifiers trained on any of these modalities utilizing features derived from any of these modalities. Particularly, we can semantically segment a modality by training a classifier on the same modality (direct approach) or by transferring predictions from other modalities (indirect approach). Hence, any established well-performing modality-specific classifier can be used for semantic segmentation of these modalities – regardless of whether they follow an end-to-end learning or feature-driven scheme.

We discuss and analyze various Ground Truth (GT) generation methods. The semi-automatic labeling leveraging the entity linking achieves consistent annotation across modalities and reduces the manual label effort to a single representation (see Figure 12). To further reduce the labeling effort to a few instances on a single modality, we combine the proposed information transfer with active learning. Subsequently, we compare the resulting classifier performances to conventional passive learning using expert annotation. In summary, we accentuate the mesh and its utility for multi-modal fusion, GT generation, multi-modal semantics, and visualization purposes.

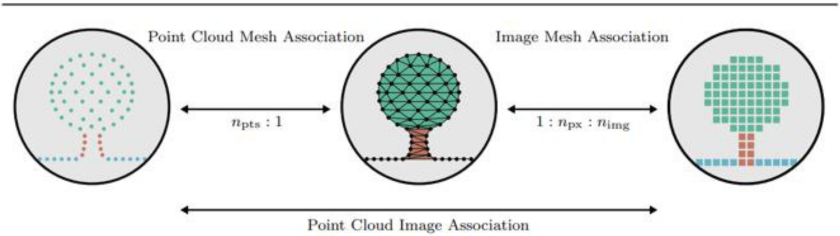

(a) Point Cloud Mesh Association (PCMA)

	Mesh $\mapsto$ PC ($1 : n_{pts}$)	PC $\mapsto$ Mesh ($n_{pts} : 1$)
Feature Transfer	Copy Value	Median Aggregation
Label Transfer	Copy Value	Majority Vote

(b) Image Mesh Association (ImgMA)

	Mesh $\mapsto$ Img ($1 : n_{px} : n_{img}$)	Img $\mapsto$ Mesh ($n_{img} : n_{px} : 1$)
Feature Transfer	Copy Value	Median Aggregation
Label Transfer	Copy Value	Majority Vote

(c) Point Cloud Image Association (PCImgA)

	PC $\mapsto$ Img	Img $\mapsto$ PC
Feature Transfer	Copy Value	Median Aggregation
Label Transfer	Copy Value	Majority Vote

Figure 11: Overview of the proposed method that links imagery, point cloud (PC), and mesh via inter-modal subprocesses a) Point Cloud Mesh Association (PCMA), b) Image Mesh Association (ImgMA), and c) Point Cloud Image Association (PCImgA). For each association mechanism, the transfer operations depend on the information type (feature or label) and the transfer direction. The pictograms on the right depict the linking of the respective entities.

Figure 12: The explicit linking of pixels, points, and faces (multi-modal data fusion) enables the information exchange across the three modalities PC (left), mesh (center), and imagery (right). The figure exemplarily depicts the label propagation from the manually annotated PC to the mesh and an oblique image (for a subset of Hessigheim 3D). Faces that cannot be linked to points remain without a label (depicted in black). Pixels that are linked to an unlabeled face are colored in black. Background and non-associated pixels are colored in reddish-brown.

An End-to-End Model for Rare Class Segmentation in Large-Scale Point Clouds

Automated semantic segmentation of point clouds is fundamental for various fields of application. Although those 3D segmentation methods developed in the computer vision community have greatly improved the segmentation accuracy, they are mostly used for general large classes in ground scans with limited space, or indoor scenes. But, the complexity and class imbalance of large-scale scenes leads to difficulties in rare class segmentation. To our knowledge, specialized segmentation methods for imbalanced rare classes in large-scale point clouds have not yet been investigated. We design an end-to-end model to overcome these difficulties. The overall structure is illustrated in Figure 13, which can be separated into three parts, feature extraction, feature fusion and classification.

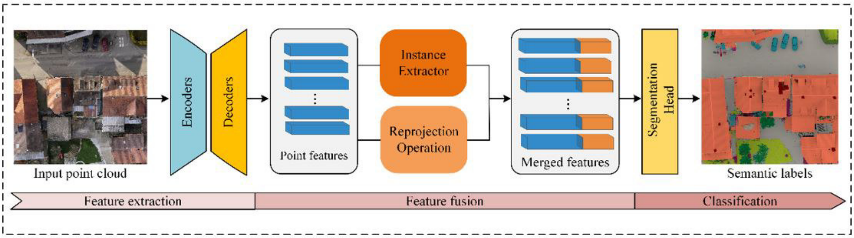

Figure 13: Structure of the proposed model.

The proposed approach is evaluated on the Hessigheim High-Resolution 3D Point Cloud (H3D) Benchmark. The confusion matrix is shown in Figure 14 (b), where the overall accuracy achieves 87.94% and the mean F1-score achieves outstanding 76.38%. In order to verify the effectiveness of the proposed model for imbalanced rare classes, i.e. vehicle class and chimney class, we compare it with the model without our proposed module. Vehicle and Chimney have achieved breakthroughs from zero to 79.87% and 77.12% in F1-score respectively, which indicates that the proposed model effectively improve the rare class segmentation in large-scale scenes, i.e. vehicle class and chimney class.

Using commercial Drones for highly precise 3D Object Reconstruction

The Institute for Photogrammetry (ifp) at the University of Stuttgart has been working intensively on high-precision, UAV-based 3D object point determination and surface reconstruction in recent years and has also investigated various camera systems. The motivation for these tests was a research project together with the Federal Institute of Hydrology (BfG) in Koblenz, in which the suitability of UAV photogrammetry for the area-based detection of ground movements was investigated using the example of the Hessigheim lock facility on the Neckar River. This project has been reported on several times. Within the scope of the research project, the project area was flown with Phase One cameras iXM 100 MPix and 150 MPix. In parallel,

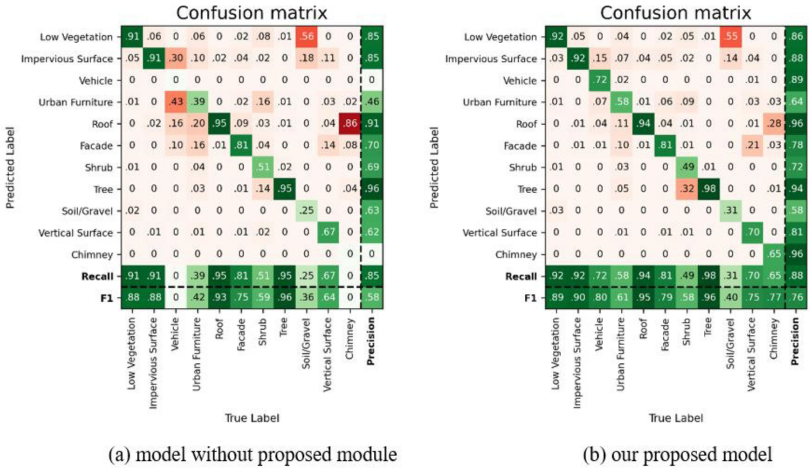

Figure 14: Detailed segmentation results from the comparative experiment.

flights with VUX-1UAV laser scanners also took place, initially on two separate UAVs. During the last flight campaign, the high-end camera and laser scanner were installed and flown together on one UAV.

In March 2022 the ship lock was flown again, but different to the previous close-to-research UAV platforms the data was captured with purely commercially available components. A DJI Matrice 300 RTK drone equipped with either a P1 camera (with 35 mm lens) or Phase One iXM 100 MPix camera (with RSM 35 mm lens) was used (see Figure 15). The Phase One system is referred to as the P3 camera in DJI's own nomenclature. The P1 camera has a diagonal angle of view of approximately 63°, the P3 is slightly wider at 76°. The project area was flown at different altitudes, the resulting GSDs are between 4 and 6 mm. With the purely control point-based bundle adjustment using ten control points (PP) distributed in the project area, the accuracies (RMS) given in Table 1 are achieved for the nadir image flights of P1 (2937 images, GSD: 6.3 mm) and P3 (986 images, GSD: 4.7 mm) from a flight altitude of 50 m from 27 and 26 independent check points (ChP), respectively. The absolute values and the accuracies in relation to the respective ground pixel size GSD are given. The georeferencing was based on the use of the same 10 control points (GCP) for both of the flights.

Table 1: Absolute accuracy of the georeferencing from control point differences for P1 and P3 camera.

	Number GCP | ChP	RMS East [m] | [%GSD]	RMS North [m] | [%GSD]	RMS Vertical [m] | [%GSD]
P1 (nadir)	10 | 26	0.0035 | 55.5	0.0031 | 49.2	0.0081 | 128.6
P3 (nadir)	10 | 27	0.0024 | 51.0	0.0021 | 44.7	0.0039 | 83.0

Figure 15: DJI Matrice 300 RTK dron with two different camera systems installed.

Table 1 shows practically identical results for the horizontal accuracy. In relation to the slightly different ground pixel sizes, both systems achieve an accuracy in the east and north of 0.5 pixel. In the vertical component, the accuracy of the P3 camera is about 40% better. On the one hand, this is due to the better intersection angle of the beams due to the slightly larger aperture angle of the optics, but on the other hand, it is also due to the fact that with the larger sensor format, significantly fewer images are necessary than with the P1 to cover the entire area. Consequently, with the same number of control points, the ratio of images to the number of control points is little worse for the P1 than for the P3. In other words, the number of images to be bridged between the control points is greater for the P1 than for the P3 camera. This is an advantage of larger format sensors. This deficit is compensated by using the RTK projection centre coordinates in the context of GNSS-based bundle triangulation, but this will not be discussed in the context of this paper.

The photogrammetric surface model (DOM) obtained by multi-image stereo evaluation is one of the most important products of photogrammetric UAV image flight evaluation. For defined, solid and well-textured surfaces, DOM accuracies can be achieved that are equivalent, and in some cases even superior, to those of laser flights. Thus, depending on the application, laser flights can be completely replaced by image flights. Figure 16 shows the differences between the two surface models calculated from P1 and P3 images, respectively. The control points used for orientation are also shown. Only the west bank with the actual lock area is shown. Here, again, there is a high degree of agreement. Larger deviations show up in areas of vegetation and especially at the edges of the image composite, outside the given control point frame, which is to be expected. On closer inspection, differences can also be seen in moving objects (cars) that were moved during the time offset of the two flights. Within the control point frame, however, there are also deviations that indicate differences in the two surface models. These occur mainly in the areas further away from the control points. This agrees with the previously discussed effect that due to the smaller image format of the P1 camera without using GNSS projection centres, the image orientation is not as good in these areas. Errors in orientation therefore also show up in the derived photogrammetric products.

The empirical comparison of two commercial camera systems of different image format and also price class shows, as was to be expected, certain quality differences. Depending on the required accuracy, however, these can be neglected under certain circumstances.

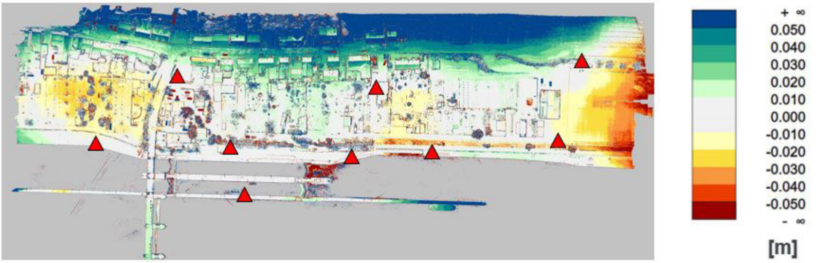

Figure 16: Comparison of the surface models from P1 and P3 evaluation (here only west bank with lock area shown). The control points are shown as triangular symbols.

References 2022

Ackermann, S., Joachim, L.: Simulation und Auswertung eines photogrammetrischen Bildverbandes aus Krankamerabildern. 42. Wissenschaftlich-Technische Jahrestagung der DGPF, 297–303. https://doi.org/10.24407/KXP:1796047422

Bill, R., Blankenbach, J., Breunig, M., Haunert, J.H., Heipke, C., Herle, S., Maas, H.G., Mayer, H., Meng, L., Rottensteiner, F., Schiewe, J., Sester, M., Sörgel, U., Werner, M.: Geospatial Information Research: State of the Art, Case Studies and Future Perspectives. PFG – Journal of Photogrammetry, Remote Sensing and Geoinformation Science. https://doi.org/10.1007/s41064-022-00217-9

Farella, E. M., Morelli, L., Remondino, F., Mills, J. P., Haala, N., Crompvoets, J.: The EUROSDR Time Benchmark for historical aerial Images. The International Archives of the Photogrammetry, Remote Sensing and Spatial Information Sciences, XLIII-B2-2022, 1175–1182. https://doi.org/10.5194/isprs-archives-XLIII-B2-2022-1175-2022

Haala, N., Kölle, M., Cramer, M., Laupheimer, D., Zimmermann, F.: Hybrid georeferencing of images and LiDAR data for UAV-based point cloud collection at millimetre accuracy. ISPRS Open Journal of Photogrammetry and Remote Sensing, 100014. https://doi.org/10.1016/j.ophoto.2022.100014

Joachim, L., Zhang, W., Haala, N., Sörgel, U.: Evaluation of the quality of real-time mapping with crane cameras and visual SLAM algorithms. The International Archives of the Photogrammetry, Remote Sensing and Spatial Information Sciences, XLIII-B2-2022, 545–552. https://doi.org/10.5194/isprs-archives-XLIII-B2-2022-545-2022

Kölle, M., Walter, V., Sörgel, U.: Learning from the Past: Crowd-driven Active Transfer Learning for Semantic Segmentation of Multi-Temporal 3D point Clouds. ISPRS Annals of the Photogrammetry, Remote Sensing and Spatial Information Sciences, V-2–2022, 259–266. https://doi.org/10.5194/isprs-annals-V-2-2022-259-2022

Laupheimer, D., Haala, N.: Multi-Modal Semantic Mesh Segmentation in Urban Scenes. ISPRS Annals of the Photogrammetry, Remote Sensing and Spatial Information Sciences, V-2–2022, 267–274. https://doi.org/10.5194/isprs-annals-V-2-2022-267-2022

Nex, F., Armenakis, C., Cramer, M., Cucci, D. A., Gerke, M., Honkavaara, E., Kukko, A., Persello, C., Skaloud, J.: UAV in the advent of the twenties: Where we stand and what is next. ISPRS Journal of Photogrammetry and Remote Sensing, 184, 215–242. https://doi.org/10.1016/j.isprsjprs.2021.12.006

Schmohl, S., Narváez Vallejo, A., Sörgel, U.: Individual Tree Detection in Urban ALS Point Clouds with 3D Convolutional Networks. Remote Sensing, 14(6), 1317. https://doi.org/10.3390/rs14061317

Schneider, P. J., Sörgel, U.: Matching Persistant Scatterer Clusters to Building Elements in Mesh Representations. ISPRS Annals of the Photogrammetry, Remote Sensing and Spatial Information Sciences, V-3–2022, 123–130. https://doi.org/10.5194/isprs-annals-V-3-2022-123-2022

Skuddis, D., Haala, N.: Globally optimal Point Cloud Registration for Robust Mobile Mapping. The International Archives of the Photogrammetry, Remote Sensing and Spatial Information Sciences, XLIII-B2-2022, 273–281. https://doi.org/10.5194/isprs-archives-XLIII-B2-2022-273-2022

Skuddis, D., Köberle, J., Haala, N.: LiDAR Ground Segmentation and Modeling for Mobile Robots in Unstructured Terrain. 8th International Conference on Automation, Robotics and Applications (ICARA), 57–61. https://doi.org/10.1109/ICARA55094.2022.9738519

Walter, V., Kölle, M., Collmar, D.: A Gamification Approach for the Improvement of Paid Crowd-based Labelling of Geospatial Data. ISPRS Annals of the Photogrammetry, Remote Sensing and Spatial Information Sciences, V-4–2022, 113–120. https://doi.org/10.5194/isprs-annals-V-4-2022-113-2022

Walter, V., Kölle, M., Collmar, D.: Measuring the Wisdom of the Crowd: How Many is Enough? PFG – Journal of Photogrammetry, Remote Sensing and Geoinformation Science. https://doi.org/10.1007/s41064-022-00202-2

Wang, J., Gong, K., Balz, T., Haala, N., Sörgel, U., Zhang, L., Liao, M.: Radargrammetric DSM Generation by Semi-Global Matching and Evaluation of Penalty Functions. Remote Sensing, 14(8), Article 8. https://doi.org/10.3390/rs14081778

Xue, R., Zhang, X., Sörgel, U.: Urban Classification based on Top-view Point Cloud and SAR Image Fusion with Swin Transformer. The International Archives of Photogrammetry, Remote Sensing and Spatial Information Sciences, 43, 559–564.

Zhang, W., Wang, S., Haala, N.: Towards robust Indoor Visual SLAM and dense Reconstruction for mobile Robots. ISPRS Annals of the Photogrammetry, Remote Sensing and Spatial Information Sciences, V-1–2022, 211–219. https://doi.org/10.5194/isprs-annals-V-1-2022-211-2022

Zhang, W., Skuddis, D., Schneider, P. J., Haala, N.: Comparison of different 2D and 3D Sensors and Algorithms for Indoor SLAM on a low-cost Robotic Platform. Tagungsband der DGPF: PFGK22 - Photogrammetrie - Fernerkundung - Geoinformatik - Kartographie, 42. Jahrestagung in Dresden 2022. https://doi.org/10.24407/KXP:1796046450

Zhang, X., Xue, R., Sörgel, U.: A two-stage Approach for rare Class Segmentation in large-scale urban Point-Clouds. The International Archives of Photogrammetry, Remote Sensing and Spatial Information Sciences, 43, 329–334.

Doctoral Theses

Laupheimer, D.: On the information transfer between imagery, point clouds, and meshes for multi-modal semantics utilizing geospatial data. http://dx.doi.org/10.18419/opus-12668

Nekouei Shahraki, M.: Design and development of a calibration solution feasible for series production of cameras for video-based driver-assistant systems. http://dx.doi.org/10.18419/opus-12188

Master Theses

Ernst, J.: Combination of Weakly Supervised Learning and Active Learning for 3D Point Cloud Classification with Minimum Labeling Effort: Supervisors: Schmohl, S., Haala, N.

Scherer, J.: Development of an Automatic Pathology Recognition System Using Machine Learning on the Basis of Clinical Raw Data from Optical Coherence Tomography. Supervisor: Sörgel, S.

Zeng, Z.: Learned Obstacle Representation from Camera Views for Mobile Robots. Supervisors: Kurz, G. (Robert Bosch GmbH), Holoch, M. (Robert Bosch GmbH), Haala, N.

Li, Y.: Stereo Camera Based Detection of Moving Objects as Basis for Collision Avoidance for an Autonomous Tower Crane. Supervisors: Joachim, L., Haala, N.

Huber, D.: Klassifikation von Defekten auf optischen Oberflächen mit synthetischen Trainingsdaten. Supervisors: Weiss, N. (Diehl Defence), Radtke, H.P. (Diehl Defence), Haala, N.

Kappler, J.: Durchsatz und Genauigkeit neuronaler Netze für die Objekterkennung im Fahrzeugbereich auf CPU-basierten Systemen. Supervisors: Hügle, D. (Vector Informatik GmbH), Haala, N.

Zhang, Y.: Photogrammetrische Bestimmung der äußeren Orientierung der Kamera am Field-of-View Prüfstand. Supervisors: Pesch, T. (Robert Bosch GmbH), Haala, N.

Nübel, H.: Improving True Ortho quality by removing moving vehicles. Supervisors: Tutzauer, P. (nFrames GmbH), Haala, N.

Schmitt, V.: Multi-View-Stereo DSM from Planetscope satellites. Supervisors: Jordahl, K. (Planet Labs Inc), Haala, N.

Hertel, V.: Probabilistic Deep Learning Methods for Capturing Uncertainty in SAR-based Water Segmentation Maps. Supervisors: Chow, C. (DLR), Schneibel, A. (DLR), Martinis, S. (DLR), Sörgel, U.

Xiang, M.: Automatic Vehicle and Occlusion Removal in Aerial and Satellite Imagery Using Deep Learning Algorithms. Supervisor: Sörgel, U.

Bachelor Theses

Ho, H.: Hochauflösende Drohnenphotogrammetrie – Ein Vergleich am Beispiel der Schleuse Hessigheim. Supervisor: Cramer, M.

Josephowitz, F.: Photogrammetrie und Laserscanning zur 3D Rekonstruktion und Visualisierung in der Höhlenforschung. Supervisor: Cramer, M.

Activities in National and International Organizations

Cramer, M.:

Secretary German Society of Photogrammetry, Remote Sensing and Geoinformation (DGPF)
Advisor ISPRS WG I/6: Orientation, Calibration and Validation of Sensors
Member of DIN Normungsausschuss NA 005-03-02 AA "Photogrammetrie und Fernerkundung"

Englich, M.:

Webmaster ISPRS

Haala, N.:

Chair ISPRS WG II/2: Point Cloud Generation and Processing
Chair EuroSDR Commission II: Modelling and Processing
Vorsitz DGPF Arbeitskreis Sensorik und Plattformen

Sörgel, U.:

President German Society for Photogrammetry, Remote Sensing and Geoinformation (DGPF)

Walter, V.:

National Correspondent of the ISPRS Commission IV

Education - Lectures/Exercises

Bachelor "Geodäsie und Geoinformatik"

Geoinformatics I (Walter)	2/2
Geoinformatics II (Walter)	1/1
Image Processing (Haala)	2/1
Integrated Fieldworks (Haala, Hobiger, Sneeuw)	0/4
Introduction into Geodesy and Geoinformatics (Cramer, Hobiger, Sneeuw, Sörgel)	2/2
Photogrammetry (Cramer)	2/1
Remote Sensing (Sörgel)	2/1
Urban Planning (Dvorak)	2/0

Master Course "Geodäsie und Geoinformatik"

Aerotriangulation (Cramer)	1/1
Computational Geometry (Walter)	1/1
Computer Vision for Image-based Acquisition of Geodata (Haala)	1/1
Databases and Geographical Information Systems (Walter)	1/1
Fundamentals in Urban Planning (Dvorak)	2/0
Georeferencing of Photogrammetric Systems (Cramer)	1/1
Modelling and Visualisation (Haala)	1/1
Pattern Recognition and Image Understanding (Haala)	1/1
Photogrammetric Acquisition of 3D Geodata (Cramer, Haala)	2/2
Project Geodesy and Geoinformatics (Haala)	4/2
Selected Chapters in Remote Sensing (Sörgel)	1/1
Signal Processing (Sörgel)	1/1
Simultaneous Localization and Mapping (SLAM) (Haala, Hobiger)	2/2
Web-based GIS (Walter)	1/1

Master Course GEOENGINE

Airborne Data Acquisition (Cramer)	2/1
Computer Vision (Haala)	2/1
Geoinformatics (Walter)	2/2
Integrated Fieldworks (Haala, Hobiger, Sneeuw)	0/4
Image Analysis (Haala, Cramer)	0/1
Signal Processing (Sörgel)	2/1
Pattern Recognition (Sörgel)	2/1
Remote Sensing (Sörgel)	2/1

Master Course "Infrastructure Planning"

Introduction to GIS (Walter)	2/0

Master Course "Aerospace Engineering"

Image Processing (Haala)	2/1
Introduction to projective Geometry (Cramer)	1/0